CHALMERS

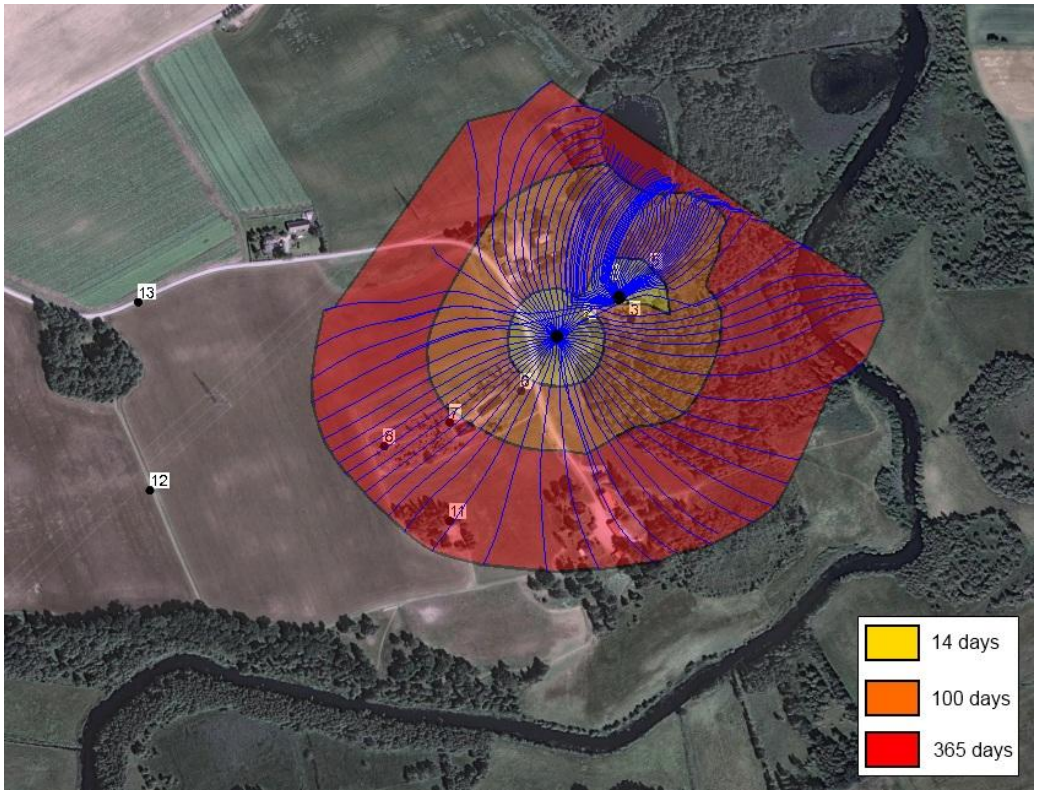

Groundwater Modelling of the Vårgårda Aquifer

Focus on the Capture Area at Storehagen

Master of Science Thesis in the Master's Programme Geo and Water Engineering

FELIX VAN DER HEIDEN
JOHANNA LITHÉN

Department of Civil and Environmental Engineering
Division of GeoEngineering

Engineering Geology Research Group

CHALMERS UNIVERSITY OF TECHNOLOGY
Göteborg, Sweden 2011
Master's Thesis 2011:130

MASTER'S THESIS 2011:130

Groundwater Modelling of the Vårgårda Aquifer

Focus on the Capture Area at Storehagen

Master of Science Thesis in the Master's Programme Geo and Water Engineering

FELIX VAN DER HEIDEN

JOHANNA LITHÉN

Department of Civil and Environmental Engineering
Division of GeoEngineering
Engineering Geology Research Group
CHALMERS UNIVERSITY OF TECHNOLOGY

Göteborg, Sweden 2011

Groundwater Modelling of the Vårgårda Aquifer
Focus on the Capture Area at Storehagen

Master of Science Thesis in the Master's Programme Geo and Water Engineering

FELIX VAN DER HEIDEN
JOHANNA LITHÉN

Examensarbete / Institutionen för bygg- och miljöteknik,
Chalmers tekniska högskola 2011:130

Department of Civil and Environmental Engineering
Division of GeoEngineering
Engineering Geology Research Group
Chalmers University of Technology
SE-412 96 Göteborg
Sweden
Telephone: + 46 (0)31-772 1000

Cover:
Capture area of the two production wells at Storehagen.

Department of Civil and Environmental Engineering
Göteborg, Sweden 2011

Groundwater Modelling of the Vårgårda Aquifer

Focus on the Capture Area at Storehagen

Master of Science Thesis in the Master's Programme Geo and Water Engineering

FELIX VAN DER HEIDEN
JOHANNA LITHÉN
Department of Civil and Environmental Engineering
Division of GeoEngineering
Engineering Geology Research Group
Chalmers University of Technology

ABSTRACT

Up to date, the extracted raw water for the Vårgårda municipality is showing high and increasing levels of nitrate. The aim of this study was to develop a numerical groundwater model that describes the flow pattern in the aquifer between Brolycke and Algutstorp, south of Vårgårda and to identify the capture zones of the production wells.

The stratigraphy and the aquifer thickness were approximated by interpolation based on several investigational borings. Indications of the hydraulic conductivity were assessed from both grain size distribution analyses and from pumping tests. In the south, the aquifer mainly consists of sand and in the northern part mainly of fine grained sand. The recharge of the aquifer was estimated from flow data along the Säve River and from the estimated extent of the capture zone of the river.

The conceptual model was transferred into a numerical model using the MODFLOW code in the GMS 7.1 software which is constructed to solve the ground water flow equation with finite difference technique.

Boundary conditions applied were Dirichlet and Neumann conditions. The Dirichlet condition represented the Säve River and the northern and southern boundaries of the aquifer. The Neumann boundary condition was used for the boundaries between the aquifer and areas of outcropping bedrock and layers of till.

The model was calibrated towards groundwater head observations, by modifying the hydraulic conductivity. The calibration technique used was indirect inverse modelling done in the automated parameter estimation program PEST, which is based on the Gauss-Marquardt-Levenberg's algorithm.

In this assessment some bias still remained as the modelled groundwater head in the periphery regularly was below the observed values.

It was concluded that the nitrate contaminated water probably originates from an area north-northeast of Siene Church. The retention time was calculated to about 30 years which implies that the nitrate problem likely will be an issue also in the future. The extension of the calculated capture zone of the abstraction wells at Storehagen coincides with the Säve River in a time perspective of one year. From Road 42 to the abstraction wells at Storehagen the transport time was determined to 4 years.

Key words: Groundwater modelling, GMS, automatic parameter estimation, indirect inverse modelling, PEST, Vårgårda, MODPATH, Gauss-Marquardt-Levenberg's algorithm, MODFLOW, finite differences, unconfined aquifer.

Groundwater Modelling of the Vårgårda Aquifer

Focus on the Capture Area at Storehagen

Master of Science Thesis in the Master's Programme Geo and Water Engineering

FELIX VAN DER HEIDEN
JOHANNA LITHÉN
Department of Civil and Environmental Engineering
Division of GeoEngineering
Engineering Geology Research Group
Chalmers University of Technology

SAMMANFATTNING

Vårgårda kommun har idag problem med höga nitrathalter i råvattnet. I denna studie har en numerisk grundvattenmodell utarbetats som beskriver flödesmönstren i akviferen mellan Brolycke och Algutstorp i syfte att identifiera tillrinningsområdet för brunnarna med höga nitrathalter.

Stratigrafin uppskattades genom interpolering av flera undersökningsborrningar i området. Den hydrauliska konduktiviteten bestämdes dels genom kornstorleksanalys och dels från provpumpningar. Akviferen består till största del av grovsand i de södra och mellersta delarna och finsand i de norra delarna. Grundvattenbildningen i modellen bestämdes genom flödesdata i Säveån och dess avrinningsområde.

Den konceptuella modellen överfördes till en numerisk modell baserad på finita differenser i MODFLOW och programmet GMS 7.1.

Randvillkoren som användes var Dirichlet och Neumann. Dirichlets randvillkor användes längsmed Säveån och modellens norra och södra gränser. Neumanns randvillkor användes mot morän och berggrund.

Serier av observerade grundvattennivåer användes för att kalibrera modellen. Modellen kalibrerades med hjälp av programmet PEST som baseras på Gauss-Marquardt-Levenberg's optimeringsalgoritm.

Modellen uppvisar dock viss bias eftersom de modellerade grundvattennivåerna i periferin understiger de observerade värdena.

Modellen visar att vattnet med de höga nitrathalterna härstammar från ett område nord-nordöst om Siene kyrka och har en uppehållstid på ungefär 30 år från detta område till uttaget i Storehagen. Detta innebär nitratproblemen kan vara ett problem även i framtiden, beroende på om föroreningen har upphört eller inte.

Tillrinningsområdet för brunnarna i Storehagen sträcker sig till Säveån i ett tidsperspektiv på cirka ett år. Från väg 42 är transporttiden cirka 4 år till uttaget i Storehagen.

Nyckelord: Grundvattenmodellering, GMS, automatisk parameteruppskattning, indirekt inversmodellering, PEST, Vårgårda, MODPATH, Gauss-Marquardt-Levenberg's algoritm, MODFLOW, finita differenser, öppen akvifer.

Contents

Preface

This report is the result of six months' work, 30 credits, of our master thesis. The project was initialized by Ramböll Sweden AB which also provided us with the computer software. During the work we received assistance from Per Sander (Ramböll Sweden AB), Lars Rosén (Chalmers University of Technology) and Lars-Ove Lång (Geological Survey of Sweden). We are grateful for the assistance we got and we would like to thank Per Sander, Lars Rosén and Lars-Ove Lång for the assistance and help with understanding the geological conditions at the site, it was very much appreciated.

We also would like to thank Per-Olof Lennartsson, Operation Technician at Vårgårda Water Board, and Robert Isberg, Chief of Vårgårda Water Board.

We believe that we from this work and from all the mistakes we done along the path, have gained rewarding insight and experience about groundwater modelling which also was our personal aim.

Gothenburg September 2011

Felix van der Heiden Johanna Lithén

1 Introduction

1.1 Background

In Sweden almost 1500 drinking water plants use groundwater as the raw water source, this compared to 170 drinking water plants that use surface water. About 130 drinking water plants use artificial groundwater from infiltration of surface water (Svenskt Vatten 2011). Vårgårda municipality, in Västra Götaland county, has until recently used natural groundwater augmented by artificial recharge to supply the municipality with drinking water. The recharge basins and production wells are located at Storehagen, south of Vårgårda, and the raw water is pumped to the treatment plant at Algutstorp, 1.5 km northeast of the production wells.

The quality of the raw water at Storehagen has been a problem for the municipality water board, due to its high nitrate levels. To improve the quality of the water, and to increase the capacity, the aquifer was up to recently, artificially recharged with surface water from the Säve River.

At the site of the drinking water treatment plant in Algutstorp there is an old groundwater supply with dug wells. This was used as Vårgårda municipality's main water source from the 1950s to the 1970s. An additional production well was in 2008 drilled 300 m north of the treatment plant to increase the capacity.

Currently, there is no reserve water supply for the municipality, and using surface water for artificial recharge increases the vulnerability of the raw water and demands a very large protection zone. To reduce the vulnerability, the old water supply in Algutstorp will be restarted and used together with the new well as a complement to the groundwater supply from Storehagen. A numerical groundwater model could contribute with important information regarding abstraction potential and groundwater flow patterns. The model could also show transport times for water or contaminants, which can be used to study different scenarios for accidents within the protection zone. In this particular case, the model was mainly used to investigate the source of the high nitrate levels at Storehagen.

The numerical groundwater modelling used in this study is based on automated parameter estimation technique, also referred to as inverse modelling, to find the optimal values of the hydraulic parameters in relation to the observed groundwater heads and flows in the water courses. This tool contributes to the development of a more accurate model that fits better with the true behaviour of the aquifer. The tool also computes the sensitivity of each parameter, which gives the user an opportunity to verify the data for the most important parameters. This assessment will further show how uncertain the model is by calculating the residual between the modelled value and the measured value.

1.2 Aim

The model was designed for interpretational use, in the sense of investigating the nitrate sources at the Storehagen abstraction wells by calculating the capture zones of the wells.

The overall aim of the project was twofold;

1) Identify the capture zones of the productions wells in Storehagen

2) Use the parameter estimation technique in order to calibrate the model.

The specific objective of the project was thus to set up a numerical groundwater model that describes the present aquifer behaviour, i.e. the distribution of head and flow pattern around Storehagen and Algutstorp, and use the model as a tool to investigate the source of the nitrate. The objective was also to use the model to investigate the capture zones of the abstraction wells in Storehagen in different time perspectives.

1.3 Limitations

The study was only aimed to identify capture area and flow pattern for which the flow conditions were unchanged from today. The model was spatially limited to the glaciofluvial deposit between Ljunghem and Algutstorp and the aquifer was simulated with steady state hydraulic conditions. No prior information was supplied for the parameters and no flow observations were used in the parameter estimation process.

2 Geological and hydrogeological description

Vårgårda municipality is located north east of Göteborg, see Figure 2.1. The municipality is supplied by groundwater from a 13 km long glaciofluvial deposit (see Appendix 1) with an estimated abstraction potential of 600 to 2 000 l/h (Lång & Persson 2011).

In the area several hydrogeological investigations have been carried out, starting in the 1950's. In 1950, 1989, 2008 and 2009 drillings were done in the area of Algutstorp (Allmänna Ingenjörsbyrån AB 1950; Kjessler & Mannestråle AB 1990; Ramböll Sverige AB 2010). In 1976, 22 drillings were made at Storehagen (Allmäna Ingenjörsbyrån AB 1976) and a decade later further drillings were carried out in the same area (Kjessler & Mannestråle AB 1990). In addition to this the Geological Survey of Sweden (SGU) has conducted numerous drillings (SGU 2004) in the aquifer and a few drillings have also been done by private land owners[1]. As a supplement to these investigational borings some geophysical investigations has also been made (SGU 2004).

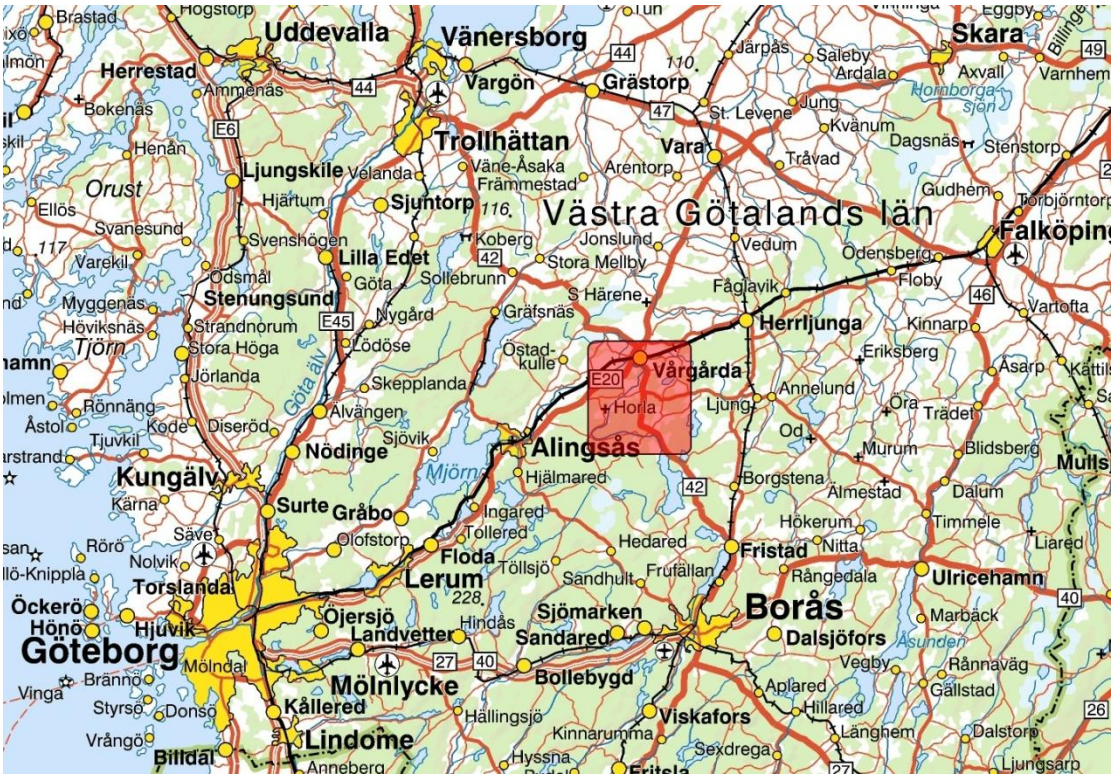

Figure 2.1 *The Vårgårda municipality is located about 60 km from Göteborg. The area of interest is highlighted with red. © Lantmäteriet Gävle 2011. Consent I 2011/0072.*

2.1 Eskers in Sweden

An esker is a glaciofluvial deposit with material that has been suspended and sorted by the inland glacier melting water streams (Andreasson 2006). Usually a distinction is made between eskers that were formed above the highest shore line and those formed below. According to the terminology convention, an esker formed above

[1] Data from the Well Archive (Brunnsarkivet). Excel file up-dated: 2006-12-06

shoreline is denoted supra-aquatic and if moulded below it is denoted as a subaquatic esker (Division of GeoEngineering, Chalmers University of Technology 2000).

A subaquatic esker was formed at the receding ice margin, see Figure 2.2. At the ice margin or at the discharging point of the stream the water velocity was drastically reduced, which resulted in that the suspended material settled (Division of GeoEngineering, Chalmers University of Technology 2000). Fine-grained materials settled at a greater distance from the discharging point than coarse-grained material, which was deposited at the vicinity of the outfall (Fredén 1994). During periods of receding ice margins the location of the deposit area moved along, and this caused the characteristic elongated shape of the esker (Division of GeoEngineering, Chalmers University of Technology 2000).

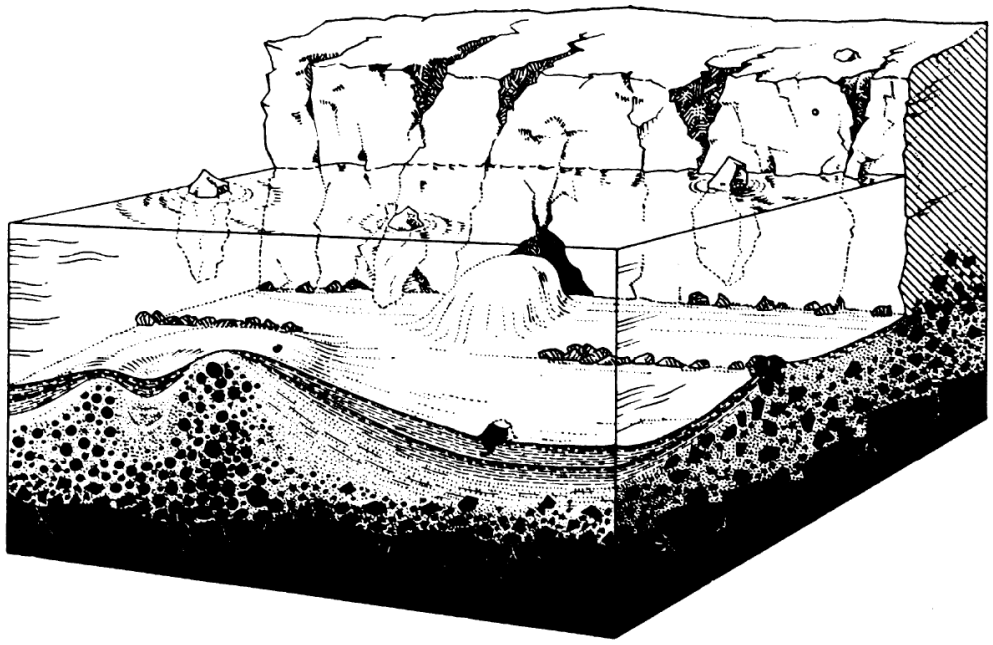

Figure 2.2 *The ice margin and the creation of a subaquatic esker (Division of GeoEngineering, Chalmers University of Technology 2000).*

The supra-aquatic type of esker was formed above the shoreline in the actual tunnels or channels in which the stream was following. This type of streams exhibits lower water velocity than the subaquatic streams, why the suspended material was free to settle inside the melt water channels (Division of GeoEngineering, Chalmers University of Technology 2000).

Glaciofluvial sediments are generally recognized by that the stratification is characterized by well sorted materials with only a few particle sizes and that the shape of the particles is smoothed (Fredén 1994).

Nevertheless during postglacial time as the land raised, subaquatic eskers were exposed to wave washing that caused re-stratification (Fredén 1994). During the wave washing process, finer-grained material fractions in the esker material was suspended and transported away from the shore. As the turbulence in the water decreased with the distance to shore, suspended material settled at different distances depending on the grain size. Thus, this process added additional sorting of the esker material since

the finer material was transported the longest way. Clay, silt and sand sediments that were washed out are all examples of post-glacial sediments, see Figure 2.3 (Division of GeoEngineering, Chalmers University of Technology 2000).

Another example of a post-glacial sediment is peat deposits. Peat deposits consist of partly decomposed plants. Figure 2.1 expressing the effect the wave washing has on a typical Swedish esker for which the prevailed wind direction was from the east.

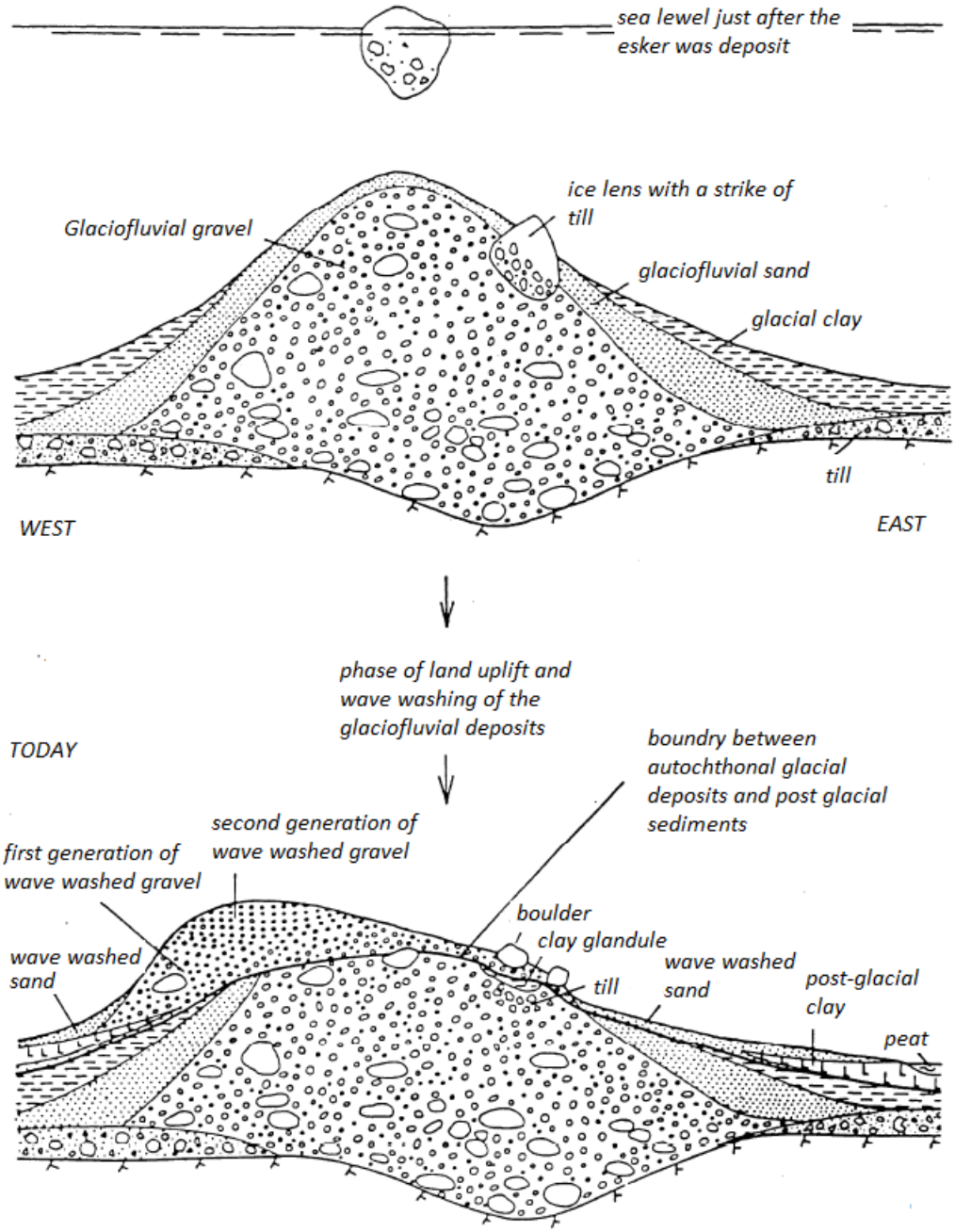

Figure 2.3 *Illustration of the post-glacial re-stratification process wave washing (Division of GeoEngineering, Chalmers University of Technology 2000).*

2.2 Geological conditions

The Vårgårda aquifer stretches from the lake Storsjön in the south to the town of Vårgårda in the north, see Appendix 1. The south part of the Vårgårda aquifer between Storsjön and Finnatorp is drained by the Säve River. Under normal conditions, there is very limited recharge to the aquifer from the river. According to the SGU the south part is hydraulically connected to the middle part of the Vårgårda aquifer, between Finnatorp and Algutstorp (Lång & Persson 2011).

The composition of soil types and their thickness vary in the area from Finnatorp to Algutstorp. Between Finnatorp and Ljunghem the drillings and the seismic profile in the area show that the soil consists of sand with a thickness of 10-15 m (SGU 2004). Along a small stream in this area, the glaciofluvial sediments are overlain by fen peat. Considering the investigational drilling R04101 carried out by the SGU (2004), the first five meters consist of silt and silty sand. The other investigational drillings in the area originates from the SGU's wells archive and may not be reliable in regard to grain size and soil type since the information is provided by the person that made the drilling.

Between Ljunghem and Siene Church, see Figure 2.4, the soil consists of sand with coarse grain size and a thickness of 15-25 m. On the east side of the river the investigational borings indicate a thickness of 3-8 m of the glaciofluvial deposits.

A seismic survey was preformed 500 m downstream Siene Church (S3-04). The survey showed a varying depth to the bedrock, between 8 and 23 m and according to the SGU (Lång & Persson 2011) the sand is overlain by silt. The drilling associated with the seismic profile (R04109) proved a depth of 13 m coarse sand. The area northwest of the seismic profile, towards Tubbetorp, was assumed to consist of a 10 m thick sand layer.

The area in and around Storehagen was believed to house a 10-20 m layer of coarse sand below a top layer of finer sediments such as fine sand, silt and in some parts clay. The grain size distribution demonstrated a hydraulic conductivity of about $4 \cdot 10^{-4}$ - $8 \cdot 10^{-4}$ m/s for the sand and the pumping test $3 \cdot 10^{-4}$ m/s for the overall hydraulic conductivity, see Appendix 2. The few investigational borings between Storehagen and Svantetorp show thick layers of fine sediments with depths of 10-14 m (drillings R11, R12 and R04111). In the small lake Lillesjön the investigational borings have shown 8 m of lake sediments. An area mainly covered by clay and peat was identified from the soil map to the southwest of Bänatorp, east of Storehagen. According to SGU these deposits may have a considerable thickness (Lång & Persson 2011), but no drillings have been done in this area to confirm this. If the non-permeable layers would stretch between Storehagen, Bänatorp and Svantetorp, this would limit the inflow of surface water from the Säve River to the aquifer in this area.

The soil in the area around the Algutstorp drinking water treatment plant is dominated by coarse sand with strikes of fine sand. The conductivity for the sand varies between about $2 \cdot 10^{-4}$ to $4 \cdot 10^{-3}$ m/s, see Appendix 2. About 500 m further north, the soil types are fine sand at the top layers, with a thickness of about 5-10 m, and silt and clay below, with a thickness of about 3-5 m. These impermeable layers together with the topography were assumed to limit the hydraulic connection to the north part of the Vårgårda aquifer; Tånga hed.

Figure 2.4 *Area of interest and location of borehole drillings (green circles). © Lantmäteriet Gävle 2011. Consent I 2011/0072.*

At the location of the Vårgårda aquifer the highest shoreline stands at an elevation of 110 to 120 meters above sea-level (masl) and the altitude of the topography in the area of the aquifer is roughly between 90 and 110 masl, see Figure 2.5, indicating that the most part of the esker probably is subaquatic. This is perhaps most true for the northern part of the aquifer since the altitude here is lower than in the southern parts. This was also confirmed by the fact that the presence of clay is more widespread and extensive in this part.

The surrounding areas with till and bedrock on the west side of the aquifer rise to a maximum level of 130 masl and on the east side to a maximum of 200 masl, see Figure 2.5. The figure also shows the topography in the modelled area, from Brolycke in South to Algutstorp in North.

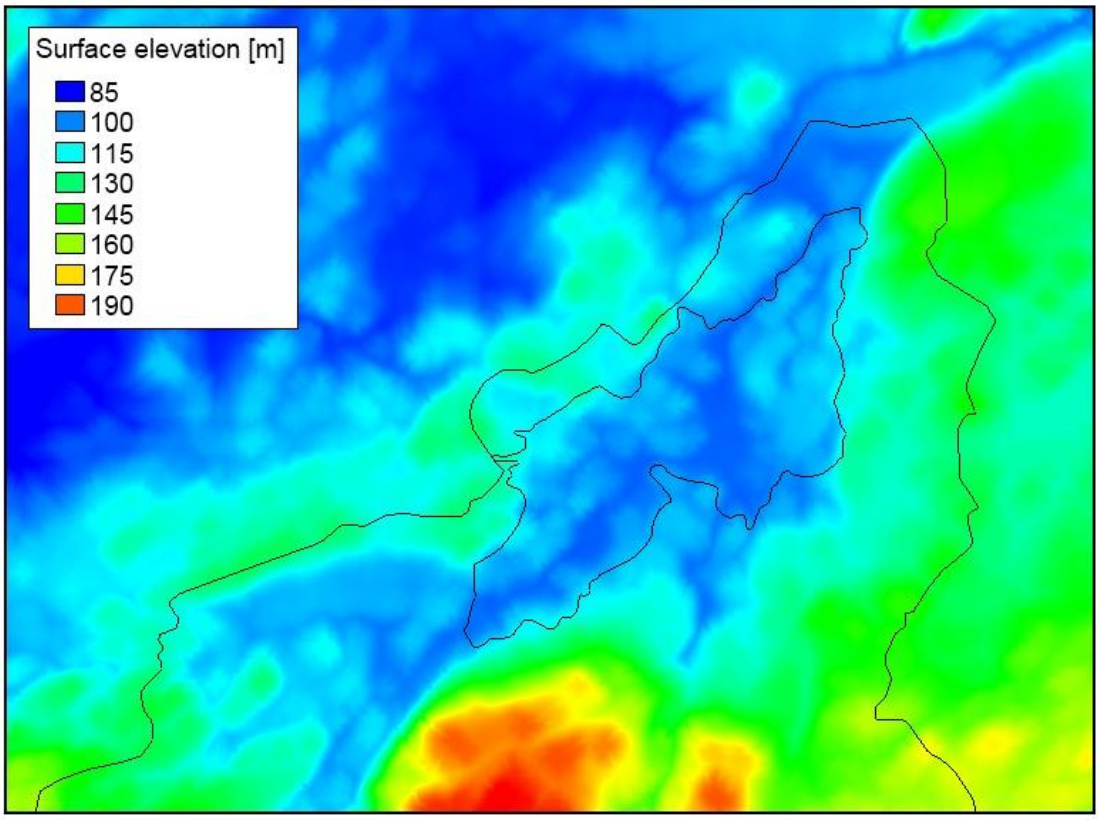

Figure 2.5 *The surface topography in the area. The outer black line represents the catchment area for the Säve River according to Vattenkartan (2011) and the inner black line represents the model domain.*

2.3 Hydraulic conductivity

The hydraulic conductivity was approximated from drawdown data obtained from two pumping tests, conducted at Storehagen and in Algutstorp and also from grain size analysis.

At Storehagen the pumping test was carried out by Allmänna Ingenjörsbyrån AB (1976) between 30 of March and 14 of April 1976. Water was abstracted from a gravel packed well denoted "Brunn 1" and the water level was observed in number of surrounding observation wells see Figure 2.6.

The resolution of the drawdown data at the initial phase and the length of the pumping session were judged as insufficient, to be used as a basis for the estimation of the type of aquifer. However, based on the stratigraphy in the area the aquifer was assumed to be unconfined.

During the pumping test the abstraction rate was changed several times and four pumping stops were recorded (Allmänna Ingenjörsbyrån AB 1976). Kresic (2007) suggests that the drawdown recovery method with adjusted pump start time should be used to calculate the transmissivity when different pumping rates have prevailed during the pumping test. The calculations carried out here (see Appendix 2) followed the rationale of the drawdown recovery method with varying pumping rate presented by Kresic (2007).

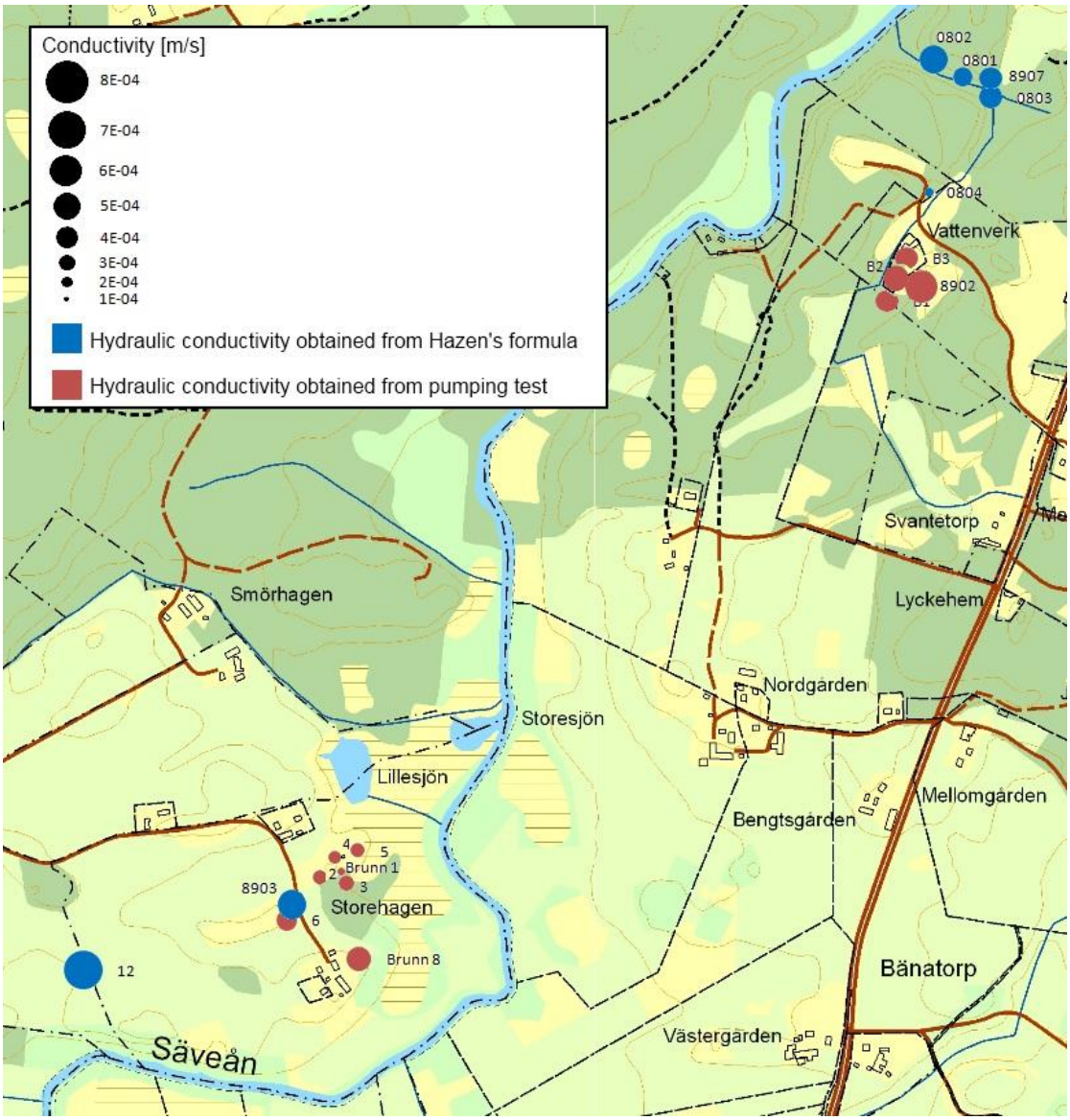

Figure 2.6 *The hydraulic conductivity per borehole relatively to each other. Blue discs represent the hydraulic conductivity obtained from Hazen's formula and the red discs from the pumping tests. The values could be seen in Appendix 2. © Lantmäteriet Gävle 2011. Consent I 2011/0072.*

The conductivity was determined by dividing the transmissivity with the saturated thickness, thus it could be claimed that the conductivity obtained in this way represents an average conductivity for the whole saturated strata.

The mean conductivity based on the pumping test was determined to $3.0 \cdot 10^{-4}$ m/s, see Appendix 2.

At Algutstorp two pumping tests were carried out in 2006-2007 (Ramböll Sverige AB 2007). The first pumping test was executed between 20 of December 2006 and 16 of January 2007 and the second between the 22 of March and 17 of April 2007.

During the first pumping test water was abstracted from production well B2 and throughout the second test water was abstracted from production well B1. In addition to the production wells the drawdown was also recorded in an old production well B3 and in observation wells R8902, G1 and G2 (Ramböll Sverige AB 2007).

The transmissivity was obtained both from drawdown data and from recovery data. The mean transmissivity obtained from the phase of drawdown for the first test was determined to $4.0 \cdot 10^{-3}$ m^2/s and for the phase of drawdown recovery to $3.4 \cdot 10^{-3}$ m^2/s. Considering the second pumping test the mean transmissivity, calculated from the phase of drawdown, was determined to $3.4 \cdot 10^{-3}$ m^2/s and from the phase of recovery to $5.6 \cdot 10^{-3}$ m^2/s (Ramböll Sverige AB 2007). Here the saturated thickness for the area was approximated to 8.4 m, and the average conductivity for the two tests was determined to $4.9 \cdot 10^{-4}$ m/s.

The hydraulic conductivity value was also approximated with the use of the Hazen's formula with an average of $6.4 \cdot 10^{-4}$ m/s at Storehagen and about $3.8 \cdot 10^{-4}$ m/s in Algutstorp, see Appendix 2. At Storehagen soil samples were taken at two locations and at a depth ranging between 8.5 and 14 m below the ground. In Algutstorp samples were taken at five locations at a depth between 6 and 15 m.

However, the approximation of the hydraulic conductivity was only done for layers with coarse material, this since no data was obtained for the other hydrogeological units present. The conductivities obtained in this way served only as a comparison.

To characterize the hydraulic conductivity in the aquifer a mean value and a 95% confidence interval was calculated based on the mean hydraulic conductivities from the pumping tests at Storehagen and Algutstorp and was determined to $3.0 \cdot 10^{-4} \pm 1.1 \cdot 10^{-4}$ m/s and $4.9 \cdot 10^{-4} \pm 1.5 \cdot 10^{-4}$ m/s, respectively, see Figure 2.7. The mean conductivity for the whole aquifer was determined to $4.0 \cdot 10^{-4}$ m/s according to the pumping test.

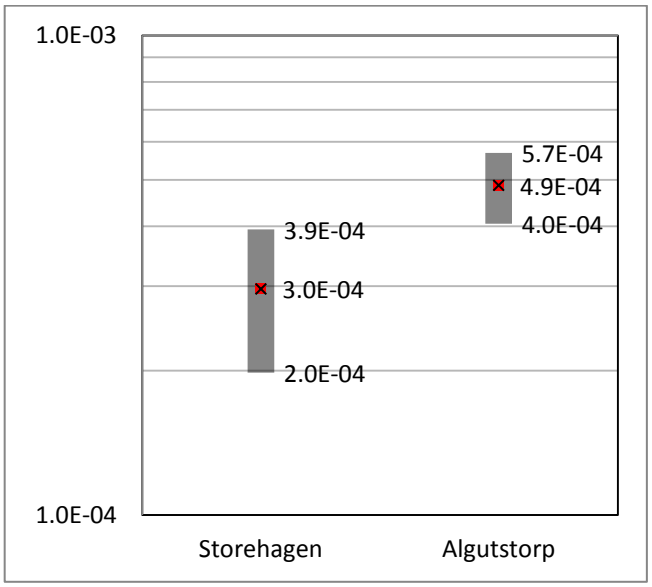

Figure 2.7 *Representative conductivity values obtained from the pumping tests with a 95% confidence interval for Algutstorp and Storehagen respectively [m/s].*

2.4 Anisotropy of the hydraulic conductivity

Anisotropy is in hydrogeology generally referred to as the difference in the magnitude between the components of the conductivity vector (Kresic 2007). In this study three main perpendicular directions were considered. The magnitude of the two perpendicular directions defining the horizontal plane was assumed to be constant and

the anisotropy factor was defined as the relation between the hydraulic conductivity in the horizontal directions and the vertical direction.

An indication of the anisotropy in the aquifer was acquired from drawdown data recorded in the production well B1 when water was extracted from the well B2 in Algutstorp (Ramböll Sverige AB 2007). The drawdown was plotted against the pumping time in a double logarithmic diagram, see Appendix 2 and the type curve that represented the best match was Theis-Boulton, r/D=1.25.

The vertical transmissivity was calculated to $1.6 \cdot 10^{-4}$ m^2/s and the anisotropy factor defined as K_r/K_z was determined to 2, see Appendix 3 (Gustafson & Gustafson 1997).

2.5 Porosity

The total porosity of the geological material is the ratio between the volume of the void and the total volume. Much of the water in the voids is generally molecularly bounded to the sediments, which means that the effective porosity usually is less than the total porosity. This is especially significant in poorly sorted and fine grained soils and less in well-sorted, coarse materials. The number of pores in a fine grained material can be very high, yielding a high porosity, but if the pores are small, a large part of the water is bounded to the pore space walls resulting in a low effective porosity (Kresic 2007).

Total porosities for different sediments can be seen in Table 2.1. The sediments in Vårgårda have a hydraulic conductivity of about $1 \cdot 10^{-5}$ to $1 \cdot 10^{-3}$ m/s, which according to Table 2.1 should give a total porosity of 25-50% (Fetter 1988).

Table 2.1 General comparison of the average porosity and hydraulic conductivity (Fetter 1988).

Soil type	Porosity range [%]	Hydraulic conductivity [m/s]
Well-sorted gravel	25-50	$1 \cdot 10^{-4}$ - $1 \cdot 10^{-2}$
Well-sorted sand	25-50	$1 \cdot 10^{-5}$ - $1 \cdot 10^{-3}$
Sand and gravel	20-35	$1 \cdot 10^{-6}$ - $1 \cdot 10^{-5}$
Silt	35-50	$1 \cdot 10^{-8}$ - $1 \cdot 10^{-6}$
Clay	33-60	$1 \cdot 10^{-11}$ - $1 \cdot 10^{-8}$
Glacial till	10-20	$1 \cdot 10^{-8}$ - $1 \cdot 10^{-6}$

The effective porosity is according to Stephens et.al (1998) often assumed to be equal to specific yield or total porosity minus specific retention. The effective porosity could therefore be seen from Figure 2.8.

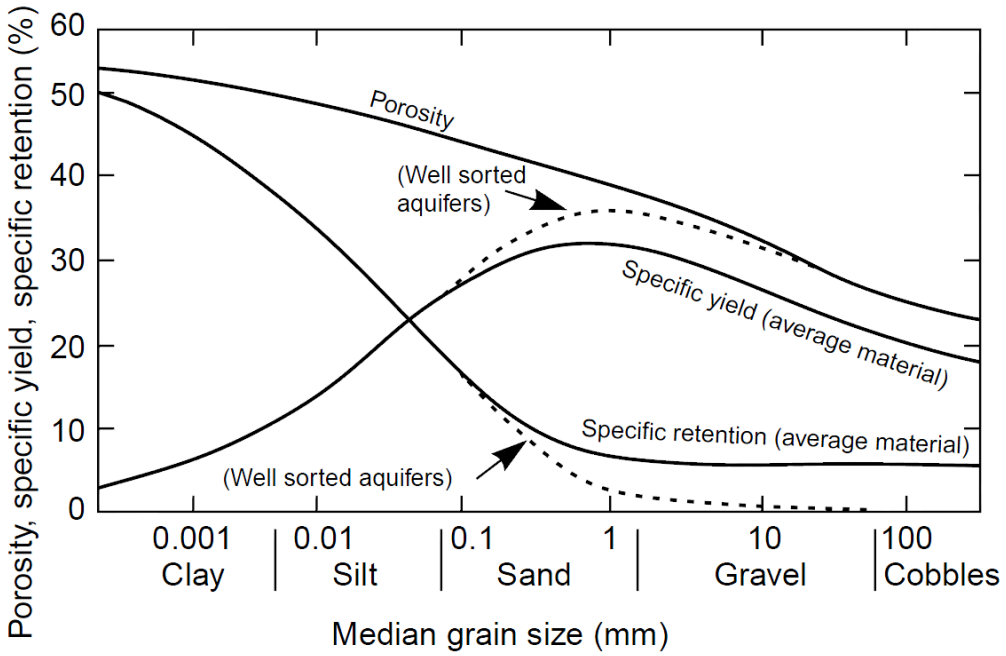

Figure 2.8 *Relationship between median grain size and water-storage properties of alluvium (Stephens et.al 1998).*

From the two arguments above, the effective porosity in all the material was therefore assumed to be between 10 and 30 %, with a most likely value of 20%. The porosity has a great impact on the transport and retention time in the aquifer, see Equation 2.1, and it is therefore important not to overestimate the porosity.

$$v = \frac{k \cdot i}{n} \tag{2.1}$$

where

v is the pore velocity

k is the hydraulic conductivity

i is the hydraulic gradient

n is the porosity

2.6 Precipitation and recharge

Based on precipitation measurements conducted from 1960 to 1990 at two rain gauging stations in the vicinity of Vårgårda city the normal precipitation was determined to 690-770 mm/year. Data considering normal monthly values can be seen in Figure 2.9 (SMHI 2009a).

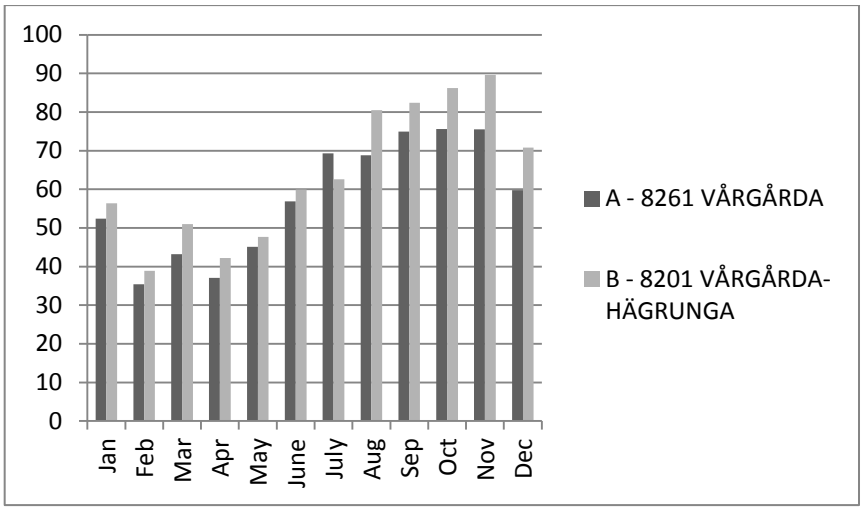

Figure 2.9 Normal values for precipitation for the years 1961-1990, [mm/month] (SMHI 2009a).

The mean value of evaporation in the region for the same period was 400-500 mm/year (SMHI 2009b), thus the runoff (overland flow) together with the groundwater flow (base flow) was 190-370 mm/year. Here this quantity is denoted effective precipitation. The actual flow in the Säve River was thought to describe the effective precipitation more accurately than the regional effective precipitation. The flow in the Säve River was used in this assessment, since the flow calculations in the Säve River was more up to date and was more precise for the area.

The drainage area for the Vårgårda aquifer between points A and C was approximated to 48 km^2 using Vattenkartan (2011), see Figure 2.10.

At two locations along the river; Kärtared (A) and Algutstorp (B), see Figure 2.10; SMHI provides information of flow rates. These flow rates are not measured, but calculated by SMHI with the flow-simulation program S-HYPE.

Information about the flow rates were readily obtained as a series of monthly mean values covering the last twenty years. However the data were modified to represent the annual mean flow for the number of years in the series. With these flow data, the effective precipitation was calculated as the difference between the mean flow rates at Kärtared and Algutstorp divided by the drainage area between them. The recharge was in this way determined to 472 ±262 mm/m^2year, see Appendix 4, with a 95% confidence interval. The standard deviation of the effective precipitation rate was calculated as the square root of the sum of the flow variances, divided by the capture area.

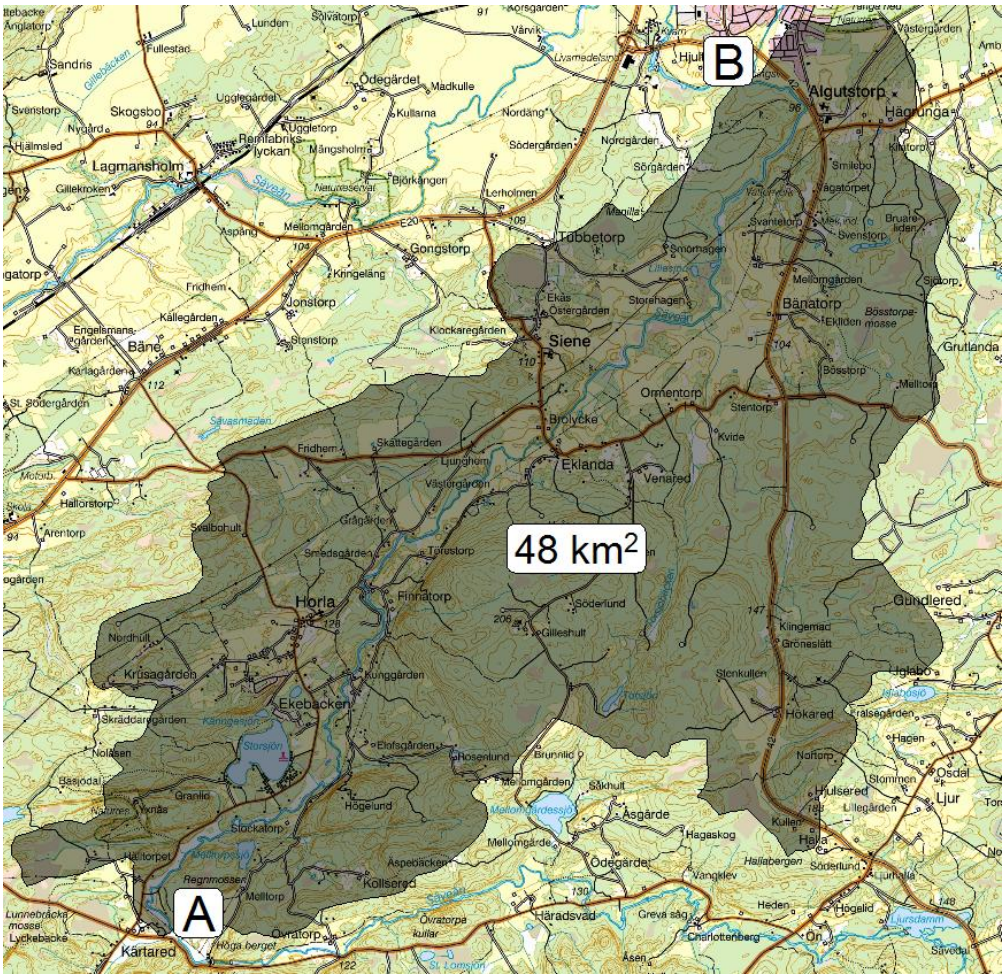

Figure 2.10 Catchment area for the Vårgårda aquifer (Vattenkartan 2011). © Lantmäteriet Gävle 2011. Consent I 2011/0072.

The evaporation is an important parameter when calculating a water balance, but it is also the most difficult parameter to determine. The evaporation depends in general on the temperature, the wind speed, the vegetation and the available amount of water (Halldin 1988).

The calculated flow rates at the two locations presented above gives thus an indication that the evaporation is most likely to be lower than 400-500 mm/year. Here it was assumed that the effective precipitation was determined most correctly by means of the flow in the river and the drainage area, as explained.

2.7 River levels

Series of monthly values of the river level have been collected at a position of the Säve River close to the abstraction wells at Storehagen, by personnel from the Vårgårda Water Board. The series cover 35 monthly values spread over the years 2007 to 2011. The mean level at the position was determined to +94.98 m with a two sided 95% confidence interval of 0.05 m. The river level was measured in RH70.

Two additional surveys of the river level have also been made but these measurements were only taken once at each location. One was carried out in June 2009and the latest

was done in May 2011. The most recent survey was carried out at two locations along the river, one at the area of Ljunghem and one further downstream at the bridge between Brolycke and Mellomgården. At Ljunghem the river level was measured to +95.18 m and at the bridge the river level was measured to +94.98 m.

The survey of June 2009 incorporated two locations along the river in the area of Algutstorp. Close to where the stream that passes through Algutstorp discharges into Säve River, the river level was measured to +94.7 m. At the intersection between the river and the north boundary of the domain, the level reached a value +94.66 m.

Since the two surveys described above only contain one measurement of the river level each, the uncertainty in the river level at these locations was not readily obtained. However the measurements of the river level carried out at Storehagen indicate a relatively constricted confidence interval and since the width and topography is generally rather similar along this stretch of the river, it was here therefore supposed that the confidence interval may serve as a general indication of the uncertainty in the river level.

2.8 Stream bottom elevations

The stream bottom elevations were investigated in field; the stream bottom elevations was in most cases located about 0.5-1 m below ground surface, but in the area of Bänatorp the streams or ditches was rather deep: 1.5-2 m below ground surface. A figure of the streams and the bottom elevation is provided in Chapter 4, Section 4.10, Figure 4.5.

2.9 Groundwater head observations

Several groundwater head measurements have been made in the area. Concerning observations at Storehagen, monthly values were assessable from 1990 to today, but for other areas the temporal data was scarce.

In Algutstorp pumping tests were carried out in August 2008 to June 2009, this means that the observed head in June 2009 was disturbed and was therefore left out from the model. Observation points with less than two observations have been excluded in the assessment. The groundwater head observations can be seen in Appendix 5.

2.10 Production wells

The well field at Storehagen consists of two production wells and ten observation wells. The total abstraction rate from the two production wells are roughly 17 l/s. Production well 1 (Brunn 1) is 15 m deep, the screen is between 10 and 13.5 m below ground surface and the diameter of the well is 0.6 m. The estimated capacity of Production well 1 is 35 l/s. Production well 2 has a depth of 16.5 m, the diameter equals 0.55 m and the screen is placed at a depth between 12.5 and 16.5 m. The assumed maximum yield of Production well 2 is 25 l/s (Ramböll Sverige AB 2011).

2.11 Summary and conceptual model

Overall the area consists of sand; fine grained sand and silt in the south-western part, coarser sand in the central parts and sand with layers of less permeable materials in the north-eastern part. The mean hydraulic conductivity for the area was believed to be about $5 \cdot 10^{-4}$ m/s, the porosity was assumed to be 20 % and the aquifer was assumed to be unconfined. A conceptual model of the soil layers can be seen in Figure 2.12 and Figure 2.13 (a-f).

The recharge to the aquifer was supposed to be equal to the effective precipitation according to the flow rates in the river; 472 mm/year.

The boundary of the model most likely has an inflow from the surrounding till and bedrock. The magnitude of the inflow was assessed based on the approximated capture areas displayed in Figure 2.11. The inflow from the north-west of Storehagen was expected to be of a lower magnitude compared to that from the eastern parts of Algutstorp and Brolycke. The south boundary of the model, at Brolycke-Eklanda, has probably a quite large inflow from the glaciofluvial deposit and the north boundary above Algutstorp most likely has a noticeable outflow.

Figure 2.11 *Estimated groundwater inflow from outside the model that contributes to the base flow across the boundaries.*

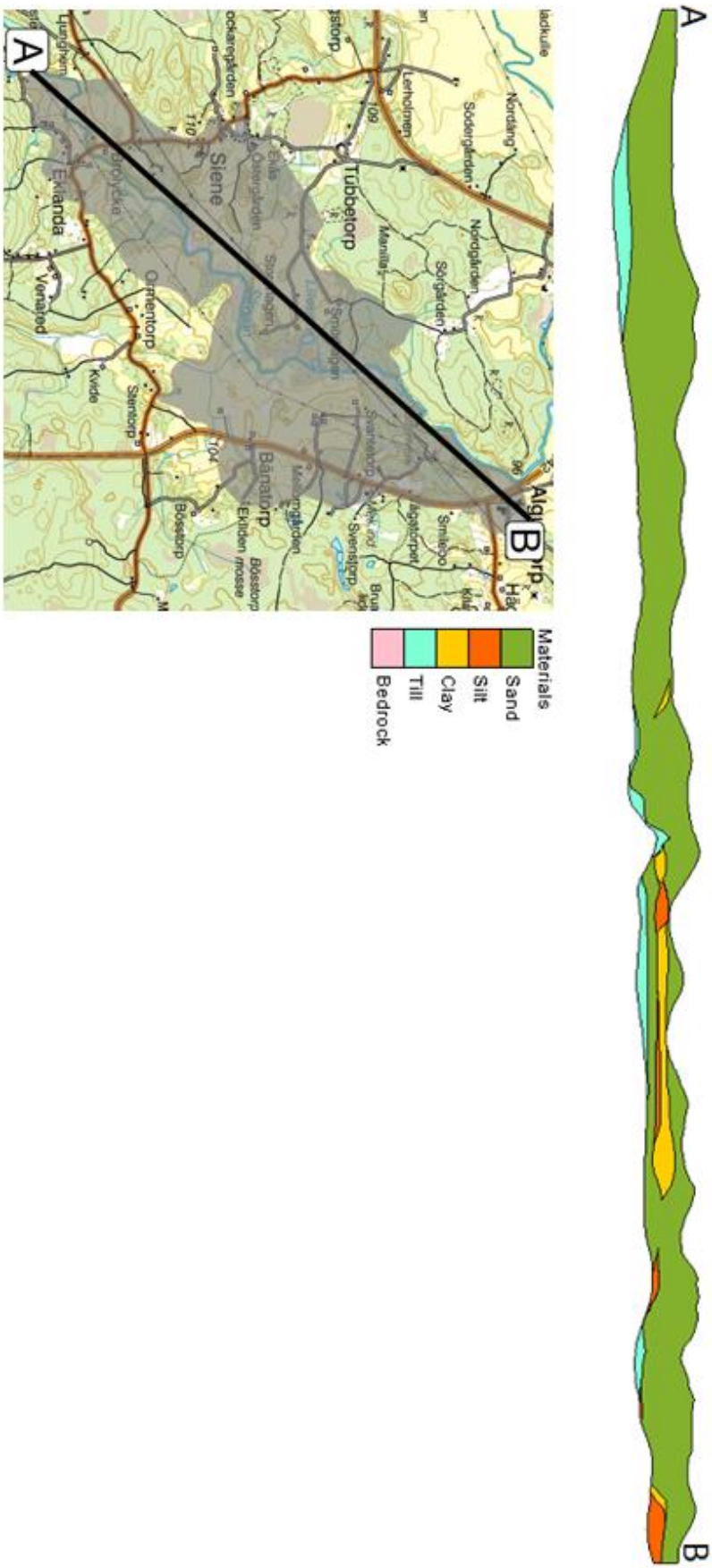

Figure 2.12 Conceptual model of the soil layers, cross section A-B. The vertical scale of the illustration is magnified by a factor of 10.

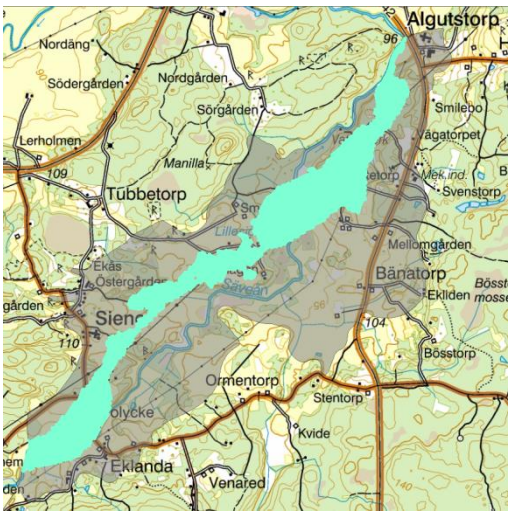

a) Layer 1 (Bottom layer): Till

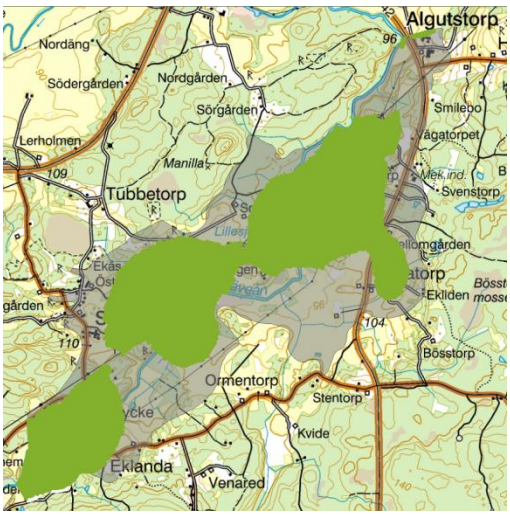

b) Layer 2: Sand

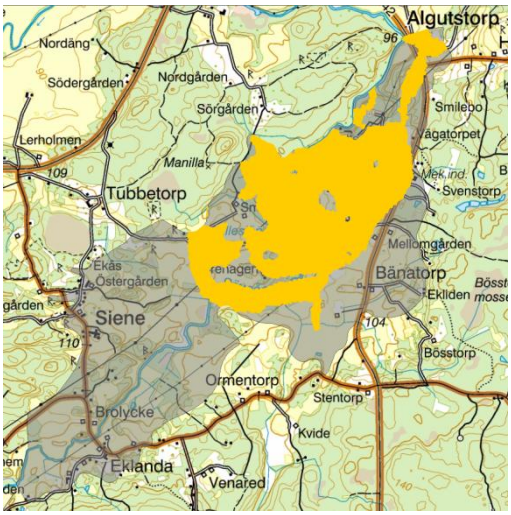

c) Layer 3: Clay

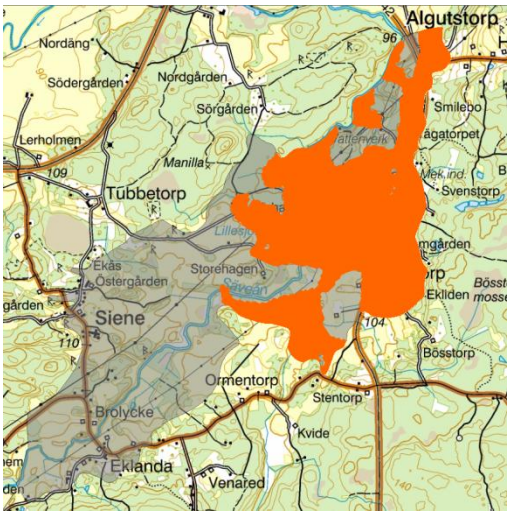

d) Layer 4: Silt

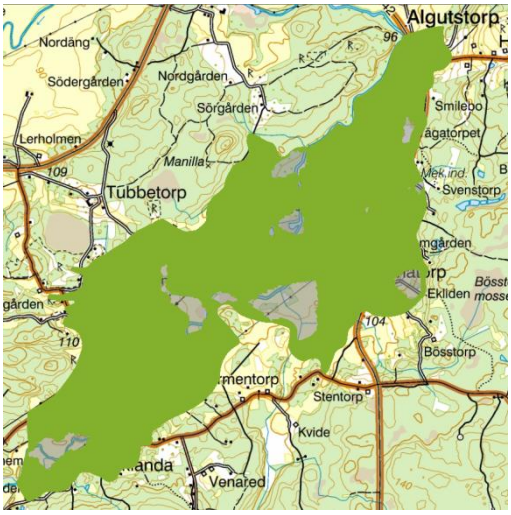

e) Layer 5 (Top layer): Sand

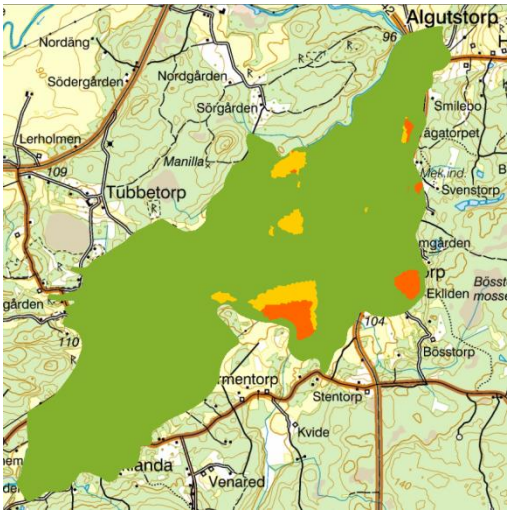

f) All layers, visible from surface

Figure 2.13(a-f) Conceptual model of the soil layers, spatial distribution of the soil layers.

3 Method

3.1 Introduction

The strategy to meet the modelling objective, i.e. to find the capture zone, basically follows the modelling protocol shown in Figure 3.1. After the definition of the purpose, a conceptual model was constructed. The conceptual model forms an idealized and simplified representation of the problem, including the spatial distribution of the geologic and hydrogeologic units, the location of system boundaries and boundary types, values on aquifer parameters and hydrogeological stresses. In order to obtain the conceptual model topology data, cross sections obtained from drillings, data from the national well archive, seismic and radar investigations, geological maps and consultation with experts in quaternary geology and hydrogeology was used (Allmänna Ingenjörsbyrån AB 1950; Allmänna Ingenjörsbyrån AB 1976; Kjessler & Mannestråle AB 1990; Lång & Persson 2011; Ramböll Sverige AB 2007; Ramböll Sverige AB 2010; SGU 2004).

Based on the conceptual model a proper mathematical model that represents the situation was chosen. A numerical method was then selected for which the mathematical model was formulated. In this case the numerical model used was the finite differences method. The next step was to select a computer program that could handle the numerical model. The computer software selected was GMS 7.1 with the application MODFLOW (Aquaveo 2011a).

In the model design stage the conceptual model was translated to a numerical form in the computer program. This means that the conceptual stratigraphy was converted to a computational domain in the form of a mesh, for which the aquifer parameters, boundary conditions, and hydrologic stresses were allocated to. Also the initial water level was assigned during this stage.

The next step was model calibration. During calibration (also known as the Parameter Estimation Process) a fine tuning of the parameters was done in such way that the model was capable of simulating heads and fluxes that match the measured field values. The parameter estimation process was carried out by the calibration program PEST.

During the calibration, sensitivities of the calculated head with respect to the parameters and parameter correlation matrix was obtained. These statistical measurements among others (see Chapter 5 Model Calibration) were used as a support in deciding which parameters to use and to reveal improved calibration.

As the model was calibrated it was used in an interpretative sense as the study of the system dynamics. In this case the investigation of the system dynamics refers to the analysis of the capture zone that yields the water to the abstraction wells at Storehagen and the flow patterns in the aquifer.

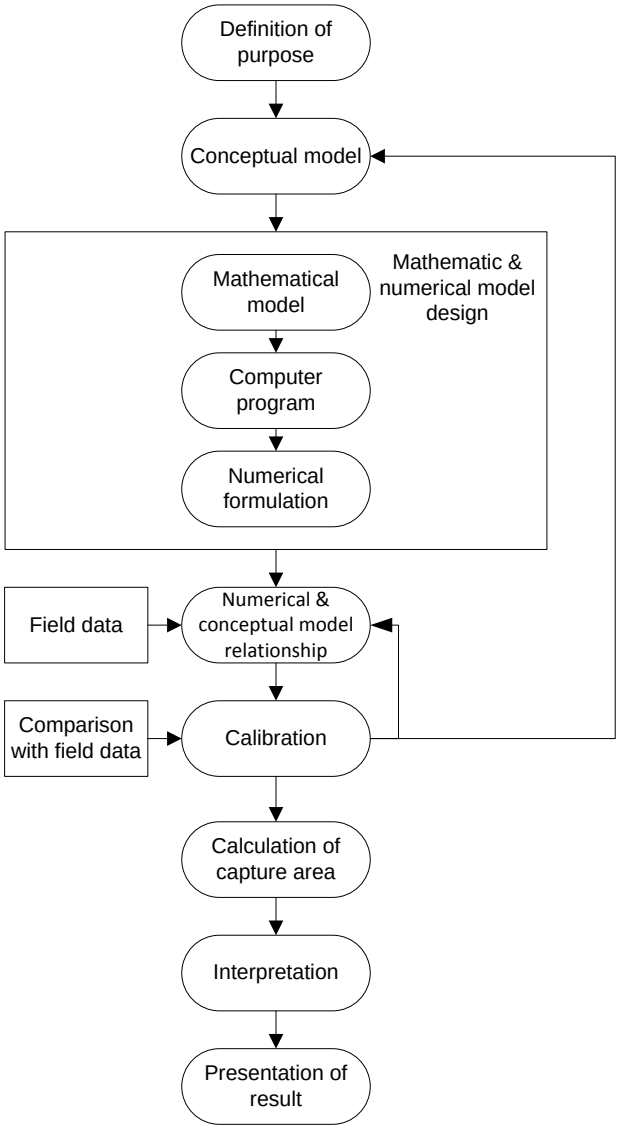

Figure 3.1 The modelling steps based on a proposal from Anderson and Woessner (1992).

3.2 Mathematical model

The mathematical model is based on the conceptual model and the intentions of the investigations. A full mathematical description of the model consists of the governing equation, boundary conditions and initial conditions (Anderson & Woessner 1992).

3.2.1 Dimensional approach

The governing equation was directly related to the dimensional approach used. If the hydraulic conductivity was approximated as uniform with depth, a two dimensional model might have been sufficiently enough. In a two dimensional model (2D model) the flow is thus assumed to be strictly horizontal. For a case of a 2D representation of a confined aquifer, the vertical flow through the confined bed can be calculated by the use of a leakage term. The leakage from above layers is proportional to the gradient, the thickness and the vertical conductivity of the confiding layer. The vertical head distribution is not calculated for a confined aquifer. The 2D approach is capable of

handling confined, unconfined, leaky-confined and mixed aquifers. Concerning the three dimensional approach, the vast difference is thus the ability to calculate the vertical head distribution within the aquifer. By using a three dimensional approach (3D approach) the hydraulic conductivity in all three directions is prescribed for the whole domain rather than identifying aquifers and confiding beds (Anderson & Woessner 1992).

It was concluded, in the formalization of the conceptual model, that the aquifer cold be considered as unconfined and the conductivity values of different layers were close to each other. The 3D approach was better suited to take account for this feature (Anderson & Woessner 1992).

A 3D approach is also a more a close description of the reality and the 3D approach was therefore used in this modelling.

Regarding the time dependency of the model two options is possible, transient or staedy state. Transient simulation is used when the model problem is assumed to be time dependent. Transient models differentiate from steady state models in that storage term and the initial condition has to be specifyed (Anderson & Woessner 1992).

Since the pumping rate at the pumping station of Storehagen has prevailed an almost uniform phase during some time and the river level is not varying that much a steady state model was found sufficient.

3.2.2 The governing equation

The governing equation can be derived by combining the equation of continuity with the constitutive relation Darcy's law (Anderson & Woessner 1992).

The equation of continuity can be obtained by applying the concept of elemental Cartesian fixed control volume, displayed in Figure 3.2, and the assumption that the fluid properties are considered to be uniform in time and space (White 2009).

In Figure 3.2 the flow in the y-direction, through the west and east side is shown. The area of the sides is denoted as $\Delta x \Delta z$, the inflow as $q_{y,in}$ and the outflow $q_{y,out}$.

The flow through the west side can be expressed as

$$q_{y,in} = v_{in} \rho \Delta x \Delta z \tag{3.1}$$

and the flow through the eastside as

$$q_{y_{out}} = \left(v_{in} + \frac{\partial v}{\partial y} \Delta y \right) \rho \Delta x \Delta z \tag{3.2}$$

where

υ is the fluid velocity in the *y*-direction and

ρ is the density of the fluid (assumed to be constant).

The change in flow between the east and west faces can be written as

$$q_{y,in} - q_{y,out} = \frac{\partial v}{\partial y} \rho \Delta y \Delta x \Delta z \tag{3.3}$$

Equations for the remaining directions could be formulated in a similar way (White 2009).

According to the conservation of mass principle a change in inflow and outflow should be equal to the change in storage within the control-volume.

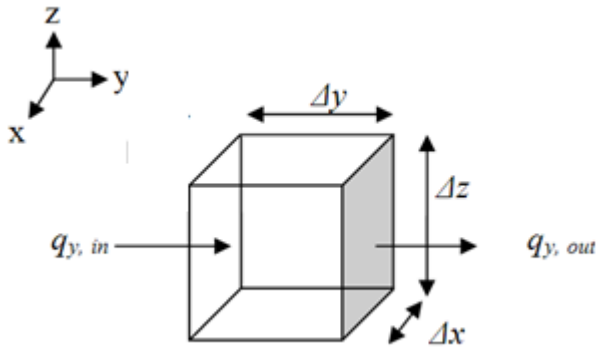

Figure 3.2 Consider a control volume, $\Delta V=\Delta x\Delta y\Delta z$, representing a cube of porous material.

The change in storage per unit change in head can be written as

$$S_s = -\frac{\Delta V_{fluid}}{\Delta h \Delta V_{storage}} \tag{3.4}$$

where

$$V_{storage} = \Delta x \Delta y \Delta z \tag{3.5}$$

A change in storage during a time, Δt, could be written as

$$\frac{\Delta V}{\Delta t} = S_s \frac{\Delta h}{\Delta t} \Delta x \Delta y \Delta z \tag{3.6}$$

Accounting for the remaining directions yields

$$\frac{\partial u}{\partial x}\rho\Delta x\Delta y\Delta z + \frac{\partial v}{\partial y}\rho\Delta x\Delta y\Delta z + \frac{\partial w}{\partial z}\rho\Delta x\Delta y\Delta z = -S_s \frac{\Delta h}{\Delta t}\Delta x\Delta y\Delta z \tag{3.7}$$

This can be simplified to

$$\frac{\partial u}{\partial x} + \frac{\partial v}{\partial y} + \frac{\partial w}{\partial z} = -S_s \frac{\Delta h}{\Delta t} \tag{3.8}$$

(Anderson & Woessner 1992)

The equation above is in Anderson and Woessner (1992) referred to as the water balance equation.

Darcy's law in three dimensions yields

$$u = -K_x \frac{\partial h}{\partial x} \tag{3.9}$$

$$v = -K_y \frac{\partial h}{\partial x} \tag{3.10}$$

$$w = -K_z \frac{\partial h}{\partial x} \tag{3.11}$$

Inserted in the continuity equation and allowing for possible internal sources and sinks, yields

$$\frac{\partial}{\partial x}\left(K_x \frac{\partial h}{\partial x}\right) + \frac{\partial}{\partial y}\left(K_y \frac{\partial h}{\partial x}\right) + \frac{\partial}{\partial z}\left(K_z \frac{\partial h}{\partial x}\right) + W = -S_s \frac{\Delta h}{\Delta t} \tag{3.12}$$

where W represents internal sinks and sources within an element. This is the governing equation for three dimensional movement of fluid in a heterogeneous and anisotropic porous media under non-equilibrium conditions (time-dependent conditions). It is further assumed that K_x, K_y and K_z are parallel to the principal coordinate directions (Kresic 2007). Under equilibrium conditions (steady-state conditions) the storage term in the equation above is set to zero (Harbaugh 2005).

3.3 Boundary conditions

Generally, three mathematical boundary conditions can be used to simulate hydrological boundaries, Dirichlet, Neumann and Cauchy conditions. In this context the Dirichlet condition represents a specified head boundary. The Neumann condition applies to the flow rate across a boundary, and could be used to prescribe an impermeable boundary. The Cauchy condition could be viewed as a mix of the Neumann and Dirichlet conditions in the sense that a flow across a boundary could be prescribed by a fixed head. Since the flow rate in the governing equation (which is based on the Darcy's law) is defined to be proportional to the derivative of the head, the use of only the Neumann condition would render a non-unique solution of the equation. Hence on at least one branch of the boundary the Dirichlet condition has to be used (Anderson & Woessner 1992).

3.4 Numerical model

The numerical method used is the finite difference method. Generally, in applications of the finite difference method the continuous domain in both time and space for which the governing equation is valid, is substituted by a discrete domain and the governing equation is described at these discrete points. The partial derivatives of the head with respect to the spatial and time dimensions can be calculated in the sense of differential calculus (Harbaugh 2005). Harbaugh (2005) uses instead a supplementary method based on the continuity equation. The description of the numerical model below follows that presented by Harbaugh (2005).

3.4.1 Background to MODFLOW

The numerical code MODFLOW is used to model the groundwater flow, using the finite difference approach. The first version of MODFLOW was developed between 1981 and 1983 and was aimed to solve the groundwater flow process (GWF) solely. Capabilities, like contaminant transport modelling and optimization were done in separate programs. In later versions however, all different capabilities were directly incorporated in the code. Different parts of the code that solves particular equations

were termed processes. Examples of the main processes are GWF, observation, sensitivity and parameter estimation-processes. The processes can be viewed as modules for which options are independent from each other. The processes can be divided into subroutines that can be used to construct either packages or procedures. A package can thus contain different procedures that when combined, treat a particular part of the simulation. A procedure can also be a part of different packages. Combination of packages is restricted by logical reasons, for example two solver packages cannot be combined (Harbaugh 2005).

3.4.2 The groundwater flow process

The groundwater flow (GWF) process and the procedures that build up the process in MODFLOW are illustrated in Figure 3.3. The process contains three nested loops, the stress loop, the time step loop and the iteration loop (also known as the outer iteration loop). The stress loop is used to proceed to different stress periods, the time step loop is used to advance in time, within a particular stress period and the iteration loop is used as a part of the solving technique for solving the flow equation at each time step. A stress period is defined as a period of time, in which the stresses are constant.

The *Allocate and read* (AR) procedure has a general function to setup the scheme. Examples of tasks are computation of conductivities for confined cells, number of cells in the grid and solution method. The *Read and prepare* (RP) procedure deals with information associated to a particular stress period. The *Advance in time* (AD) procedure calculates time step lengths etc.

The iteration loop contains the *Formulate* (FM) and *Approximate* (AP) procedures. Considering nonlinear problems like unconfined aquifers the horizontal conductance may change as the water table changes, thus in the *Formulate* (FM) procedure an updated conductance is calculated based on the precedent head level. In the *Approximate* (AP) procedure the head distribution for the nodes is calculated or approximated and the new head values is updated to the FM procedure, this loop carries on until convergence is met, according to convergence criteria. The convergence criteria used, are descried later in this chapter. The approach that the (FM) procedure utilize to compute the conductance is future described in the text, and for additional information readers may refer to (Harbaugh 2005).

Hydraulic conductance for confined cells is based on the conductivity and thickens of the confined layers. The confined layer thickness is assumed to be constant during the simulation, why these values can be calculated in the AR-procedure (Harbaugh 2005).

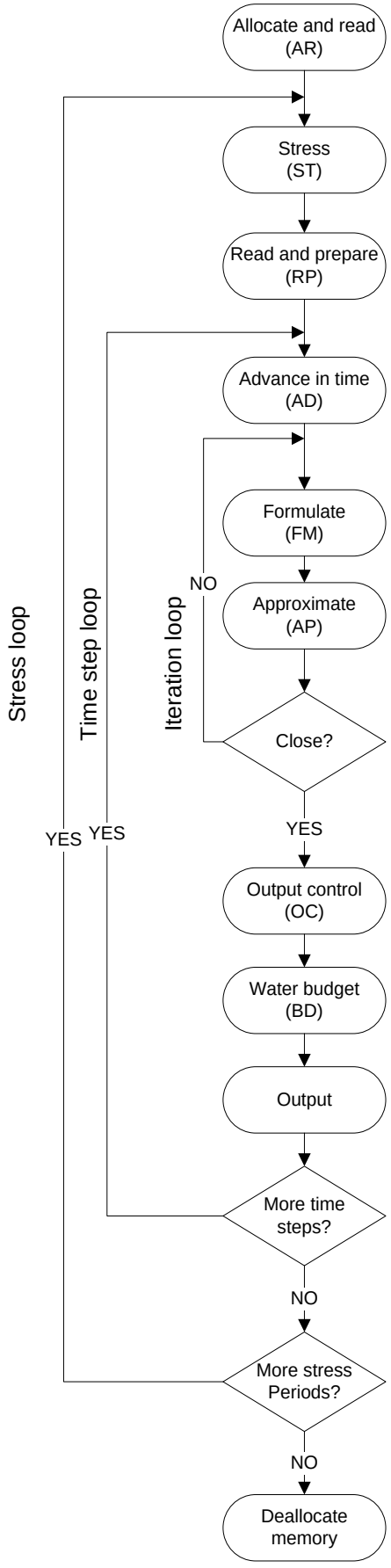

Figure 3.3 Flowchart of program to simulate groundwater flow (Harbaugh 2005).

3.4.3 MODFLOW packages

The GWF process can be constructed by so called packages. There are three different types of packages used; Basic package, Hydrological packages and Solver packages. The hydrological packages can further be divided in internal flow packages and stress packages, see Figure 3.4.

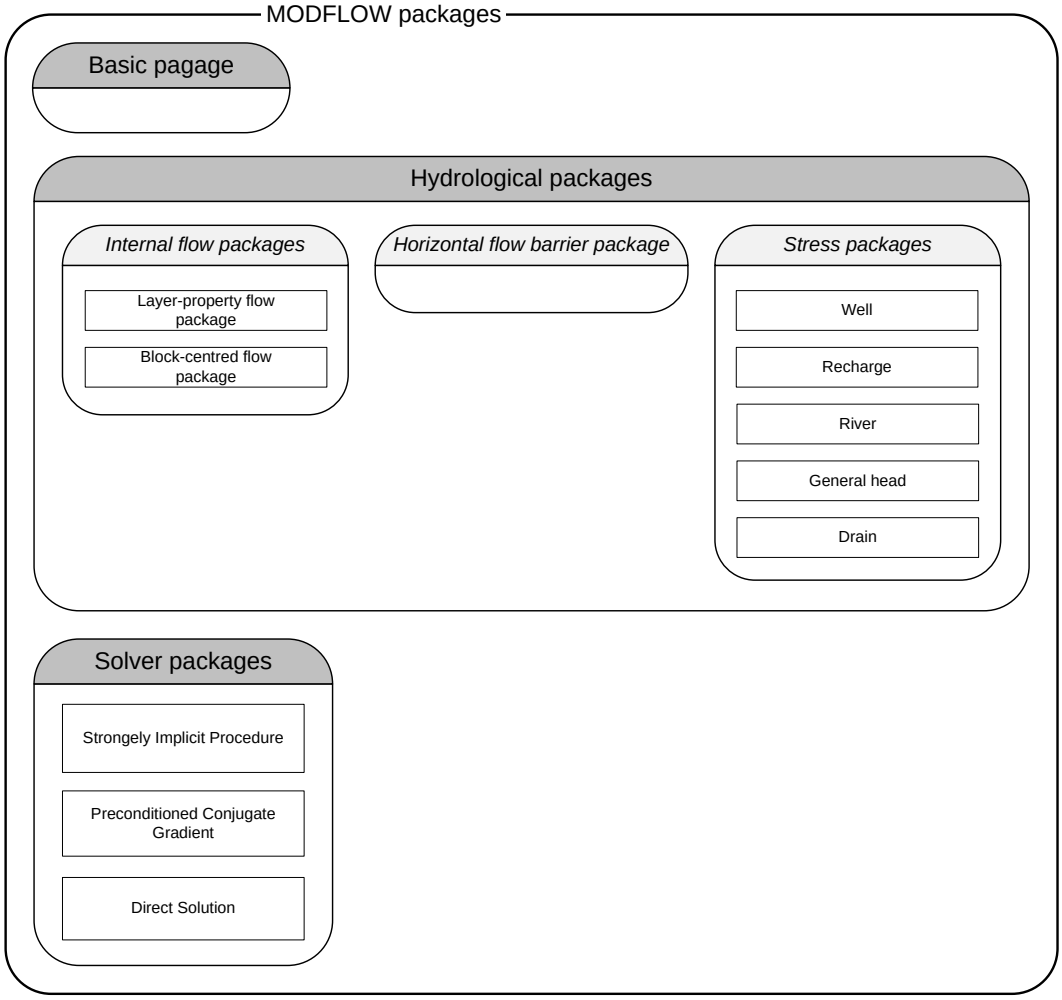

Figure 3.4 MODFLOW packages

The different package contains to some extent the same subroutines and it is possible to combine some packages, also those with the same subroutine. However not all combinations are possible. Two solver packages cannot be used at the same time and the same goes for the internal flow packages.

The basic package contains four procedures that are not represented in the others, that are the *Stress* (ST), *Advance in time* (AD), *Output control* (OC) and *Output* (OT) procedures. The basic package can hence be seen as a package that mainly treats administrative tasks. The function of the internal flow package is primarily to calculate and prescribe conductance terms.

The stress package can be seen as the part of the hydrological package that deals with the boundary conditions. The stress package contains primarily the five packages; *Well*, *Recharge*, *River*, *General head* and *Drain* package, displayed in Figure 3.4. The *General head* and the *River* package treat the same feature, but in a slight different

way. The *River* package was judged to be a more close representation of the true behaviour of a river, compared to the general head package, why it was used here. The other packages used in the modelling will be *Well*, *Recharge*, *General-head (*north and south boundary*)* and *Drain* packages. In the solver packages the numerical model is approximated. Three types of methods are generally possible, which are the *Strongly Implicit Procedure*, the *Preconditioned Conjugate Gradient* and the *Direct solution*. The solver packages represent primary the approximate (AP) subroutine, however the FM procedure is invoked during the solution process of a nonlinear problem.

3.4.4 Numerical formulation

3.4.4.1 Spatial discretization

The technique used here to discretize the spatial domain, is called the block-centred formulation. The approach bases on that a continuous domain is divided in to blocks, also called cells. The function is then formulated at the centre of each cell, i.e. at the node of the cell. The discretization could also be done by application of the mesh-centred grid technique. The difference between the methods is primarily in how the boundaries are formulated. The formulation of boundaries is seen to be easier to handle by using block-centred formulation (Anderson & Woessner 1992). The discretization teqnicue precented here follovs the block centered formulation, which also is the method that MODFLOW uses.

When formulating the model on the discritized domain, an underpinning assumption is that the shape of the grid is rectangular both vertically and horizontally. Altough MODFLOW allows vertical disortion of the grid, the transmisivity is still seen as either constant whithin a cell or linearly varying between two adjencent nodes (Harbaugh 2005).

The discretized concontinuity equation, assuming constant density, of the fluid states that

$$\sum Q_i = S_s \frac{\Delta h}{\Delta t} \Delta V \tag{3.13}$$

where

Q_i is flow rate into a cell [m^3/s]

S_s is the specific storage coefficient [1/m]

ΔV is the volume of the cell [m^3]

Δh is the change in head [m] over the time interval Δt *[s]*

Consider a cell surrounded by cells at each face. If the cell in the center is denoted *i,j,k* where *i* is the row index, *j* is the collum index and *k* layer index, the six surrounding cells could be denoted as (assuming that the row and cloumn directions conicide with the principial cardinal directions)

the cell next to the north side *i-1,j,k*

the cell next to the south side *i+1,j,k*

the cell next to the west side *i,j-1,k*

the cell next to the east side *i,j+1,k*

the cell nest to the upper side *i,j,k-1*

the cell nex to the bottom side *i,j,k+1*

The flow to into the middle cell can be described by using one dimensional Darcy's law between all the adjacent cells and the middle cell. The flow from the north cell into the middle is described below

$$q_{i,j-1,k\to i,j,k} = K_{i,j-1,k\to i,j,k}\Delta c_i \Delta v_k \left(\frac{h_{i,j-1,k} - h_{i,j,k}}{\Delta r_{i,j-1,k\to i,j,k}} \right) \tag{3.14}$$

where

$h_{i,j,k}$ is the head at node in the middle cell, similar for the north cell

$q_{i,j,k}$ is the flow between the middle and north node

$K_{i,j-1,k\to i,j,k}$ is the hydraulic conductivity between the middle and north node

$\Delta c_i \, \Delta v_k$ is the cell cross-sectional area normal to the flow direction

$\Delta r_{i,j-1,k\to i,j,k}$ is the distance between the north and middle node.

The flow from the remaining cells is described in a similar way. The Darcy's laws can be rewritten by lumping together the hydraulic conductivity between the middle cell and one adjacent cell, the cell cross-sectional area between the two cells and the distance between the two cells into a single term known as conductance.

In order to model boundary conditions and stresses, additional terms has to be included in the discredited continuity equation. Assuming that the flow in to a cell either can be stated solely or as a linear function of the head the following expression holds

$$\sum_{n=1}^{N} a_{i,j,k,n} = \sum_{n=1}^{N} p_{i,j,k,n} h_{i,j,k} + \sum_{n=1}^{N} q_{i,j,k,n} \tag{3.15}$$

where

N represents the number of sources yielding fluid to cell *i,j,k*

$p_{i,j,k,n}$ and $q_{i,j,k,n}$ are constants

$a_{i,j,k,n}$ represents the flow to the middle cell from source n

$h_{i,j,k,}$ is the head in the middle cell node.

If the discretized groundwater flow equation now is formulated considering the flow into the centred cell from the neighbouring cells, the finite approximation for cell *i,j,k,* yields as follows

$$\begin{aligned} &C_{i,j-1,k\to i,j,k}\left(h_{i,j-1,k} - h_{i,j,k}\right) + C_{i,j+1,k\to i,j,k}\left(h_{i,j+1,k} - h_{i,j,k}\right) + \\ &C_{i-1,j,k\to i,j,k}\left(h_{i-1,j,k} - h_{i,j,k}\right) + C_{i+1,j,k\to i,j,k}\left(h_{i+1,j,k} - h_{i,j,k}\right) + \\ &C_{i,j,k-1\to i,j,k}\left(h_{i,j,k-1} - h_{i,j,k}\right) + C_{i,j,k+1\to i,j,k}\left(h_{i,j,k+1} - h_{i,j,k}\right) + \\ &P_{i,j,k} h_{i,j,k} + Q_{i,j,k} = SS_{i,j,k}\left(\Delta r_j \Delta c_i \Delta v_k\right)\frac{\Delta h_{i,j,k}}{\Delta t} \end{aligned} \tag{3.16}$$

where

$$P_{i,j,k} = \sum_{n=1}^{N} p_{i,j,k,n} \tag{3.17}$$

and

$$Q_{i,j,k} = \sum_{n=1}^{N} q_{i,j,k,n} \tag{3.18}$$

(Harbaugh 2005)

3.4.4.2 Discretization of time

Discretization means the transformation of a continuous domain into a set of discrete points and the reformulation of the governing equations at those points. Here this was done for the time dimension instead of the spatial dimension. The technique used in MODFLOW is the backward difference approach, which is unconditionally stable. Compared to the backward difference approach a forward technique is unstable which means that once an error is introduced, there is a risk that the errors grow and propagate during the solution process (Harbaugh 2005).

In the backward differential approach the derivative of the head with respect to time is calculated based on the head distribution at the nodes for two succesive time steps, where one of the head distributions is determined from a previous soulution of the equation. The soulution method is thus an itterative process, and therefore demands an initial head distribution (Harbaugh 2005).

The time derivative of the head is approximated as follows

$$\frac{\Delta h_{i,j,k}}{\Delta t} \approx \frac{h^{m}_{i,j,k} - h^{m-1}_{i,j,k}}{t^{m} - t^{m-1}} \tag{3.19}$$

where

t^m denotes the time at which the solution is evaluated

t^{m-1} denotes the time prior to time t^m

$h^m{}_{i,j,k}$ is the head in node i,j,k at time t^m

$h^{m-1}{}_{i,j,k}$ is the head in node i,j,k at time t^{m-1}

Applying the backward-difference technique to the discretized groundwater flow equation yields

$$\begin{aligned} &C_{i,j-1,k\to i,j,k}\left(h^{m}{}_{i,j-1,k} - h^{m}{}_{i,j,k}\right) + C_{i,j+1,k\to i,j,k}\left(h^{m}{}_{i,j+1,k} - h^{m}{}_{i,j,k}\right) + \\ &C_{i-1,j,k\to i,j,k}\left(h^{m}{}_{i-1,j,k} - h_{i,j,k}\right) + C_{i+1,j,k\to i,j,k}\left(h^{m}{}_{i+1,j,k} - h^{m}{}_{i,j,k}\right) + \\ &C_{i,j,k-1\to i,j,k}\left(h^{m}{}_{i,j,k-1} - h^{m}{}_{i,j,k}\right) + C_{i,j,k+1\to i,j,k}\left(h^{m}{}_{i,j,k+1} - h^{m}{}_{i,j,k}\right) + \\ &P_{i,j,k}h^{m}{}_{i,j,k} + Q_{i,j,k} = SS_{i,j,k}\left(\Delta r_j \Delta c_i \Delta v_k\right)\frac{h^{m}_{i,j,k} - h^{m-1}_{i,j,k}}{t^{m} - t^{m-1}} \end{aligned} \tag{3.20}$$

To solve this equation for all nodes in the domain, it is reformulated. This is done by grouping all coefficients that is associated to a specific node, together.

$$
\begin{aligned}
&C_{i,j-1,k\to i,j,k}h^{m}{}_{i,j-1,k} + C_{i,j+1,k\to i,j,k}h^{m}{}_{i,j+1,k} + \\
&C_{i-1,j,k\to i,j,k}h^{m}{}_{i-1,j,k} + C_{i+1,j,k\to i,j,k}h^{m}{}_{i+1,j,k} + \\
&C_{i,j,k-1\to i,j,k}h^{m}{}_{i,j-1,k} + C_{i,j,k+1\to i,j,k}h^{m}{}_{i,j,k+1} - \\
&\left(\begin{array}{l}
C_{i,j-1,k\to i,j,k} + C_{i,j+1,k\to i,j,k} + C_{i-1,j,k\to i,j,k} + \\
C_{i+1,j,k\to i,j,k} + C_{i,j,k-1\to i,j,k} + C_{i,j,k+1\to i,j,k} + \\
\left(P_{i,j,k} + \dfrac{S_{s\,i,j,k}\left(\Delta r_j \Delta c_i \Delta v_k\right)}{t^{m} - t^{m-1}}\right)
\end{array}\right) h^{m}{}_{i,j,k} \\
&= -Q_{i,j,k} - S_{s,i,j,k}\left(\Delta r_j \Delta c_i \Delta v_k\right)\frac{h^{m-1}_{i,j,k}}{t^{m} - t^{m-1}}
\end{aligned}
\tag{3.21}
$$

(Harbaugh 2005)

Accounting for each node in the spatial domain a system of equations emerges and could be formulated as

$$\underline{\underline{A}}\underline{h} = \underline{q} \tag{3.22}$$

where

$\underline{\underline{A}}$ is the coefficient matrix

$\underline{h}$ is the head values vector

$\underline{q}$ is a vector containing constant terms like the constant flow terms from boundary or stress sources etc.

The solution technique of solving for the head distribution at each time step, differ between the solvers packages. Nevertheless they all rely on the iteration technique meaning that an initial head distribution has to be supplied regardless of whether the problem to be solved is transient or at steady state. The equation (3.21) above is formulated for each node in the domain, and at arbitrary node the head is calculated based on the precursor heads in the surrounding nodes. The calculation is done for all the nodes in the domain and a new head distribution is obtained. With the updated head distribution this process can continue, thus successive improving the head distribution to be more close to the head distribution that satisfies the system of equation (3.22). Each cycle of calculations through the computational domain is here referred to iteration. The iteration procedure terminate when a convergence criteria is met and the solution is said to have converged. One example of convergence criteria is the difference in head change between two successive iterations.

In MODFLOW the simulation of a steady state problem is achieved by only using a single time step with in a single stress period and with the prescription of the storage term to zero.

3.4.4.3 Conductance

The conductance terms are among other features like storage flow and cell drying-rewetting are treated in the internal flow packages (Harbaugh 2005). The internal flow package that was used here was the Layer-property flow package (LPF-package). The reason why Layer-property flow package (LPF-package) was used was because that the Block-centred flow package (BCF-package) not supports the parameter estimation process (Aquaveo 2009a). Principles of how the conductance terms are treated in the LPF-package are given in the text below.

In the LPF-package two possible options on how the layers should be treated are presented, i.e. confined or convertible, this compared to the BCF-package where four options are available. The main difference between the confined and convertible option is whether the transmissivity is constant during simulation or not, which type of storage term to be used, the possibility of drying and rewetting of the cells and vertical flow correction. In the convertible option the transmissivity of the cells is allowed to change during simulation, the storage is formulated as a combination of the specific yield and specific storage, the cell drying and cell wetting is possible and vertical flow correction is possible. In the confined option the transmissivity is constant throughout the simulation, the storage is formulated as specific storage and no drying and wetting of cells is possible etc. (Harbaugh 2005).

In the system of equations representing the discretized flow equation, the conductance is prescribed between nodes of neighbouring cells. This formulation of the conductance is referred to in MODFLOW as branch conductance. Generally, in the internal flow packages, these values of conductance are calculated based on conductivity and dimensions for specific cells. There is however different approaches present in the internal flow packages on how these calculations are carried out. The methods used in the LPF-package, to calculate the horizontal conductances are denoted the logarithmic-mean interblock transmissivity method, the arithmetic-mean thickness and logarithmic-mean hydraulic conductivity method and the harmonic mean method. Here the harmonic mean method was used. The harmonic mean method is based on the assumption that the transmissivity is constant throughout a cell, this in contrast to the other methods, for which it is assumed that the transmissivity and the conductivity, varies linearly between the nodes (Harbaugh 2005).

The formulation for vertical conductance is similar to the harmonic mean method for calculating the horizontal conductance. Unlike the formulations for the horizontal flow, there are however some additional features related to the vertical flow that has to be accounted for, see below (Harbaugh 2005).

The hydraulic conductance for a single cell can be defined as

$$C = \frac{KA}{L} \tag{3.23}$$

or as

$$C = \frac{TW}{L} \tag{3.24}$$

where

K is the conductivity of the material in the flow direction [m/T]

A is the cross-sectional are perpendicular to the flow direction [m^2]

L is the length of the cell [m]

T is the transitivity in the flow direction [m^2/T]

W is the cell width [m]

Generally in the LPF package the horizontal transmissivity for a cell is calculated as

$$T = \Delta v K \tag{3.25}$$

For a confined cell the Δv is the thickness of a cell, whether in the case of an unconfined cell Δv is the saturated thickness of a cell. In MODFLOW the subsequent scheme is used to calculate the saturated thickness under unconfined. The term convertible layer is in MODFLOW synonymous to the term unconfined.

$$\begin{aligned}
&if \quad h^{new}_{i,j,k} \geq h^{top}{}_{i,j,k} && \xrightarrow{then} && \Delta v_{i,j,k} = h^{top}{}_{i,j,k} - h^{bot}{}_{i,j,k} \\
&if \quad h^{top}{}_{i,j,k} > h^{new}_{i,j,k} > h^{top}{}_{i,j,k} && \xrightarrow{then} && \Delta v_{i,j,k} = h^{new}_{i,j,k} - h^{bot}{}_{i,j,k} \\
&if \quad h^{new}_{i,j,k} \leq h^{bot}{}_{i,j,k} && \xrightarrow{then} && \Delta v_{i,j,k} = 0
\end{aligned} \tag{3.26}$$

where

$h^{new}{}_{i,j,k}$ is the head calculated in the most recent iteration

$h^{top}{}_{i,j,k}$ is the top elevation in the cell i,j,k

$h^{bot}{}_{i,j,k}$ is the bottom elevation in the cell i,j,k (Harbaugh 2005).

Using the convertible option (in which the transmissivity is allowed to vary with the head stage) it could be that the water level drops below the bottom elevation of some cell. When this is the case, the cell is prescribed as dry in MODFLOW. During the solution process as the water table fluctuates, the water table in a cell below a cell that recently was prescribed to dry can become higher than the boundary level towards the uppermost cell. Under situations like this, the possibility of rewetting of the dry cell has to be accounted for.

MODFLOW poses two alternatives to wetting a cell for the LPF-package and the BCF-package, either when the head in adjacent cells in the same plane surpass a given value (so called threshold), or if the head goes beyond a given value of the cell beneath. The thresholds are to be determined by trial and error to obtain a well-functioning model. Too high values might render a more non unique solution and to small might cause in oscillations between wetting and drying. For the same reason (oscillations) carefulness should also be taken when the initial estimate of the water table is prescribed. One method that MODFLOW offers to deal with the oscillations is to convert a cell to wet only at specific iteration intervals. Interested readers are referred to (Harbaugh 2005) for additional details.

Consider a series of two cells parallel to the direction of the flow, the equivalent conductance for the whole series can be calculated as

$$C_{a \to b} = \frac{c_a c_b}{c_a + c_b} \tag{3.27}$$

where

C is the equivalent conductance

c_a and c_b are the conductance for two arbitrary cells respectively.

(Harbaugh 2005)

The derivation of the harmonic-mean method is underpinned by two assumptions; the nodes are at the centre and the transmissivity is uniformed in the interior of the cells. If c_a and c_b in the equation above are replaced by the formula for the conductance given in (2.25), considering that (2.25) now represents a half cell, the following equation for the equivalent conductance between two adjacent cells can be written as

$$C_{a\to b} = \frac{\left(\frac{TW}{\frac{1}{2}L}\right)_a \left(\frac{TW}{\frac{1}{2}L}\right)_b}{\left(\frac{TW}{\frac{1}{2}L}\right)_a + \left(\frac{TW}{\frac{1}{2}L}\right)_b} \tag{3.28}$$

The general formula for which the vertical conductivity is calculated is derived by inserting (2.24) in the inverse off (2.28) giving that

$$\frac{1}{C_{a\to b}} = \frac{1}{\left(\frac{KA}{\frac{1}{2}L}\right)_a} + \frac{1}{\left(\frac{KA}{\frac{1}{2}L}\right)_b} \tag{3.29}$$

Denoting $A = \Delta r \Delta c$ and $L = \Delta v$ the formula above could be simplified as

$$C_{a\to b} = \frac{2\Delta r \Delta c}{\left(\frac{\Delta v}{K}\right)_a + \left(\frac{\Delta v}{K}\right)_b} \tag{3.30}$$

Considering the vertical flow between two cells, a situation can emerge for which the bottommost cell becomes unconfined whereas the topmost cell become still is saturated. Under a situation like this the flow downward is no longer dependent on the head stage in the bottommost cell. Substituting the head stage in the bottommost cell with the level of the bottommost top face, in the equation (2.22), render the matrix asymmetric. MODFLOW instead adds corrections terms based on the head stage in the topmost cell at the precedent iteration and the level of the bottommost top face to the two affected cells (Harbaugh 2005).

3.4.4.4 Well

Abstraction or injection in a well could be seen as a point source or sink. High gradients are naturally likely to occur close to this type of feature. In finite differences a point source or sink is represented by the cell for which the point source or sink is located to. This way of treating the point sources and sinks render a poor approximation of the head in the vicinity of the well (Anderson & Woessner 1992).

Mesh refinement may be needed around a well in order to treat the steep gradients in more proper way. However it should be noticed that the finite difference expression for an irregular mesh only is correct to the first order (Anderson & Woessner 1992). Under quasi steady state conditions the Thiem-equation based on the computed head in the cell and the effective well block radius can be used to give a better estimate of the head in the well (Anderson & Woessner 1992).

In MODFLOW the abstraction or recharge to a well is prescribed in Q in the discretized flow equation. A negative value represents abstraction (Harbaugh 2005).

3.4.4.5 Recharge

The type of recharge handled with this package was the areal recharge due to precipitation. The recharge cannot be applied to more than one cell in a column at the same time. The recharge flow rate from a cell is calculated as precipitation rate over a cell times the cell area. The recharge flow rate from the cells is added to the flow term Q in the discretized flow equation (Harbaugh 2005).

3.4.4.6 River

The river package is aimed to treat seepage back and forth between a river and an aquifer. The way this is implemented is underpinned by the assumptions that the cells below the riverbed are saturated, only the riverbed yields the head losses and the river stage is uniform and constant in every stress period. The flow through the riverbed is calculated as

$$\begin{aligned} Q_{river,n\to i,j,k} &= C_{riverbed,n}\left(h_{river} - h_{i,j,k}\right) && h_{i,j,k} > h_{riverbottom} \\ Q_{river,n\to i,j,k} &= C_{riverbed,n}\left(h_{river} - h_{riverbottom}\right) && h_{i,j,k} \le h_{riverbottom} \end{aligned} \tag{3.31}$$

where

$$C_{riverbed,n} = \left(\frac{K \cdot L \cdot W}{M}\right)_n \tag{3.32}$$

and

K is the hydraulic conductivity of the riverbed in cell n

L is the length of the riverbed in the cell n

W is the width of the river in cell n

M is the thickness of the riverbed in cell n

Thus when the head in the aquifer exceeds the river stage, the aquifer yields water to the river. The flow to the aquifer varies linearly as the head in the aquifer is located between the bottom of the river and the river level. When the head in the aquifer is lower than the river bottom the flow is set to be constant. The seepage from each cell that contains a river segment are added or subtracted to the Q term in the discretized flow equation depending on the direction of the flow (Harbaugh 2005).

Since the river package is not intended to simulate the flow in the river and the river level is assumed to be constant (Harbaugh 2005), there is a potential risk that the simulated seepage to the aquifer is greater than actual amount of water which is being conveyed in the river (Anderson & Woessner 1992). Nevertheless it was here

assumed that the abstraction rate from the wells is much less than the amount of water conveyed by the river, and will therefore not affect the river level.

3.4.4.7 Drain

The drain package is aimed to simulate abstraction only. This situation is typical for ditches, small creeks or drains. The abstraction is calculated as the difference between computed head and the drain elevation multiplied with a lumped conductance (Harbaugh 2005).

$$\begin{aligned} Q_{i,j,k\rightarrow drain,n} &= C_{drain,n}\left(h_{drain} - h_{i,j,k}\right) && h_{i,j,k} > h_{drainbottom} \\ Q_{i,j,k\rightarrow drain,n} &= 0 && h_{i,j,k} < h_{drainbottom} \end{aligned} \tag{3.33}$$

The drain conductance can be difficult to measure and is therefore often adjusted during model calibration (Harbaugh 2005).

3.4.5 The solver used

The solver used was the Preconditioned Conjugate-Gradient package (PCG package). This solver uses both inner and outer iterations. The outer iterations invoke the loop containing the FM and the AP procedure, and it is in this loop the account is taken to nonlinear terms that emerge for an unconfined aquifer. The inner iteration loop is allocated within the AP procedure and is used to calculate the interim head stage for some user supplied number of iterations between the loops through the FM procedure in which the transmissivity terms may change. Harbaugh (2005) recommended that a number of 20 or more inner iterations and five or more outer iterations should be used when to solve non-linear problems. Regarding convergence criteria the PCG-package uses bout head-change and residual criteria. The head change criteria states that the iteration procedure has to continue until the maximum head change, regarding all cells, between two successive iterations is less than a user supplied value. The residual criterion is referring to the flow difference between cells. If the maximum difference between, regarding all the cells, is less than a specific amount prescribed by the user the solution is said to have converged. However it should be noticed that both the criteria should be met in order for the solution to converge. The process terminates without having converged if convergence not has been accomplished within the number of user supplied amount of iterations (Harbaugh 2005).

3.5 Description of MODPATH

Based on a MODFLOW solution of the flow equation, the post processing program MODPATH is able to do a particle tracing procedure. Here the capture area was calculated via MODPATH. The following text follows what is described by Pollock (1994).

MODPATH evaluate the particle tracking on a cell to cell basis, meaning that the starting location for the particle at its intercellular journey is equal to the exit location for a previously passed cell. In order for MODPATH to execute the tracing the velocity field and the very first starting locations of the fictive particle has to be assigned.

In MODPATH the intercellular velocity field is approximated as described below.

The solution or approximation of the flow equation yields a distribution of heads calculated at the cell nodes. When the head distribution is obtained, the flow a cross each of the cell boundaries is evaluated using the Darcy's law. Based on these flow rates, the fluid velocity at each of the cell faces can be calculated. Considering the velocity at one of the cell faces in the x-direction, the velocity at cell face *x1* is calculated as

$$u_{face,x1} = \frac{q_{face,x1}}{n\Delta A_{face,x1}} \tag{3.34}$$

where

n is the porosity

$q_{face,x1}$ is the flow rate across the cell face *x1*

$\Delta A_{face,x1}$ is the area of the cell face *x1* at which the flow rate is evaluated

The velocities at the remaining cell faces are calculated in a similar way.

Based on the velocity at the faces MODPATH uses linear interpolation to produce a "continuous" velocity field within the cells. The internal velocity in the x-direction is calculated as

$$u_x = G_x(x - x_{face,x1}) + u_{face,x1} \tag{3.35}$$

where

G_x represents the velocity gradient within the cell and is evaluated as

$$G_x = \frac{u_{face,x2} - u_{face,x1}}{\Delta x} \tag{3.36}$$

The interpolation scheme presented above is carried out in a similar way for the remaining directions.

The location of the particles at different times can be evaluated by integrating the particle acceleration in order to achieve the particle velocity as a function of time. If now the velocity obtained by the integration of the particle acceleration is substituted with the interpolation scheme described above, a function of the particle location with respect to the velocity gradients, the velocity at the particle entrance cell face, the location of this cell face, the time of travel and the velocity at the initial location of the particle, the particle location can be obtained. The procedure is further described below (Pollock 1994).

The acceleration of a particle in the x-direction at the particle location *p* can be evaluated as

$$\left.\frac{\partial u_x}{\partial t}\right|_p = \frac{\partial u_x}{\partial x} \cdot \left.\frac{\partial x}{\partial t}\right|_p \tag{3.37}$$

Analytical integration yields

$$\ln\left(\frac{u_x(t_2)\big|_p}{u_x(t_1)\big|_p}\right) = G_x \Delta t \tag{3.38}$$

The particle velocity evaluated after a time step Δt is then formulated as

$$u_x(t_2)\big|_p = u_x(t_1)\big|_p e^{G_x \Delta t} \tag{3.39}$$

This can be reorganized to

$$x(t_2)\big|_p = \frac{u_x(t_1)\big|_p e^{G_x \Delta t} - u_{face,x1}}{G_x} + x_{face,x1} \tag{3.40}$$

After first identifying that

$$u_x(t_2)\big|_p = G_x(x - x_{face,x1}) + u_{face,x1} \tag{3.41}$$

The above is comparable for the other directions.

In a three dimensional case the determination of the particle exit location is done by first evaluating the exit face. The possible time needed for the particle to reach each and every one of the probable exit faces is computed and the direction that constitutes the shortest time determines the exit face. Once this time is calculated it is used in the equations for the particle location in order to calculate the exact location at this face. This location serves then the purpose as a starting location for the successive cell for which the particle enters. To calculate the capture zone, the theory as described above is still used with the exception that all velocities now are multiplied by -1 (Pollock 1994).

4 Integration of Numerical and Conceptual Models

4.1 Hydrogeological units

As concluded in Chapter 2, the aquifer was initially characterized by four types of hydrogeological units which were assumed to be approximately distributed on five horizons. These hydrogeological units were then assumed to correspond to different materials namely sand, silt, clay and till. The classification was based on the notations in the borehole protocols, see Appendix 6.

However, during the model calibration it was concluded that the layers of silt and clay most likely are not continuous. Therefore the hydrogeological units within these layers were assigned higher conductivity values than normal for silt and clay.

A solid which aimed to describe the geology in the aquifer in a conceptual fashion was constructed from the borehole data. The solid was then used to allocate the height, bottom and location of the hydrogeological units to the finite element mesh.

MODFLOW provides different options to translate the solid to the grid. Here the mesh was constructed by using the so called boundary matching option. The boundary matching option assigns the location of the layers in a way that the layer follows the stratigraphic units as closely as possible (Aquaveo 2009b). This option renders different heights of the layers within each column depending on the vertical expansion of the hydrogeological units, see example in Figure 4.1.

At a number of locations in the domain, the solid was very thin (<0.2 m). To circumvent the creation of very thin layer a minimum thickness were assigned to 0.2 m. If a layer then was thinner than 0.2 m MODFLOW prescribed the surrounding material instead (Aquaveo 2009b).

Figure 4.1 Cross section to illustrate the different thicknesses of the horizontal layers.

4.2 Grid settings

According to the orientation of the grid, the horizontal plane was aligned in a SW-NE direction, since the aquifer mainly is extended in this direction, see Figure 4.2. The governing equation is underpinned by the assumption that the principal directions of the hydraulic conductivity tensor are coincident with the coordinate axis of the model (Anderson & Woessner 1992). This assumption may be true at the central parts of the domain but not at some parts near the boundaries.

The size of the grid was determined so the natural boundaries would match the model boundaries. Meaning that aim was to assign boundaries as either no flux boundary (Neumann condition) or as specified head boundaries (Dirichlet conditions).

Concerning the discretization in the horizontal directions, the cell width and length were assigned to be constant to a value of 10x10 m throughout the domain. The grid

size in the horizontal plane was prescribed by trial and error and was a compromise between model accuracy and computational time.

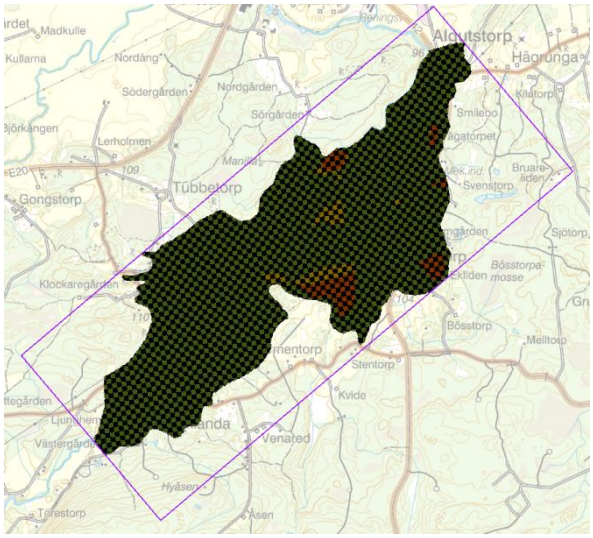

Figure 4.2 Orientation and spatial extent of the grid

4.3 Hydraulic boundaries

According to Anderson and Woessner (1992) the selection of proper boundaries is one of the most crucial parts in a steady state modelling survey.

Regarding the selection of the boundaries, Anderson and Woessner (1992) suggest that a contrast in hydraulic conductivity of a factor of 100 between two materials may serve as a no-flow boundary. Their motivation is that the high contrast in the conductivity between the layers deflects the flow lines from being almost vertical in the low conductivity material to almost horizontal in the highly permeable material. Considering the specified head boundary condition Anderson and Woessner (1992) recommend the allocation of this boundary condition to coincide with features like rivers.

In this study only no-flow and specified head boundary conditions were used. Along the horizontal perimeter of the aquifer the no-flow conditions were assigned to represent the margin between the aquifer and regions consisting of till or bedrock. This was done since it was anticipated that the difference in magnitude of the hydraulic conductivity between the till and the glaciofluvial deposit and between the bedrock and the glaciofluvial deposit was equal to or higher than two orders of magnitude.

The no-flow condition was assigned to the northwest side of the aquifer between Sörgården and Ljunghem and at the southeast boundary between the Västergården and Algutstorp.

The specified head condition was applied along the Säve River, the stream Torsjöbäcken (passing through Ormentorp) and the stream that passes through Algutstorp water treatment plant.

The specified head condition was also used as a boundary condition across the aquifer along the southwest boundary between Ljunghem and Västergården and along the

north boundary that lies between Algutstorp and Tånga Hed. However it should be pointed out that this was an assumption. Due to this reason, the length of these boundaries was assigned as short as possible. The allocation of the specified head condition was motivated by that earlier model runs indicated that the head contours were parallel to these boundaries. The boundary conditions could be seen in Figure 4.3.

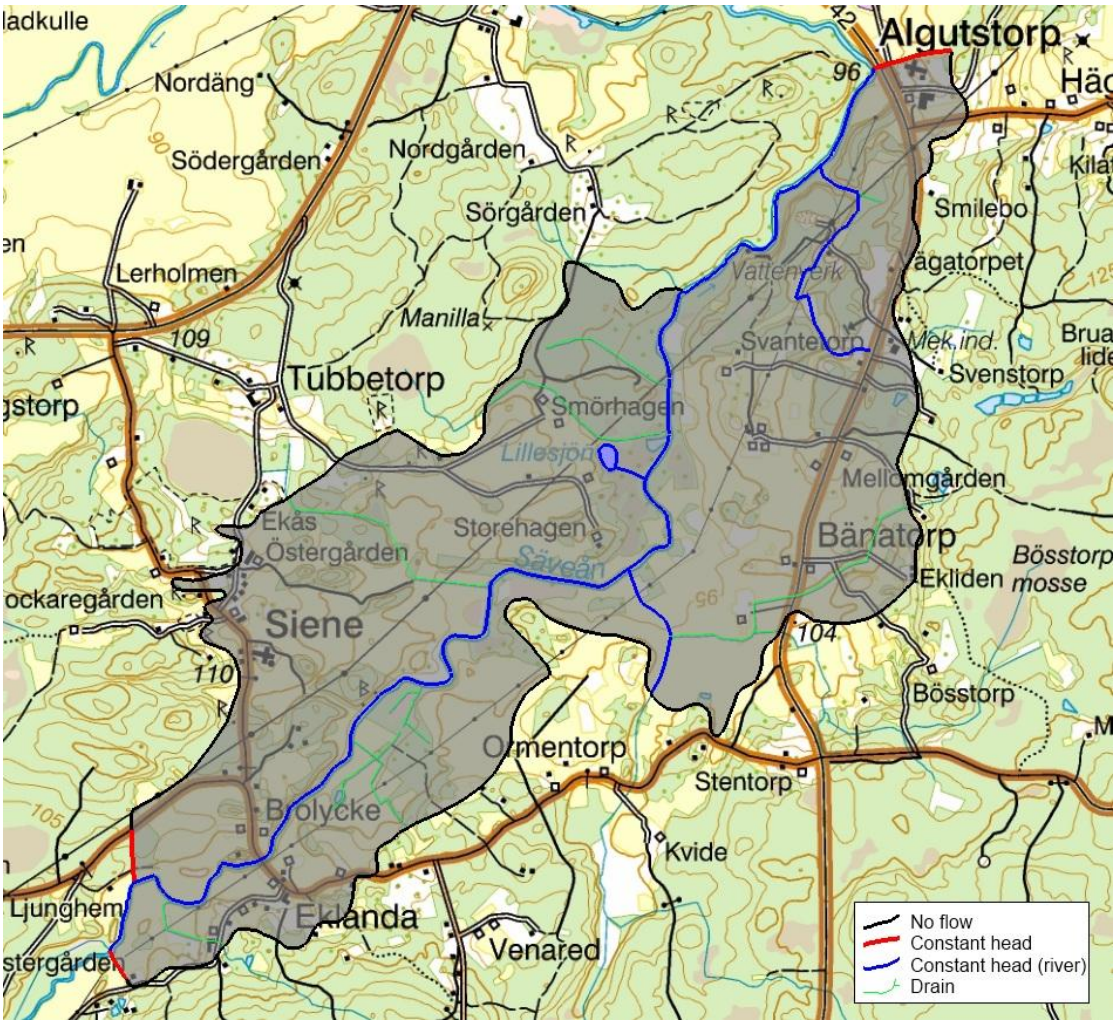

Figure 4.3 *Boundaries for the modelled part of the aquifer. © Lantmäteriet Gävle 2011. Consent I 2011/0072.*

Vertically, the aquifer domain was bounded by the water table and the boundary towards the bedrock.

The topography of the aquifer area was obtained from Digitala Kartbiblioteket (2011) and was consisted of measurements at a spacing of fifty meters. A Triangulated Irregular Network (TIN) representing the surface was constructed by linear interpolation of the measurements.

The bottom boundary of the glaciofluvial deposit was interpolated from borehole data. At the perimeter of the modelled area the borehole data was scarcer. But since the soil map showed bedrock at the surface at these locations, the boundary of the model was

given a depth of three meters. The bottom depth was then interpolated to a TIN with the interpolation method Clough-Toucher.

4.4 Initial hydraulic conductivity

It was concluded in Chapter 2 that the difference between the mean conductivity calculated from the aquifer analysis and from Hazen's formula was rather small. Since the conductivity calculated by Hazen's formula represents a somewhat coarse material, the small difference may indicate that the rest of the material also has a relatively high conductivity or that the layers of silt and clay layers are rather thin. One interpretation of the result could be that the clay and silt layer is disrupted with coarser material. The initial values of the hydrogeological units where therefore set to $5 \cdot 10^{-4}$ m/s for the sand, since this was the outcome of Hazen's formula, and $1 \cdot 10^{-5}$ m/s for the other layers, since the overall mean from the aquifer analysis was $4 \cdot 10^{-5}$ m/s, see Table 4.1.

Table 4.1 Initial conductivity values for the different hydrogeological units (HGU).

HGU	Initial conductivity value [m/s]
Sand	$5 \cdot 10^{-4}$
Silt	$1 \cdot 10^{-5}$
Clay	$1 \cdot 10^{-5}$
Till	$1 \cdot 10^{-5}$

4.5 Riverbed conductance

The river bed conductance were determined as the riverbed conductance per meter unit length of the river, this because MODFLOW internally multiplies the user supplied conductance by the length of the river (Aquaveo 2010). The formula used is given in Chapter 3 Method. The initial conductivity used in the formula was judged to be equivalent to the typical value of sand namely $1 \cdot 10^{-4}$ m/s. The river bed thickness was assumed to be 1 m. Based on some rough measurements of the river width taken from aerial photography, the river width was assumed to be 17.5 m. The riverbed conductance was therefore set to $1.75 \cdot 10^{-3}$ m^2/s. The uncertainty in the width was assumed to be negligible compared to the uncertainty of the conductivity.

4.6 Drain conductance

Most of the streams in the area as well as the ditches, see Figure 4.3, were assumed to drain the aquifer rather than contribute with a recharge and are therefore assessed as drains in the model. As for the riverbed, the drain conductance was based on the conductivity of $1 \cdot 10^{-4}$ m/s. The width of the drains was approximated in field to roughly 1 m and the thickness of the drain bed was estimated, by some digging in the

bottom material at some investigated drains, to roughly 0.2 m. The conductance was therefore determined to $5 \cdot 10^{-4}$ m^2/s.

4.7 Anisotropy

According to Chapter 2 Section 2.3 the pumping test in Algutstorp indicated an anisotropy factor (K_r/K_z) of 2. The uncertainty in the anisotropy could not be assessed since only one measurement was obtained. In the trial and error process, a better fit was obtained when the horizontal and vertical conductivities were equal.

4.8 Allocation of the recharge rates

Groundwater recharge is generally said to occur when infiltrated water reach the water table (Kresic 2007) but in MODFLOW the recharge rate is defined as the flow rate that is added to a receiving cell at every iteration (Harbaugh 2005). It was therefore interpreted as that the MODFLOW definition of the recharge rate is not related to the amount of water that arrive at the water table.

In this assessment, the recharge rate was generally set to equal that of the effective precipitation. It could be argued that this was a rather high value. However the main motivation for this choice was that the draining of the upper most soil layers was incorporated in the model, hence it was anticipated that the excess water would form runoff which would be diverted through the drains. One additional motivation, that is in some way related to what is stated above, was that the surface runoff was judged to be of a low magnitude because the topography is rather flat and the soil material fairly coarse.

If draining of the topmost layers were not included, the theory of flow hydrographs and base flow separation might be used instead.

The no-flow boundaries (Neumann conditions) were assigned to coincide with the assumed boundary between the aquifer and the surrounding areas of bedrock or till. It was believed that this type of boundary allocation was correct regarding groundwater flow occurring at some depth in the aquifer, but surface flow or flow in the very top layers might pass over the boundary to some extent.

The parts of the boundary where this surface-water migration likely occurs were identified. The influence from the surface flow was modelled by allocation of an extra recharge rate over areas of the computational domain close to these parts of the boundary, see Figure 4.4.

Figure 4.4 shows the capture zone of the Säve River between Kärtared and Algutstorp, The dark grey areas in the figure were assumed not to be drained by the watercourses. These areas are instead supposed to contribute to the groundwater recharge in relation to their size. The extra groundwater recharge was approximated as the effective precipitation multiplied by the capture area and added on the nearby cells, coloured light grey in Figure 4.4.

Figure 4.4 *Groundwater recharge outside the modelled area. Dark grey areas represent areas that were assumed to contribute to the groundwater recharge in the model. Light grey areas were assigned a higher recharge, which corresponds to the size of the adjoining dark grey area.*

4.9 River levels

In GMS the rivers are defined as arcs and the river level along the arcs is interpolated from prescribed values at the end nodes of the arcs (Aquaveo 2009c).

Here the river levels were defined at eight nodes, of which five were measured in field. These nodes were used to characterize the overall river level. At the nodes for which the river levels were not measured in field, the river levels were assigned by using the surface TIN. However since the TIN was constructed by measurements with a spacing of 50 m, the river valley was not readily identified. This problem was solved by assigning the head level for the node to the lowest value of the TIN that was present in the absolutely vicinity to the node. The remaining two nodes were placed at 50 m and 180 m north respectively south of the measures node at the Ljunghem area. The value of the river level of the node downstream the measured node was approximated by interpolation and the other by extrapolation.

4.10 Drain bottom elevations

The drain bottom elevations were at the confluence with the river assigned to the river level. Six upstream nodes were assigned to field measured values and for the remaining drains the upstream nodes were assigned to a specified depth below the ground surface see Figure 4.5 below.

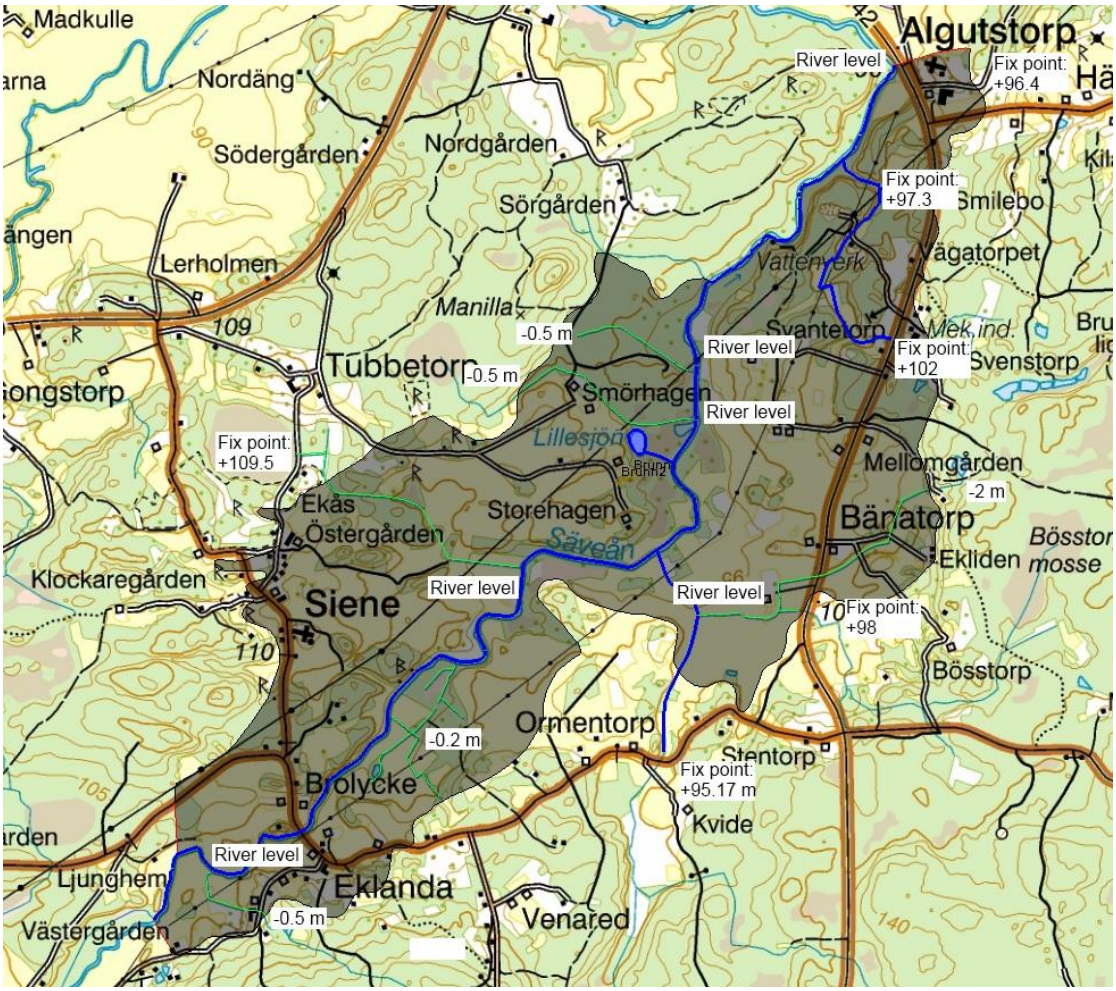

Figure 4.5 *Drain bottom elevations, set off from the surface TIN if not described as a fix point or river stage. © Lantmäteriet Gävle 2011. Consent I 2011/0072.*

4.11 Internal stresses

The abstraction rate applied to both the wells was the set to 8.7 l/s which equal half of the total amount abstracted. Temporal variations in the abstraction were not included in the assessment.

4.12 MODFLOW settings

MODFLOW settings can be seen in Appendix 7. The settings were based on recommendations in the PEST user manual (Watermark Numerical Computing 2005) and the convergence criteria was refined though out the calibration process.

5 Model Calibration

The aim of the calibration process was to obtain a model in which the output matches field measured values. The output and measured values are here defined as head. To obtain the desired result of the calibration process the model parameters are changed or fine-tuned to optimal values. Examples of model parameters are the hydraulic conductivity and recharge rate (Hill & Tiedeman 2007).

Model calibration can be carried out by manual trial and error adjustments of the parameters, or it can be done automatically. Here the calibration was done automatically. The automated calibration technique used here is formally referred to as indirect inverse modelling or parameter estimation and applies an objective function to quantify the match between simulated and computed observations.

The parameter estimation problem could be linear or nonlinear (Hill & Tiedeman 2007). The technique used is general, thus capable of handle both situations. However linear parameter estimation is carried out much faster than the nonlinear one, which is solved using an iterative procedure. Most problems in this context are nonlinear (Watermark Numerical Computing 2005). Understanding of the nonlinearity referred to here, can be archived by glancing at the Darcy's law, where it could be noticed that the head is a nonlinear function of the conductivity (Hill & Tiedeman 2007).

The benefits of using inverse modelling compared to manual trial and error calibration are that it produce more transparent models, and is less time consuming and less subjective. Other benefits with inverse modelling are the possibility to reveal and quantify model shortcomings like parameter insensitivity towards observations and non-uniqueness of parameters. Once these problems are revealed, changes in the definition of the parameters or the number of parameter could be made to improve the model. Parameter sensitivity could be comprehended as the information that the observations provide to the parameters or how well the parameters are supported by the observations. Parameter uniqueness could be interpreted as the extent to which sets of different parameter values produce nearly the same objective function value (Hill & Tiedeman 2007).

5.1 Automated calibration – the background theory

In indirect inverse modelling an objective function is formulated describing the difference between the model output and the observations. The aim of inverse modelling is then to find the parameter set that minimize the objective function (Hill & Tiedeman 2007).

The program used when carrying out the calibration process is called PEST. The objective function that PEST uses is the weighted least squares objective function and is for a linear problem generally defined as below. The objective function defined below is after local linearization of a nonlinear problem also used, however in some modified form, as will be explained later in this chapter.

$$\phi = (\underline{o_m} - \underline{\underline{X}}\,\underline{b})^t \underline{\underline{W}} (\underline{o_m} - \underline{\underline{X}}\,\underline{b}) \tag{5.1}$$

where

$\underline{\underline{W}}$ is a $m \times m$ weight matrix which is either a diagonal matrix weight matrix or a full weight matrix depending on whether the observation uncertainty for different observations is assumed to be correlated or not, se future below.

$\underline{o_m}$ is a vector of order n consisting of field measured observations

$\underline{\underline{X}}$ is a $m \times n$ matrix which is constant and independent to $\underline{o_m}$

$\underline{b}$ is a vector of order n consisting of the parameters for which are about to be evaluated

m represents the number of observations and n represents the number of parameter to be estimated (Watermark Numerical Computing 2005).

When calculating the value of the objective function the units of the residuals have to be of the same type. In order to allow for different types of observations and to account for observations with different accuracy weighting is introduced (Hill & Tiedeman 2007). If it is assumed that no correlation in observation uncertainty between observations is present, then the weights are said to be correctly assigned if the weights are proportional to the inverse of the standard deviation pertaining to the observations. Under this circumstance the square of the weights is housed in a diagonal matrix. If however correlation is in fact present then a full weights matrix should be assigned to be proportional to the inverse of the observation covariance matrix (Watermark Numerical Computing 2005). Readers may refer to Watermark Numerical Computing (2005) for additional information on how PEST incorporates the full weight matrix. The correlation of the observation uncertainty between the observations can be evaluated by investigating the weighted residuals against weighted observation values. The residuals should be randomly distributed with a mean of zero if no correlation is present (Watermark Numerical Computing 2005). Here a diagonal weight matrix was used.

The weights that MODFLOW provides are calculated in compliance with the first condition stated above. MODFLOW offers also a possibility to account for a so called group weight, but this was not done in the modelling effort (Aquaveo 2011b).

The set of parameters that minimize objective function above could be obtained by solving

$$\frac{\partial}{\partial \underline{b}} (\underline{o_m} - \underline{\underline{X}}\,\underline{b})^{t} \underline{\underline{W}} (\underline{o_m} - \underline{\underline{X}}\,\underline{b}) = 0 \tag{5.2}$$

(Hill & Tiedeman 2007)

and the normal equations that constitutes the solution are generally formulated as

$$\underline{b} = (\underline{\underline{X}}^{t} \underline{\underline{W}} \underline{\underline{X}})^{-1} \underline{\underline{X}}^{t} \underline{\underline{W}} \underline{o_m} \tag{5.3}$$

Here the model was nonlinear why nonlinear parameter estimation has to be done. In PEST nonlinear parameter estimation is executed using the Gauss-Marquardt-Levenberg algorithm. The theory which underpins the Gauss-Marquardt-Levenberg algorithm is shortly described below.

The foundation of the algorithm is that the model output related to an observation for a nonlinear model is locally linearized around a parameter set, $\underline{b_0}$, by the Taylor theorem. Considering the general relation between the model output and the parameters, described as

$$\underline{o_C} = f(\underline{b}) \tag{5.4}$$

where

$\underline{o_c}$ is a model calculated observation.

The linearized approximation could then be formulated as

$$\underline{o_C} = \underline{o_{C,0}} + \left.\frac{\partial f(\underline{b})}{\partial \underline{b}}\right|_{\underline{b}=\underline{b_0}} \Delta \underline{b} \tag{5.5}$$

$$\underline{o_{C,0}} = f(\underline{b}_0) \tag{5.6}$$

noting that

$$\left.\frac{\partial f(\underline{b})}{\partial \underline{b}}\right|_{\underline{b}=\underline{b_0}} = \underline{\underline{J}} \tag{5.7}$$

where $\underline{\underline{J}}$ is the Jacobian matrix of $(\underline{b})$, for which $\underline{\underline{J}}_{m,n}$ is the derivative of the observation m with respect to parameter n. The objective function is now denoted linearized objective function and could be formulated as

$$\phi = \left[\underline{o_m} - \underline{o_{C,0}} - \underline{\underline{J}}\Delta \underline{b})\right]^t \underline{\underline{W}} \left[\underline{o_m} - \underline{o_{C,0}} - \underline{\underline{J}}\Delta \underline{b})\right] \tag{5.8}$$

Minimizing the linearized objective function with respect to parameter upgrade vector, $\Delta\underline{b}$, yields

$$\Delta \underline{b} = (\underline{\underline{J}}^t \underline{\underline{W}}\, \underline{\underline{J}})^{-1}\, \underline{\underline{J}}^t \underline{\underline{W}} (\underline{o_m} - \underline{o_c}) \tag{5.9}$$

A better approximation of the parameter sett, $\underline{b}$, can now be estimated as

$$\underline{b} = \underline{b}_0 + \Delta \underline{b} \tag{5.10}$$

Realising that the parameter sett, $\underline{b_0}$, successive can become improved yields the following iterative procedure

$$\underline{b}_{new} = \underline{b}_{old} + \Delta \underline{b} \tag{5.11}$$

Consequently adding $\Delta\underline{b}$ to the old parameter sett gives a new parameter set for which the objective function is even further lowered. The Jacobian matrix is then once again evaluated around this new parameter sett and a next parameter upgrade vector, $\Delta\underline{b}$, can be evaluated. This procedure will carry on until the convergence is reached, which is determined by a set of convergence criteria. Figure 5.1 illustrates the process. Readers may refer to Watermark Numerical Computing (2005) for additional information concerning the convergence criteria.

The process described above could be rationalized if account is taken to the direction of the parameter upgrade vector in respect to the contours of equal objective function value (Watermark Numerical Computing 2005).

According to Watermark Numerical Computing (2005) it is advantageous if the direction of the parameter upgrade vector is aligned with the direction of steepest decent. This can be accomplished by using the so-called Marquardt parameter, α. Introduced the parameter upgrade vector takes the following shape

$$\Delta \underline{b} = (\underline{\underline{J}}^t \underline{\underline{W}} \underline{\underline{J}} + \alpha \underline{\underline{I}})^{-1} \underline{\underline{J}}^t \underline{\underline{W}} (\underline{o_m} - \underline{o_c}) \quad (5.12)$$

where $\underline{\underline{I}}$ is the identity matrix. During the approximation process PEST evaluates the Marquardt parameter and raises its value if the value of the objective function was increased and vice versa (Watermark Numerical Computing 2005).

Since there is a possibility that the elements in the Jacobian matrix exhibit immense difference in magnitude, because different type of parameters may be considered, scaling of the elements might be needed. In PEST this is done by adding a scaling matrix to the equation for the parameter upgrade vector (Watermark Numerical Computing 2005). PEST is also capable of changing the mangitude of the parameter uppgrade vector to an optimal length. Readers may refer to Watermark Numerical Computing (2005) for additional information.

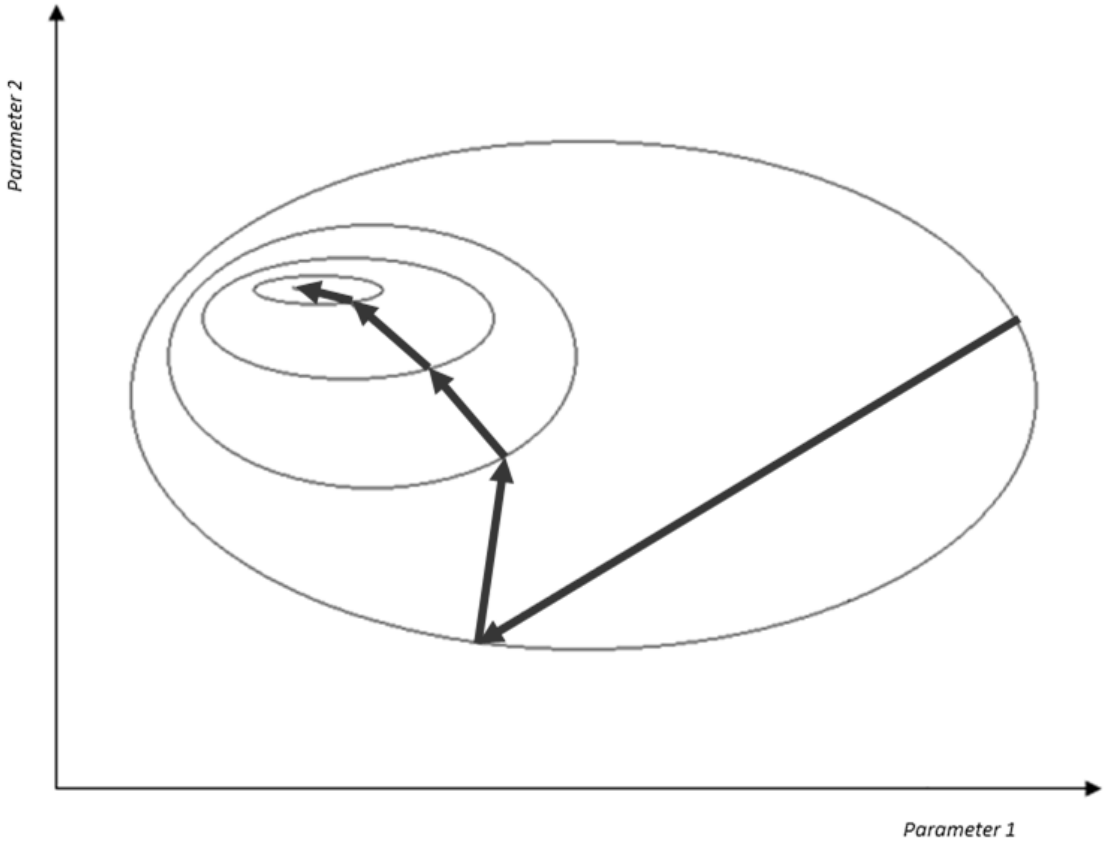

Figure 5.1 *Objective function contours for a two parameter problem and the upgraded parameter vectors.*

5.2 Weights and calibration targets used

Considering head observations Aquaveo (2011b) propose that if head measurements at different times are provided the mean and the standard deviation of this data could be used to calculate the observation weights and the expected value of the head observation. This was also done. However the number of measurements taken at each observation well at Storehagen was by far more than the number of measurements taken at Algutstorp. The measurements at Storehagen were done every month compared to 2-4 measurement in total for Algutstorp, which also only were conducted during the summer months.

The mean value of the standard deviation of the groundwater head observation was for the observation wells at Storehagen 0.21 m, for Algutstorp 0.30 m and for the observations made by SGU in the private wells 0.22 m. The standard deviation for the observations at Algutstorp that were used to calculate the weight was multiplied by two in an attempt to reflect the fact that the measurements of the observations not reflect other seasons. See Appendix 5 regarding the spatially location of the observation wells.

Hill and Tiedeman (2007) recommend that it is beneficial to use many types of observations, e.g. flow rate across the aquifer boundary, and not just head observations. Initially, flow rates were also accounted for and the flow observation for the flow to and from the aquifer was determined as the difference in the river flow rate between the two end nodes of the Säve River.

The standard deviation of the flows at the two points was calculated in a similar way as was done for the head. However in accordance to Hill and Tiedeman (2007) the standard deviation for the difference in the flow between the two locations was calculated as the square root of the summed variances of the flow at the two locations.

However the flow between the aquifer and the Säve River was not measured but instead calculated and it was assumed that the calculations were rather incorrect why this type of observation was omitted. For example, flow rate was calculated based on the very same numbers as for the effective precipitation and no account was taken to the flow that was drained by the drains. Also the incorporation of general heads as boundaries across the aquifer introduced additional uncertainty in the flow terms.

After omitting the flow observation, the recharge rate was estimated to unreasonable values in the parameter estimation. It was interpreted that this parameter was constrained the most by the flow observation. Instead of letting the flow observation constrain the recharge rate, this parameter was set to a fixed value. This could also be motivated by that the sensitivity of the recharge rate towards the flow observation was lower than for the other defined parameters.

5.3 PEST settings

According to Watermark Numerical Computing (2005) it is possible that an insensitive parameter can dominate the parameter upgrade vector and because PEST also applies maximum bounds for parameter change at each optimisation iteration there is a risk that the objective function will not be reduced. This could be solved if Automatic User Intervention (AUI) is specified. If automated user intervention is used PEST is capable of setting insensitive parameters to be fixed at their current values during the rest of optimisation iteration. In the succeeding iteration PEST then evaluates the sensitivity once again to justify whether the parameters should be allowed to vary (Watermark Numerical Computing 2005).

Other settings like the maximum parameter change bounds and convergence settings were set to default values. Readers might refer to Watermark Numerical Computing (2005) for additional information about the default settings.

In PEST the user has to supply initial parameter values and ranges. The values that were used are given in Table 5.1.

Table 5.1 Starting hydraulic conductivity values for PEST-parameters.

Parameter	Start value [m/s]	Min value [m/s]	Max value [m/s]
Sand	$5 \cdot 10^{-4}$	$1 \cdot 10^{-7}$	$1 \cdot 10^{-1}$
Silt	$1 \cdot 10^{-5}$	$1 \cdot 10^{-12}$	$1 \cdot 10^{-2}$
Clay	$1 \cdot 10^{-5}$	$1 \cdot 10^{-12}$	$1 \cdot 10^{-2}$
Till	$1 \cdot 10^{-5}$	$1 \cdot 10^{-12}$	$1 \cdot 10^{-2}$

5.4 Statistics used as a support in parameter estimation process

Statistics derived from sensitivity analysis and weighting rather than from residuals are denoted as fit-independent statistics by Hill & Tiedeman (2007).

Fit-independent statistics aim to reveal the potential affect that observations have on the parameters and offer guidance in the selection of the most suited parameters to include in the regression analysis. The fit-independent statistics are in much based on the sensitivity of the model calculated observation with respect to the different parameters used in the model. The sensitivity of a model calculated observations with respect to a particular parameter reveal in some sense the prominence of the observation to that parameter or formulated in another way, the amount of information that the observation offer to the parameter (Hill & Tiedeman 2007).

Examples on fit-independent statistics that are described by Hill & Tiedeman (2007) are composite scaled sensitivities and parameter correlation coefficients.

5.4.1 Composite sensitivities

Composite scaled sensitivities (*css*) could be interpreted as the average change in per cent of calculated observations standard deviation based on one per cent change in a particular parameter value. The composite scaled sensitivities could also be seen as the sum of information that all of the used observations give to one parameter. A value of the composite scaled sensitivity lower than the noise in the data, the influence of the observation uncertainties, could reduce the possibilities for the regression to approximate the parameters. Hill and Tiedeman (2007) recommend that the composite scaled sensitivity of a parameter not should be lower than one.

PEST offers a composite parameter sensitivity which is slightly different compared to the composite scaled sensitivity described in "*Effective groundwater model calibration"* (Hill & Tiedeman 2007) in that the composite scaled sensitivity is calculated as the composite parameter sensitivity times the actual parameter value. The composite scaled sensitivity is in PEST refered to as the relatively composite sensitivity (Watermark Numerical Computing 2005).

The composite parameter sensitivity is in PEST calculated (Watermark Numerical Computing 2005) as

$$s_i = \frac{\left(\underline{\underline{J}}^t \underline{\underline{W}} \underline{\underline{J}}\right)_{ii}^{1/2}}{m} \tag{5.13}$$

and the relatively composite sensitivity or the composite scaled sensitivity was here calculated as

$$css_i = s_i \cdot b_i \tag{5.14}$$

where b_i is the i'th parameter

The composite scaled sensitivities (Hill & Tiedeman 2007) and the composite parameter sensitivity (Watermark Numerical Computing 2005) could be used in order to facilitate the choice on which parameters to be used in the regression and those that should be set to a constant value. Here composite parameter sensitivity was used as a support to decide which parameters to include.

The composite parameter sensitivities for the final PEST run are given in Figure 5.2 and the composite scaled sensitivities in Figure 5.3. It was noticed that the observations provide the most information about the hydrogeological-unit sand and the least to silt. However all the composite scaled sensitivities were way below one, why the information provided from the observations was probably insufficient.

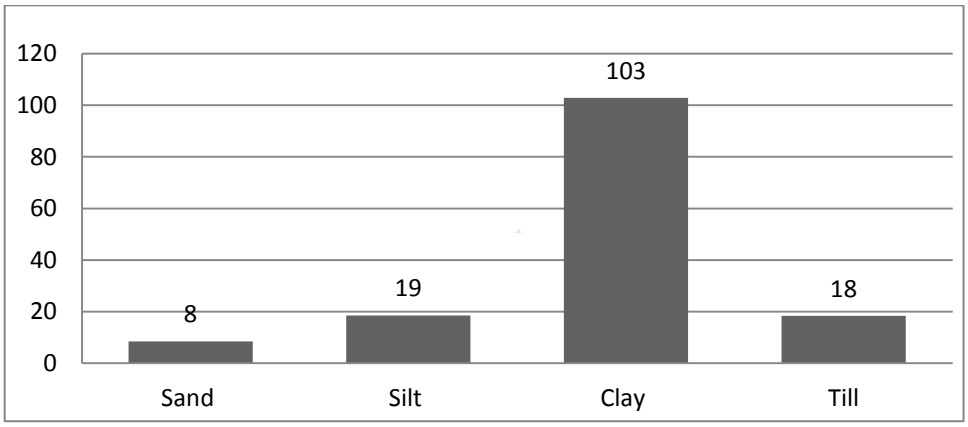

Figure 5.2 Composite parameter sensitivities for observation group "head" [s/m].

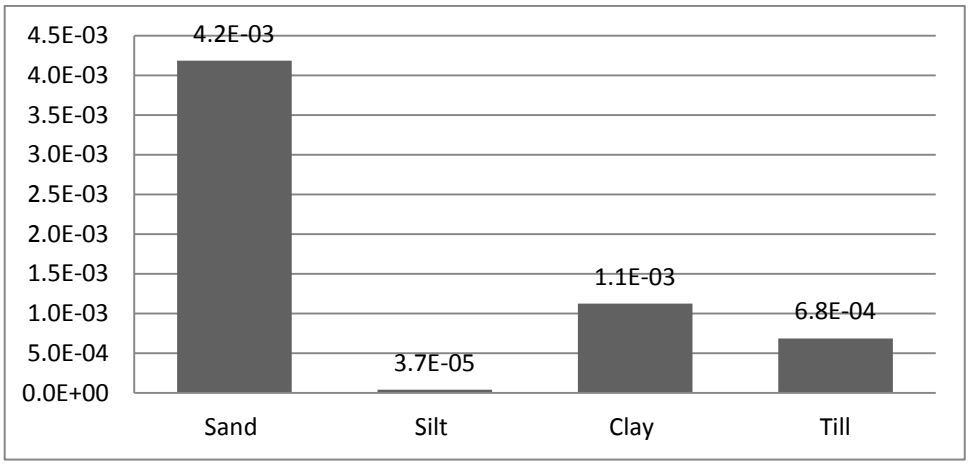

Figure 5.3 Composite scaled sensitivities for observation group "head" [-].

5.4.2 Parameter correlation coefficient matrix

The parameter correlation matrix is a matrix consisting of correlation coefficients between two parameters. Each of the correlation coefficients is calculated as the covariance divided by the standard deviation of one of the parameters multiplied with the other (Hill 1998). Interpreted in the context here, the correlation between two parameters in the correlation matrix should reflect a possible synchronized change in the parameters that yield the same objective function value (Hill & Tiedeman 2007).

According to Hill and Tiedeman (2007) the correlation coefficient can be used as an indicator on whether the parameter values can be estimated uniquely. Hill and Tiedeman (2007) proposes a rule of thumb that if the absolute values of the parameter correlation coefficients are less than 0.95 it is to be expected that the parameters can be estimated unique.

In PEST the covariance's between two parameters and the variance of the parameters is housed in a covariance matrix which is calculated in a different way whether the observation weights are unity or not. The covariance matrix is determined as

$$C(\underline{b}) = \sigma^2 \left(\underline{\underline{J}}^t \underline{\underline{W}} \, \underline{\underline{J}} \right)^{-1} \tag{5.15}$$

where σ^2 is calculated as

$$\sigma^2 = \frac{\phi}{m - n} \tag{5.16}$$

(Watermark Numerical Computing 2005)

The quantity σ^2 is by Hill (1998) referred to as the calculated error variance and by Watermark Numerical Computing (2005) as the reference variance. Readers may refer to Hill and Tiedeman (2007) concerning the proof of the covariance matrix defined above.

According to Hill and Tiedeman (2007) high parameter correlation could be resolved by including more observations, redefining parameters and including prior information to the parameters that exhibit high correlation. Moreover, Watermark Numerical Computing (2005) claim that high parameter correlation could emerge in models with a high number of parameters. Hill and Tiedeman (2007) also suggest that different types of observations should be used to compel the regression.

In the initial stages of the modelling effort the parameters exhibit great non-uniqueness. At this stage only a few more observations than defined parameters were used. The model was then redesigned with account taken to the above recommendations. The primary changes that were done to the model were that fewer parameters were prescribed, and more head observations were added.

The use more observations and less parameter were shown to have a great impact on the high parameter correlations which initially was severe. To facilitate the use of fever parameters, some parameters were lumped together and some were put to fixed values. One example on parameters that was prescribed to fixed values was the two parameters controlling the recharge rate. Also the river conductance was shown to have low sensitivity why this parameter was set to a fixed value.

Table 5.2 shows the parameter correlation coefficient matrix for the final PEST run. By glancing at the matrix, one could notice that no correlation coefficient exceeds the

critical absolute value of 0.95. In accordance to Hill and Tiedeman (2007) this was an indication that the parameter set obtained was unique.

Table 5.2 Parameter correlation coefficient matrix

	Sand	Silt	Clay	Till
Sand	1.00	-0.57	-0.38	-0.06
Silt	-0.57	1.00	-0.05	0.03
Clay	-0.38	-0.05	1.00	0.02
Till	-0.06	0.03	0.02	1.00

5.5 Goodness of model fit

5.5.1 Correlation coefficient

The correlation coefficient, *r*, functions as an overall measurement of model fit. The correlation coefficient indicates to what extent modelled values follow measured counterparts (Hill & Tiedeman 2007). The benefit of using the correlation coefficient, *r*, as an overall measure of goodness of fit compared to the objective function value is that it could be compared for altered models. This is possible since it is independent to the uncertainty in the observations and to the number of observations (Watermark Numerical Computing 2005).

In PEST the correlation coefficient for the weighted observations and the weighted simulated value is calculated as

$$r = \frac{\sum\left(\underline{\underline{W}}_i^{1/2} o_{m,i} - \overline{\underline{\underline{W}}^{1/2} o_m}\right)\left(\underline{\underline{W}}_i^{1/2} o_{c,i} - \overline{\underline{\underline{W}}^{1/2} o_c}\right)}{\left[\sum\left(\underline{\underline{W}}_i^{1/2} o_{m,i} - \overline{\underline{\underline{W}}^{1/2} o_m}\right)\left(\underline{\underline{W}}_i^{1/2} o_{m,i} - \overline{\underline{\underline{W}}^{1/2} o_m}\right)\sum\left(\underline{\underline{W}}_i^{1/2} o_{c,i} - \overline{\underline{\underline{W}}^{1/2} o_c}\right)\left(\underline{\underline{W}}_i^{1/2} o_{c,i} - \overline{\underline{\underline{W}}^{1/2} o_c}\right)\right]^{1/2}} \quad (5.17)$$

where

$\underline{\underline{W}}_i$ is the weight linked to observation *i*.

$o_{m,i}$ is the field measured observation value at the *i'th* observation

$o_{c,i}$ is the calculated observation value at the *i'th* observation

$\overline{\underline{\underline{W}}^{1/2} o_m}$ is the mean value of the weighted field measured observations

$\overline{\underline{\underline{W}}^{1/2} o_c}$ is the mean value of the weighted calculated observations

According to Hill (1998), a value of the correlation coefficient larger than 0.9 indicates an acceptable match between the weighted observations and the weighted

calculated counterparts. Here the correlation coefficient was determined to 0.9999 and the fit is illustrated in Figure 5.3 below. The match in the perspective of the correlation coefficient, *r*, was thus sufficient in accordance to what is described in (Tiedeman & Hill, 2007).

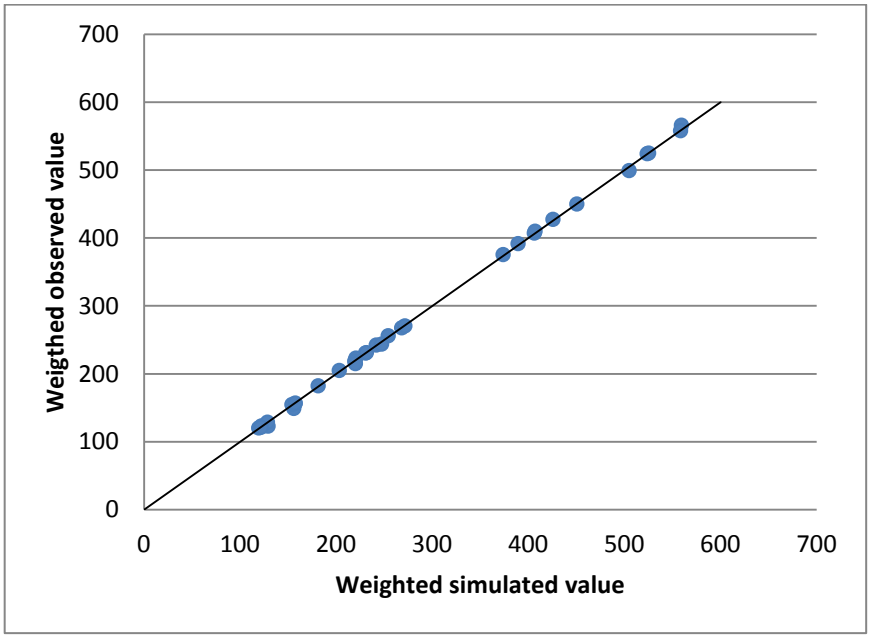

Figure 5.3 Weighted observed values plotted against weighted simulated values [-].

5.5.2 Residuals

The difference between the simulated values and the field observations is here referred to as residuals. Weighted residuals are calculated by multiplying the residuals with the pertaining weights.

A model error is said to be present if the model does not capture the true behaviour of the aquifer. Model bias is referred to a systematically misfit between the model output and the observations that is due to model error. Weighted residuals that exhibit randomness indicate, in conjunction with reasonably optimized parameters, a good model fit and vice versa (Hill & Tiedeman 2007). According to Hill and Tiedeman (2007) weighting could not be applied to reduce model bias.

Reasonably optimized parameters are here referred to optimized parameters that are close to what were to be expected based on what is known on beforehand (Hill & Tiedeman 2007). One example of a common source of model misfit described by Hill and Tiedeman (2007) is that often the wells are screened at a highly permeable layer which may be of a minor extent. Thus the conductivities obtained from a pumping test poorly represent the other material layers.

Here model bias was recognised in earlier model runs, by that the residuals close to the river all were negative. In this case it was concluded that the river level was incorrectly assigned.

Figure 5.4 displays a scatter data set of which the weighted residuals were plotted against weighted modelled values of the head. The scatter data originated from a MODFLOW run with the optimal parameter set. The mean value of the weighted

residuals was determined to 0.1 with a max of 6.77 and min of -6.72. Since the mean value of the residuals should be zero some model bias could be present.

By glancing at the plot it was assumed that the residuals were fairly random by considering all of them, but if the residuals were investigated with regard to their location a different situation emerges. The model calculated head stage at the perimeter of the model were found to be consistently lower than the measured values and at the centre of the aquifer the computed heads were found to be more randomly distributed around zero, see Figure 5.5. It was here believed that the reason for this pattern could be that either the conductivity was lower than earlier anticipated or some unaccounted base flow across the boundary may be present.

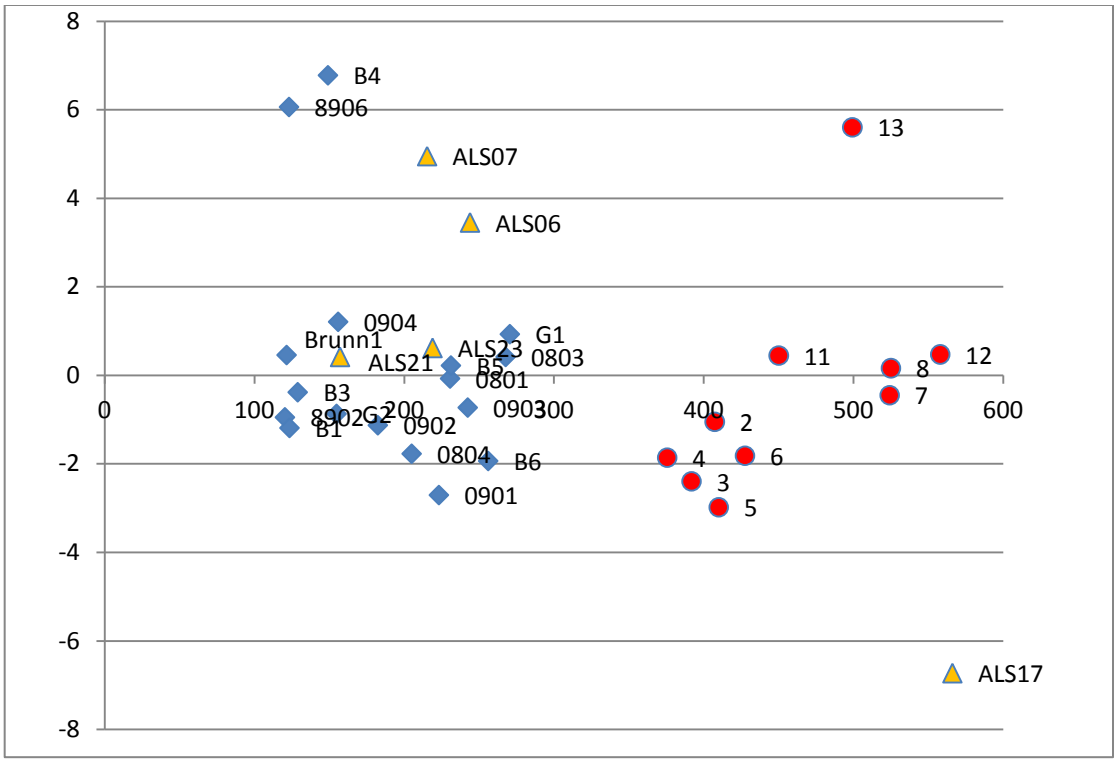

Figure 5.4 *Subset of weighted residuals plotted against weighted simulated values [-]. The red circles represent Storehagen, the blue diamonds Algutstorp and the yellow triangles private wells scatted around the aquifer.*

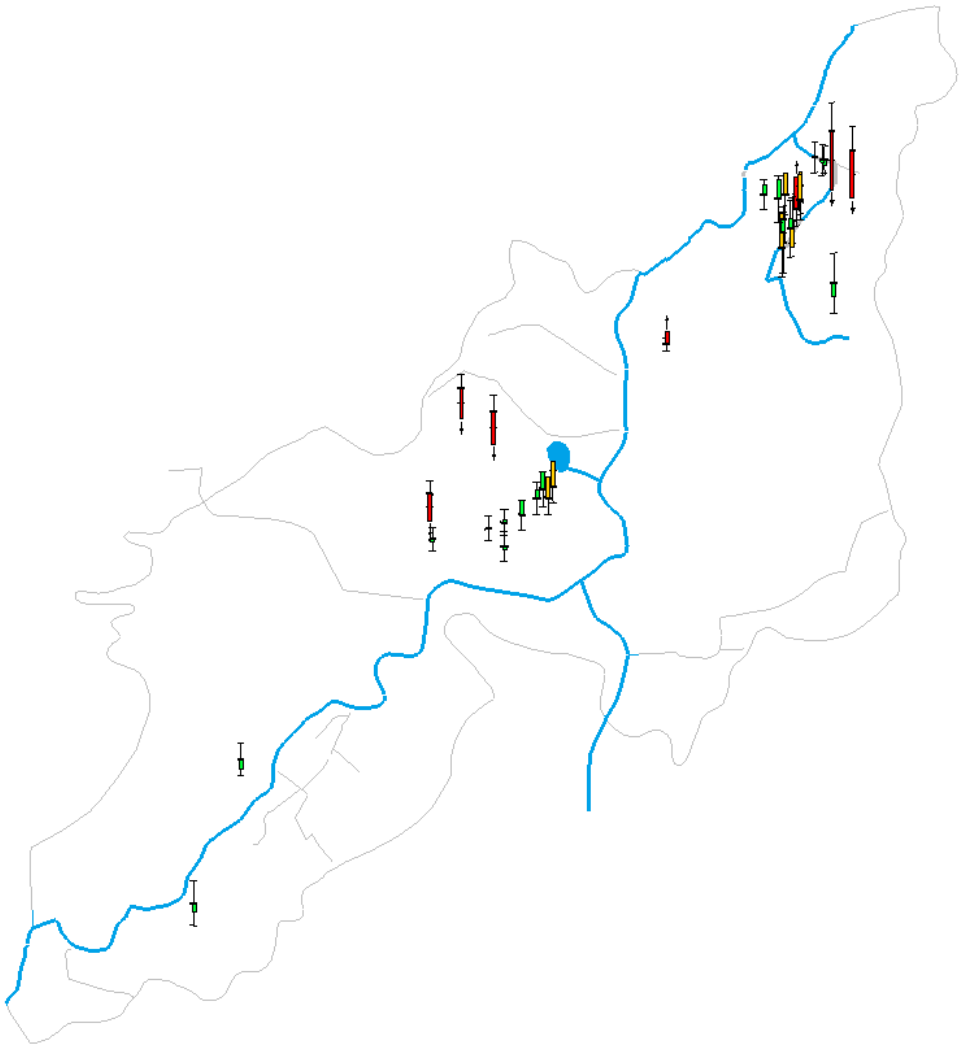

Figure 5.5 The residuals displayed at their respective spatially location.

5.5.3 Calculated error variance

The calculated error variance is in PEST referred to reference variance and calculated as shown in Section 5.4.2, as the sum of the weighted squared residuals divided by the number of degrees of freedom (calculated as the number of observations minus the number of parameters used). The calculated error variance and the standard error of regression (calculated as the square root of the calculated error variance) could also be used as a measure of the model fit. The calculated error variance or the standard error could be seen as a measurement of whether the fit between the model calculated head values and the observations is consistent with the uncertainty in the observations.

An indication of that the model fit is consistent with the weighting is apprised if the calculated error variance or the model error equals one. This could be envisioned by noting that the uncertainty in the observations is described by the standard deviation of the observation value and the weights pertaining to the observations are proportional to the reciprocal of the variance of the observation value.

If the calculated error variance is substantially different from 1, Hill and Tiedeman (2007) recommend that an investigation of the calculated error variance confidence interval could be done. The fit is by Hill and Tiedeman (2007) seen as inconsistent to

the weighting if a two sided 95% confidence interval of the calculated error variance does not include 1.

It may be that the observation weights used not believed to represent the uncertainty in the observation value in a truly correct manner. To evaluate the magnitude of the weights for which the model fit is consistent to, so-called individual fit consistent statistics could be applied. The magnitude of the new weights is calculated by just multiplying the observation standard deviation with the standard error of regression. If the new weighting seems fairly reasonably and could be motivated and if the weighted residuals are randomly distributed, a model could still be valid despite having a confidence interval of the calculated error variance that not include 1.

If the magnitude of the new weights could not be motivated and the residuals still are randomly distributed, there is a reason to believe that the model suffers from model error. However the model could still be functional in a predictive sense. If the residuals not are randomly distributed and if the new weights are unrealistic the model may very well be useless (Hill & Tiedeman 2007).

Here the calculated error variance was determined to 8.63 and the standard error of regression to 2.93 why the confidence interval was determined and investigated. The confidence interval limits was calculated in accordance with Hill and Tiedeman (2007) and was calculated as the number of degrees of freedom multiplied with the calculated error variance divided by the upper and lower tail value of the chi-square distribution respectively. The upper and lower tail value of the chi-square distribution was obtained from using the program Distribution Calculator (Virtual Insitute of Applied Science 2010). With 28 degrees of freedom and a significance level of 0.05 the confidence limits were determined to 5.4 m^2 and 15.8 m^2. The new standard deviations of the observations that was used to calculate the weighting was consequently 2.9 times larger than those initially used. The largest new observation standard deviation was 2.38 m (Observation Well 8902) and the smallest was 0.49 m (Observation Well 12) see Figure 5.6. The mean of the new observation standard deviations that the model fit was consistent to was 1.25 m.

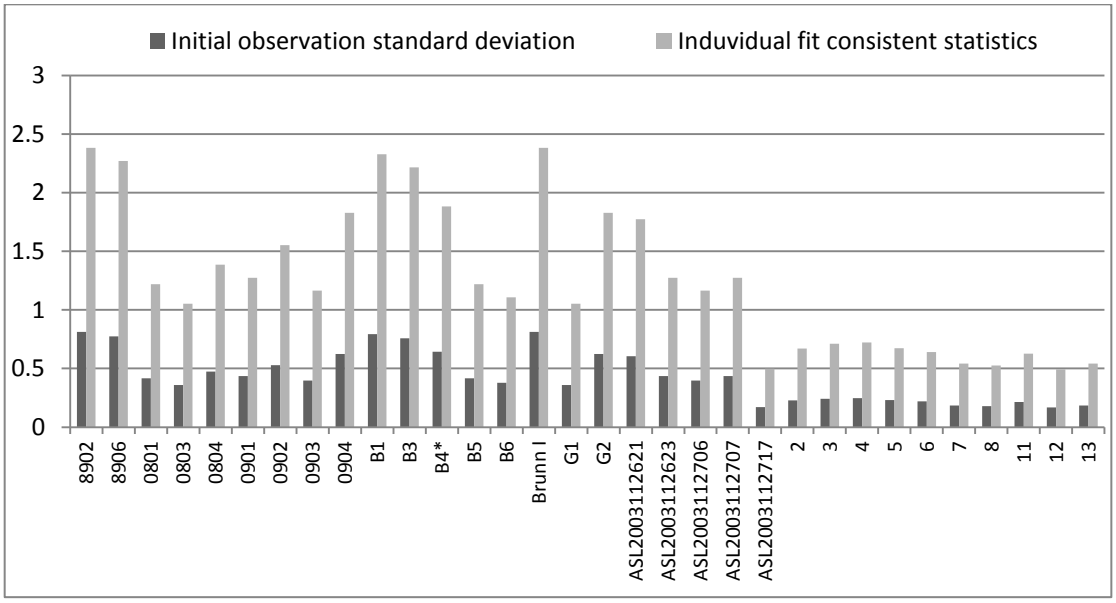

Figure 5.6 Comparison of the individual fit consistent statistics and the initial observation standard deviation [m].

It was here believed that the fitted error statistics barely could be motivated. However it could be useful to put the standard deviations in the context of the size of the aquifer (roughly 7 km long, 1 km wide and 15 m deep). Given this relatively large area, a mean value of the observation standard deviation of 1.25 m could perhaps be adequate.

5.6 Optimal parameter set compared to reasonable ranges

In Figure 5.7 the parameter set is compared with typical ranges of the type of material that the parameters should represent. The parameter value representing the hydraulic conductivity for sand seems reasonable. Considering the other materials the parameter estimates has shown to be rather inconsistent towards what was known beforehand about the hydraulic conductivity. This could indicate model bias (Hill & Tiedeman 2007). As discussed in Chapter 2 Geological and hydrogeological description of the area, it was believed that the silt and clay layers are disrupted with layers of highly permeable materials and thus the overall conductivity for these layers is higher than what would be expected if the layers were continuous. It was also anticipated that most of the material in the aquifer is sand, why optimal parameter set was believed to be rather reasonable.

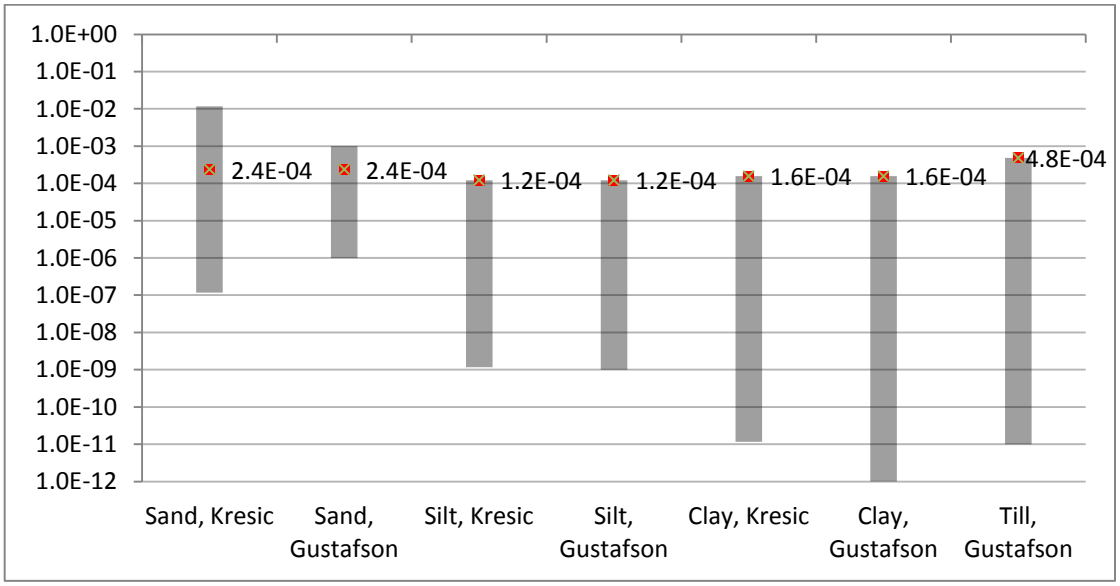

Figure 5.7 *Parameter estimates (red mark) compared with reasonably ranges for different material hydraulic conductivity for which they should represent [m/s].*

5.7 Linear individual confidence interval

Figure 5.8 is the optimized parameter displayed with their linear individual confidence intervals provided from PEST. The linear confidence interval (95%) is not truly representing the confidence interval if the model is nonlinear (Hill & Tiedeman 2007). A possible nonlinear confidence interval may be further enhanced (Watermark Numerical Computing 2005). However a linear confidence interval demand only very little computation compared with nonlinear confidence interval (Hill & Tiedeman 2007) and the linear confidence intervals of the parameters cold be seen as an

indicator of the precision of the parameter estimates compared to each other (Watermark Numerical Computing 2005).

Note that the axis is not logarithmically scaled and that the lower limit of the confidence interval contains negatively values.

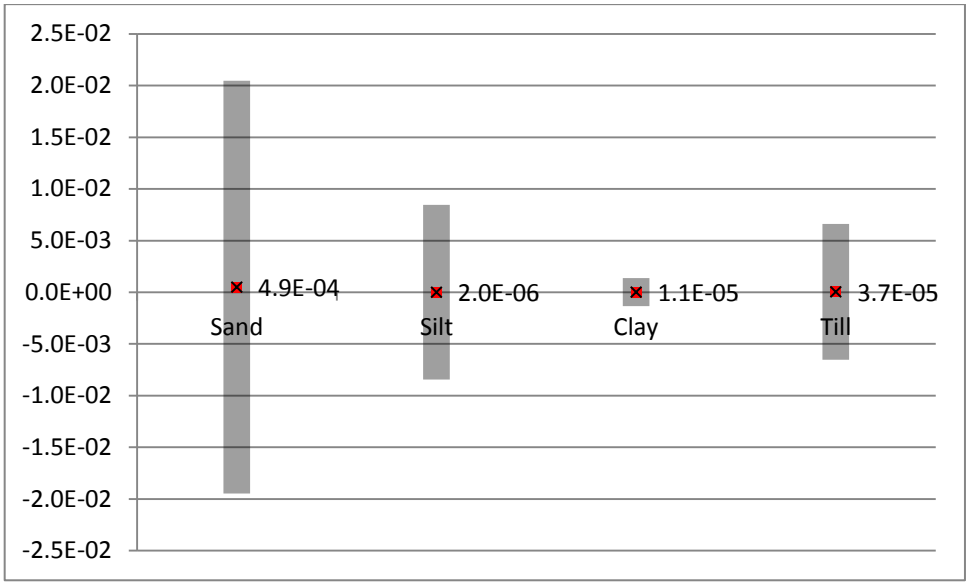

Figure 5.8 Estimated parameter values with linear individual confidence intervals [m/s].

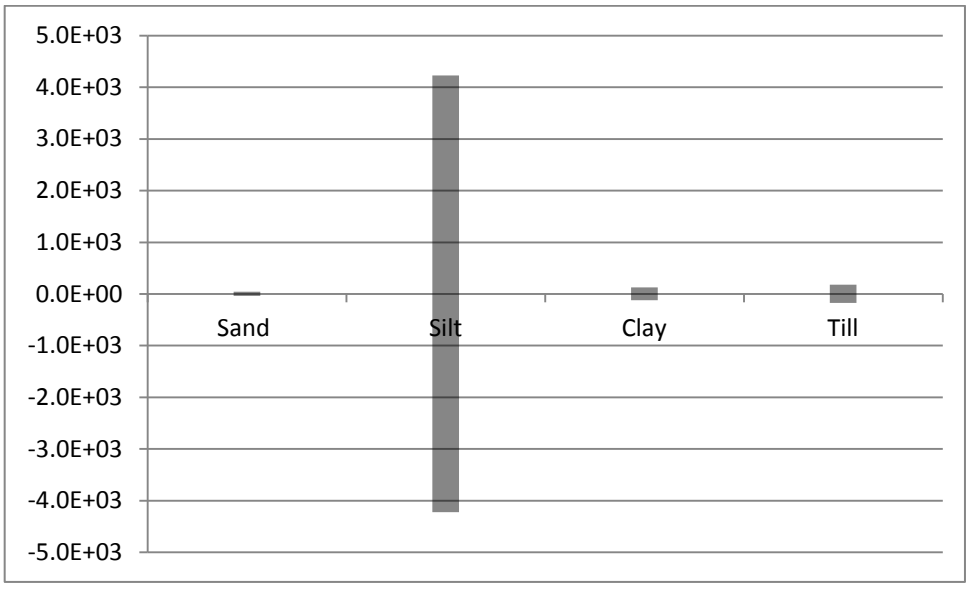

Figure 5.9 Linear confidence interval in relation to each parameter value [-].

From Figure 5.9 it could be noticed that the parameter representing sand has, in real numbers, the largest linear confidence interval and thus one could suspect his parameter to be the least accurately estimated. However in relation to the value of the parameter it could be concluded, from Figure 5.9 Linear confidence interval in relation to each parameter value [-].Figure 5.9, that the parameter representing silt was the least accurate in comparison with the others. This makes sense by recalling that

the parameter representing sand had the highest composite scaled sensitivity and the parameter representing silt the lowest.

If a linear confidence interval should apply, the model should truly represent the system and it was assumed the weighted residuals should be random and normally distributed. The assumption of normality is due to that t-statistics should be used to calculate the confidence interval. In Figure 5.10 is the residuals plotted against the cumulative probability and compared with the normal distribution based on the mean value and the standard distribution of the weighted residuals (Hill & Tiedeman 2007).

The cumulative probability was calculated as

$$p = \frac{(k - 0.5)}{n} \tag{5.18}$$

where

n is the number of weighted residuals here 32 and

k is striding from one to n.

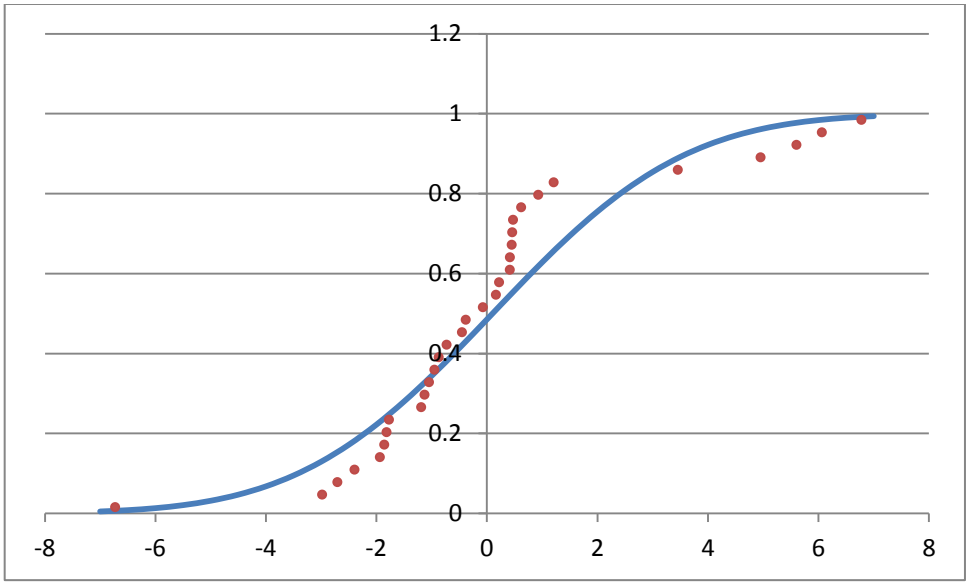

Figure 5.10 *Weighted residuals [-] plotted against the cumulative probability. The curve represents the normal distribution based on the mean and standard deviation of the series of residuals.*

The correlation coefficient was calculated to 0.20 using the formula:

$$R_N^2 = \frac{\left(\left(\underline{e_0} - \underline{m}\right)^T \underline{\tau}\right)^2}{\left(\underline{e_0} - \underline{m}\right)^T \left(\underline{e_0} - \underline{m}\right)\left(\underline{\tau}^T - \underline{\tau}\right)} \tag{5.19}$$

where

$\underline{e_0}$ represents a vector housing weighted residuals (sorted from smallest to largest value)

$\underline{m}$ is a vector housing the mean value of the weighted residuals at all positions

$\underline{\tau}$ is a vector housing the elements of

$$p = \frac{(k - 0.5)}{n} \tag{5.20}$$

(Hill & Tiedeman 2007)

A value of the correlation coefficient of one describes a perfect fit, and indicates that the residuals are independent and normally distributed. Here the fit was judged to be rather poor, why the linear confidence interval for the parameters should be used and interpreted with caution.

5.8 Effect of cell drying and rewetting

When cells prescribed to dry or rewetted a discontinuity between calculated observations and the adjusted parameters are introduced, this since MODFLOW prescribes a dry cell as inactive. Also if cells representing boundary conditions like constant head or river are prescribed as dry, severe effects of the model could be expected. This possible discontinuity degrades PEST's performance. To mitigate the effect of cell drying and rewetting PEST adjust the normal MODFLOW procedure of wetting and rewetting (Watermark Numerical Computing 2005). Still, however, Watermark Numerical Computing (2005) recommends that wetting and re-wetting of cells should be avoided.

Hill and Tiedeman (2007) recommend the use of confined layers as often as possible to circumvent the creation of dry cells.

5.9 Final head distribution

The final head distribution over the different layers in the model can be seen in Figure 5.11 (a-e). The figure shows the massive extent of dry cells in the top layer (Figure 5.11 a) and that the highest groundwater levels can be found in the northeast part of the domain.

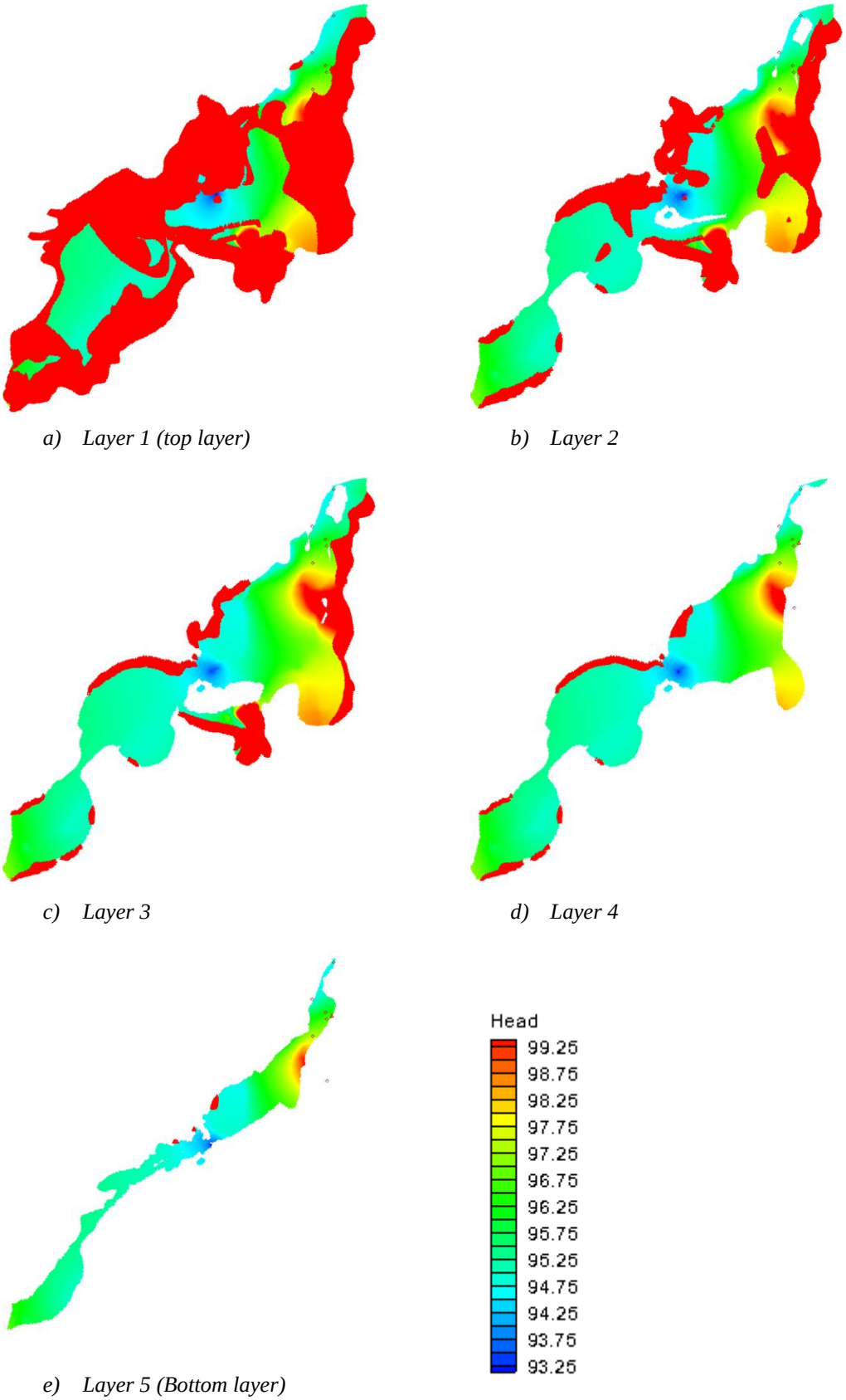

a) Layer 1 (top layer)

b) Layer 2

c) Layer 3

d) Layer 4

e) Layer 5 (Bottom layer)

Figure 5.11 Head distribution by layer

6 Results

The capture zone for the production wells at Storehagen was calculated using MODPATH. The results for different retention times, with a porosity of 20%, can be seen in Figure 6.1. The yellow area in the figures shows the capture zone for a retention time of 14 days. This is the time limit for which raw water from artificial recharge can be regarded as natural groundwater (Livsmedelsverket 2006). The capture zone for a retention time of 100 days is illustrated by the orange area, which is the guideline value for the boundary between the primary and secondary groundwater protection zone, recommended by the Swedish EPA (Naturvårdsverket 2011). The guideline value for the outer boundary of the secondary protection zone is one year (Naturvårdsverket 2011).

This capture zone could be compared with Figure 6.2, where the porosity was set to 10 % and therefore resulted in a higher groundwater velocity and a larger capture zone. The porosity of 20 % (Figure 6.1) was assumed to be more realistic than a porosity of 10 % (Figure 6.2), due to the reasons described in Chapter 2, Section 2.5.

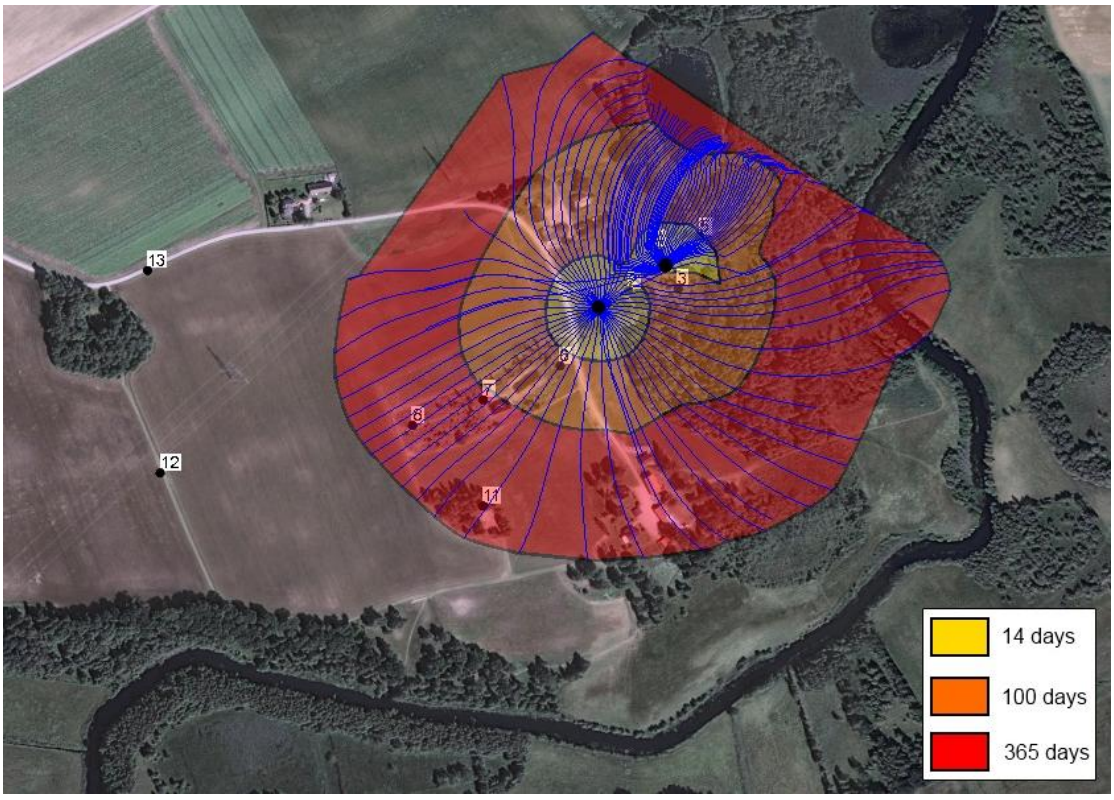

Figure 6.1 Capture zone of the two production wells at Storehagen with a porosity of 20 %.

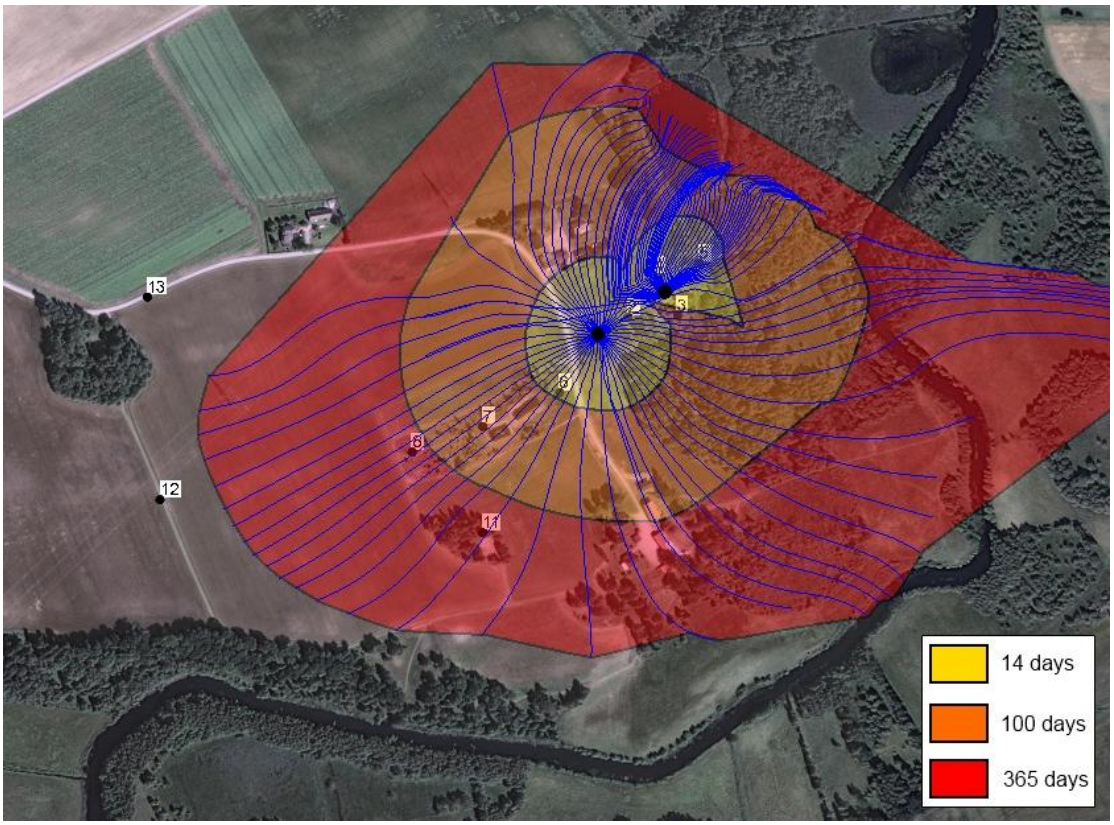

Figure 6.2 Capture zone of the two production wells at Storehagen with a porosity of 10 %.

Figure 6.3 demonstrates the total capture zone according to the model. The extent of the model domain was limited in a number of directions (marked with a dotted line in the figure) and the possible flow from these directions was not included. Approximately 1 km of the Säve River is included in the capture zone.

The influence of the recharge rate on the capture area and transport time was investigated by changing the recharge rate to the upper and lower value of the confidence interval given in Chapter 2 Section 2.6. It was concluded that the recharge rate mainly affected the water levels and that the capture zone and transport time remain mostly unchanged.

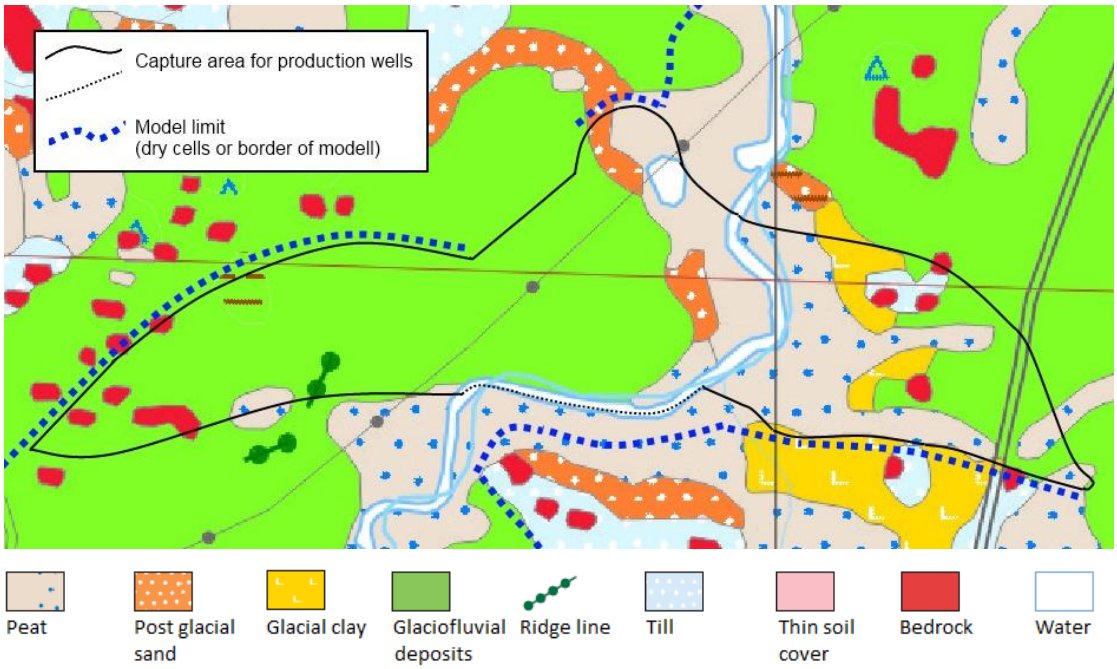

Figure 6.3 Total capture zone of the two production wells at Storehagen.

The flow patterns according to the model can be seen in Figure 6.4. In most parts of the area, the flow directions is primarily towards the river but close to Storehagen the river function as a source to the production wells.

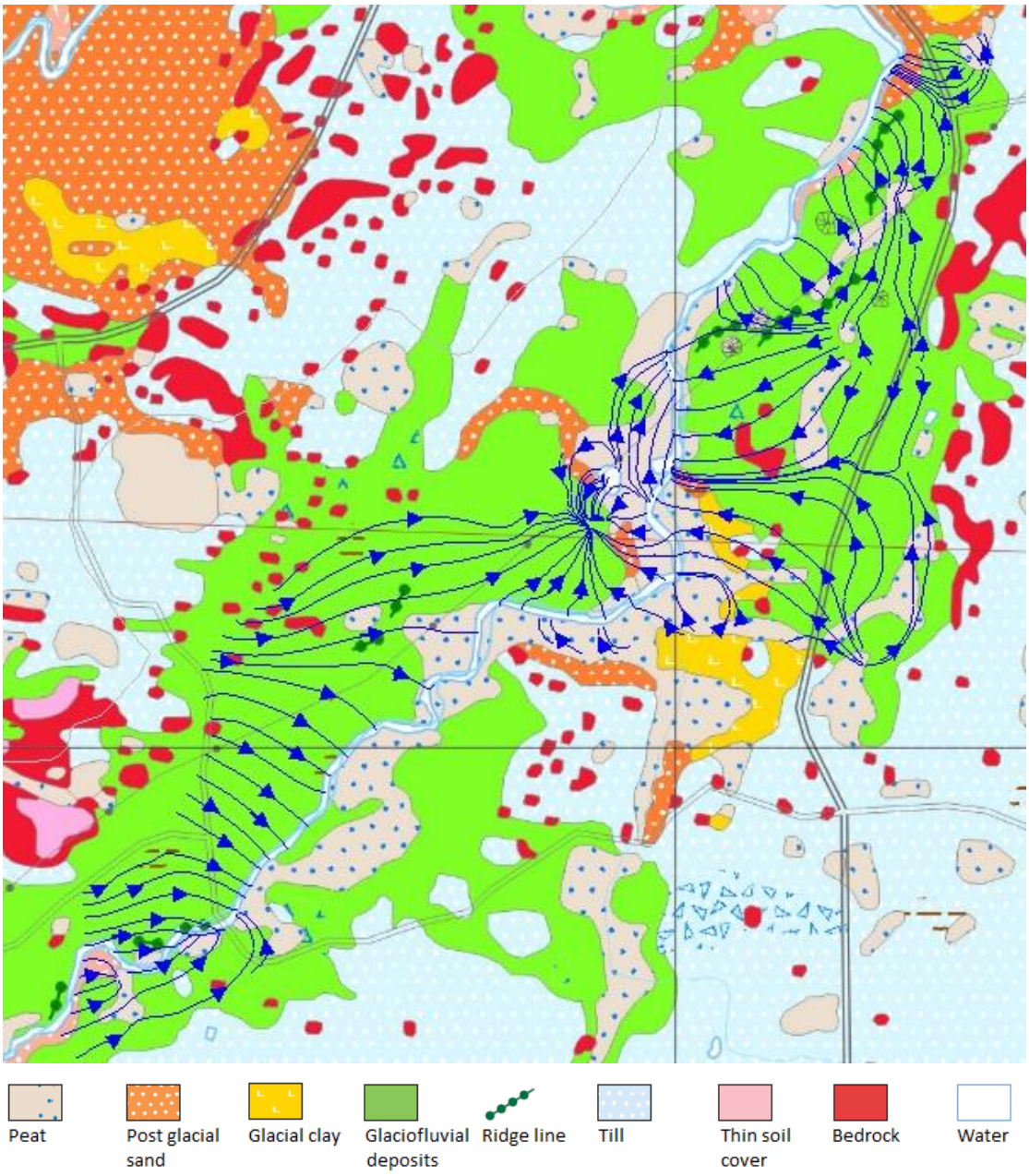

Figure 6.4 Flow patterns in the aquifer according to the model.

In observation wells 12 and 13 high levels of nitrate were detected. The model indicated that the capture zone of observation well 12 may include a farm about 1 km to the west of the production wells, see Figure 6.5. The retention time was estimated to about 30 years from the farm to the observation well and an additional two and a half years to the abstraction well when the porosity was assumed to be 20 %. When the porosity was assumed to be 10 %, the retention time from the farm to the observation well was reduced to 15 years and an additional 1.2 years from the observation well to the abstraction well.

Also in observation well 13 the level of nitrate was high. The flow to the production well from observation well 13 and further back can be seen in Figure 6.5. The calculated pathway through observation well 13 was adjacent to dry cells, which may have limited a possible flow from the north.

Figure 6.5 *Flow patterns to production well via observation wells 13, 12, 8 and 11.*

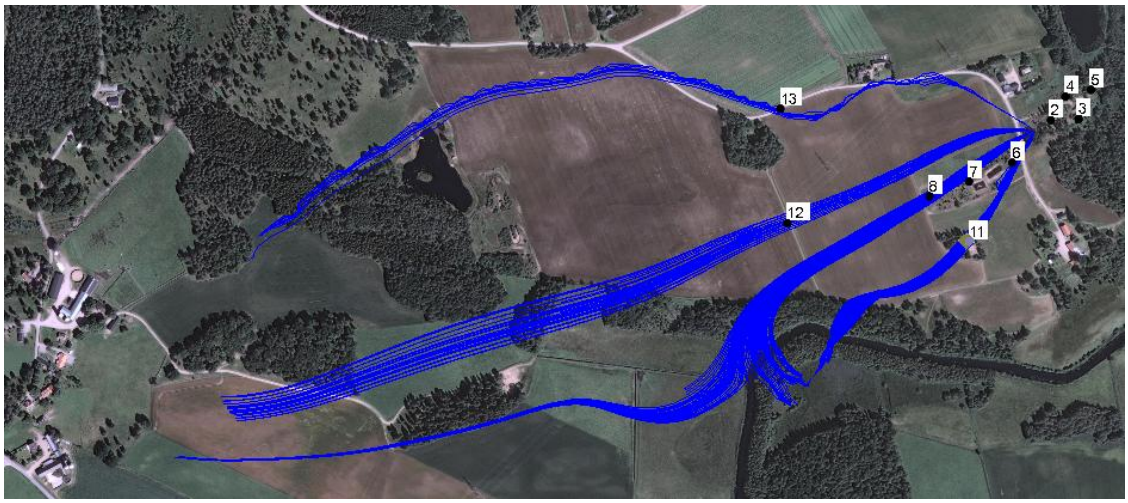

Figure 6.6 *Changed flow patterns with a lower recharge rate. Recharge rate was set to the lower confidence limit: 213 mm/year.*

Figure 6.7 *Changed flow patterns with a higher recharge rate. Recharge rate was set to the upper confidence limit: 737 mm/year.*

If an accident would occur at Road 42 at Bänatorp, the estimated time of travel from the road to the abstraction wells was estimated to four years with a porosity of 20 % (see Figure 6.8) and half this time when the porosity was set to 10 %. The simulation showed that if the abstraction at Storehagen cease, the groundwater flow originating from Road 42 would likely end up in the Säve River and consequently not reach the area of the production wells at Storehagen. The transport time and the flow patterns on the east side of the Säve River were found out to be fairly insensitive to abstraction at Storehagen.

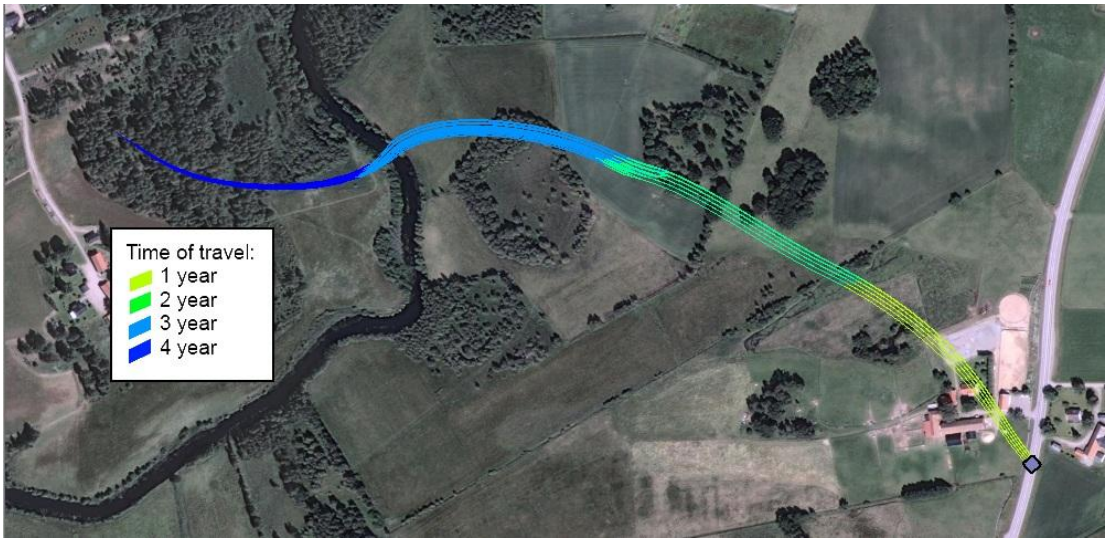

Figure 6.8 Flow path from Road 42 around Bänatorp to the production wells at Storehagen.

It was supposed that the surrounding soil layers have low thickness and that the runoff likely follows the surface. Figure 6.9 is an attempt to show how the flow patterns outside the modelled area could look like, under the assumption that the flow basically follows the topography. The figure also illustrate the calculated flow pattern from the western boundary to the abstraction wells at Storehagen (the flow to the production wells from other directions was not included in this figure).

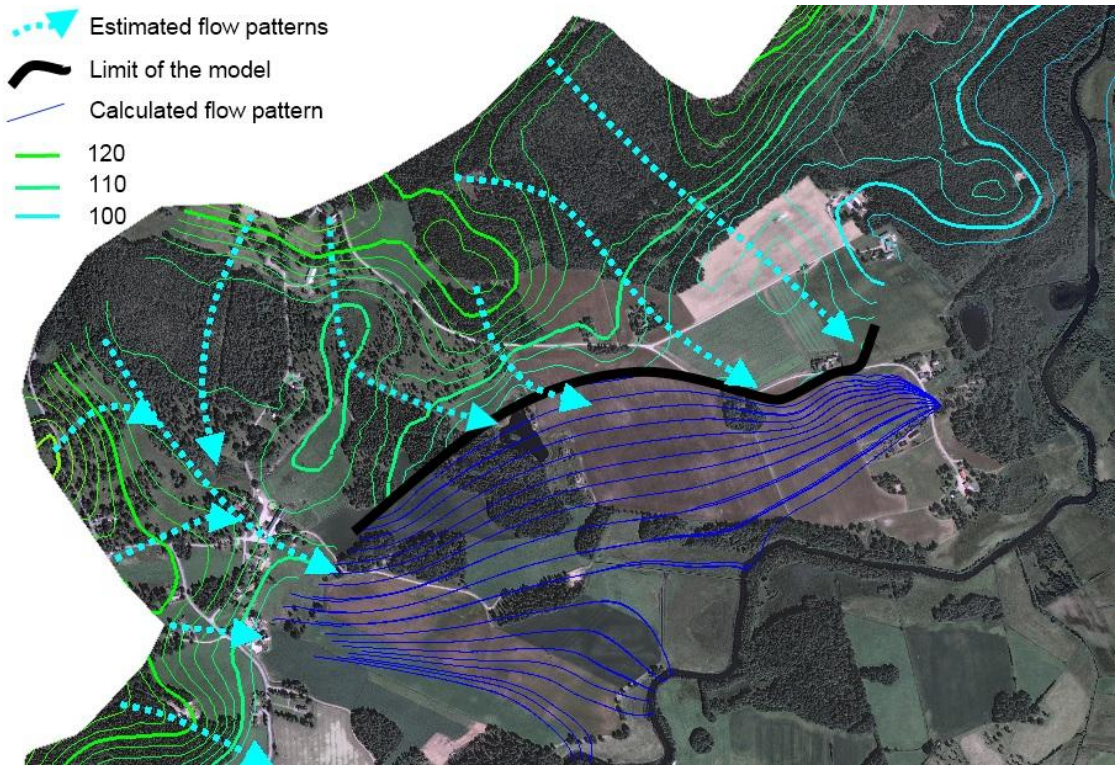

Figure 6.9 *Illustration of flow patterns west of Storehagen. The map is cropped to the catchment area according to Vattenkartan (2011).*

7 Discussion

7.1 Model settings and conceptual model

The model was constructed by a surface TIN, a bottom TIN and borehole data. The surface TIN has grid of 50 m and the mean error of the elevation was ±2 m (Lantmäteriet, 2010). This resolution was belived to be adequate for the topography, since it not is the surface flow that is modeled. However it should be pointed out that these errors also were transmitted to the modeled stratigraphy, this because the surface TIN also was used to prescribe the vertical location of the stratigraphy. It is assumed that these errors have a small influence on the final result.

The limited number of boreholes drilled to bedrock has been an issue in the development of the bottom TIN. Very few drillings has been done in the periphery of the model and the bottom location was in many places estimated by professional judgment and interpretations of the soil map and the surface topography. The bottom TIN has a great impact on the final result and probably also a greate influence on the dry cells north-northwest of Storehagen.

The borehole data ranges from the 1950's to today, and the investigational boreholes are mostly limited to the two areas of Storehagen and Algutstorp. The soil classes in the borehole protocoll was mainly determined in field and not by grain size analysis. The different soil classes in the borehole protocoll has been divided into five hydrogeological units in the conceptual modell. As refered to in Chapter 4 Section 4.1 the hydrogeological unit classification can be seen in Appendix 6. The hydrogeological unit sand includes a whide range of fractions, starting from fine sand/silt to gravel. To combine these into one hydrogeological unit probably affected both the conductivity values and the flow pattern, but it would have been unreasonable to construct a solid with five different sand types. The drillings indicated that the dominating soil type in the area arround Storehagen and Algutstorp is coarse and medium fine sand. The coarser material, such as gravel, as well as the most fine grained sand was assumed to be present in limited areas. The single type of sand in the hyderogeological unit was therefore assumed to probably be correct.

The river and stream bed conductances have a direct impact on the groundwater levels. In this study these values were estimated and no field test were made. To improve the results carefull investigation of the stream beds, especially the small stream through Algutstorp and the larger Torsjöbäcken through at Ormentorp, could be done. At an early stage of the calibration process, the river and the stream bed conductance was parameterized (included in the calibration). The result from the calibration revealed that the these conductances were fairly insensitive in comparison to the other parameters. These conductivities were therefore given fixed values. Even though the sensitivities calculated by PEST were low, it was belived that the conductance has a great impact on the groundwater levels.

As stated in Chapter 5 Section 5.6, the optimal hydraulic conductivity was determined to rather high values for the silt, clay and till layers. The reason for this might be that the less permeable layers, like the clay and silt layers, actually are thinner and less continuous than anticipated. The area consists mostly of sand, why this parameter probably has the most significant influence on the result. The pumping tests indicated that the general conductivity of the aquifer is rather close to the values obtained from the parameter estimation process and it was therefore assumed that the result from the parameter estimation regarding the parameter values was fairly reasonable.

However it should be pointed out that the parameter values for silt, clay and sand obtained from the parameter estimation process was not in a perfect agreement with the reasonable ranges for these materials, and this *could* indicate model bias.

The boundaries of the model were assigned either as a no-flow boundary or a constant head boundary. Considering the recharge and possible inflow from the surrounding till and bedrock, extra recharge was added to the outer areas of the model. A more accurate conceptualisation would possible be to assign a constant flow boundary to simulate the flow from these areas. In this assessment, there were especially two parts of the boundary, northeast of Algutstorp towards Hägrunga and north of Storehagen, which might have been better represented with this type of boundary condition.

7.2 Summary and interpretations of the model calibration

According to the rule of thumb presented by Hill and Tiedeman (2007) the parameter correlation matrix indicated that the parameter set was unique and the correlation coefficient that the fit was very good. With regard to the weighted residuals, the model was judged to be less as good, this because they were believed to not be sufficiently randomly distributed around zero. The residuals belonging to observation wells allocated in the peripheral parts of the area were also shown to be consistently positive and thus indicating model bias.

If more parameters were used in the regression analysis, it might have been possible to obtain an even better model fit. However during the calibration process, emphasis was put on keeping the number of parameters to a minimum, since a high number of parameters might render a non-unique solution. It may be, that a simulation of an aquifer of this size demands numerous parameters, but then it follows that more observations have to be applied to compel the non-uniqueness that could emerge.

The model fit was rather reasonable in the central parts of the model but not at the perimeter. This model bias was supposed to emerge from either too low hydraulic conductivity, from too low base flow across the defined model boundary or from a combination of too low base flow and hydraulic conductivity. However, the aquifer is an esker and when deposited at this altitude the presence of clay should not be very extensive. According to the borehole logs the material in the aquifer is also mostly sand and the hydraulic conductivity determined from aquifer field test fits well to that of sand. Since the hydraulic conductivity values were judged to be fairly reasonable, the model bias was probably due to unaccounted or incorrect base flow /surface runoff across the boundaries.

There is little information of the soil depths and about the head levels at the perimeter of the boundary. At the boundary, the aquifer is mostly facing outcrops of bedrock or layers of till. Initially these till layers were assumed to be thin and with respect to the generally low hydraulic conductivity of till these boundaries were assigned as no-flow boundaries. However some surface runoff across the boundary was expected at a number of locations. These flows were modelled by the allocation of an extra recharge at areas close to the boundary to enable parameterization. Nevertheless this treatment of the boundary conditions could be erroneous and the problem might have been better solved if constant flow conditions had been applied.

The depth of the model domain at the boundaries was also a weak point. The depth at the model boundaries were assigned to approximately the surface elevation minus

three meters, as the extent of bedrock outcrops was of great magnitude there. This might also be an erroneous assumption, and resulted in an extensive amount of dry cells close to the boundaries, which is negative for the parameter estimation procedure. Also since MODFLOW prescribe dry cells as inactive, the added recharge at the boundary was changed and this was identified as one cause of the possible erroneous base flow.

Particularly at the west side of Storehagen and at the northeast side of Algutstorp it was suspected that the till layer might be of a significant depth. Little data was obtained about the aquifer thickness at the boundaries. Thus, this was identified as something that could be investigated further if a more accurate model of the area should be developed.

East of Algutstorp there is a hill that reaches almost 150 masl and the hill was believed to contribute to the groundwater recharge of the aquifer via the till deposit. It is likely that the surface runoff from this hill has a great influence on the water level in the northeast part of Algutstorp. To the southwest of Storehagen the topography is typically 20 m lower than the hill close to Algutstorp, and the area that could yield water is as a result of minor extent here compared to Algutstorp. Also the presence of drains is more common here, why the surface runoff or base flow from this area was judged to be of minor importance. The obtained head distribution at this area can therefore still be relatively correct.

Hill and Tiedeman (2007) recommend that confined layers might be used to overcome the problem of dry cells, but the general characteristics of the aquifer was understood to be of such a type (unconfined) that it would be difficult to motivate this choice. For instance, the top layer (sand) was assumed to be of a great thickness. A possible more suitable approach could have been to just define one layer and move the boundaries more towards the centre of the aquifer.

7.3 Analysis of the results

The calculated groundwater levels at Algutstorp was shown to have a less good fit compared to measured levels than the rest of the model and the flow patterns obtained indicated that this specific area was poorly represented by the model. The topography implies that the esker continues from the northwest, towards Hägrunga, why a significant inflow from this area could be expected. In this assessment the inflow has been assessed by extra recharge, but the calculated groundwater levels indicated that this might not have been a good simplification. The stream through Algutstorp has probably a too large influence on the model, this was seen when the model was compared to data from the pumping tests.

The flow pattern at Storehagen was judged to be reliable, since the area most likely consists of sand and has more or less the same geological formation history and therefore assumed to have approximately the same conductivity. The spatial distribution of the soil types at Storehagen was assumed to be fairly accurate, since 30 investigational drillings have been made in the area. Also since the inflow from the surrounding till and bedrock was assumed to be of minor magnitude the occurrence of dry cells here, might not have affected the flow pattern as much as on other locations. The pathways to the wells were therefore judged as trustworthy, even though the transport time was different.

Observation well 13 is located close to the border of the model and the flow to the observation well runs along this border. This means that a potential flow from the north was limited in the model and the flow path to this well was more uncertain than e.g. the pathways to observation well 12. Along the pathway of the flow though observation well 13 a pond is located. This pond was not included in the model and might have influenced the flow pattern.

According to the model, the water in observation well 12 and 13 originates from the area of a farm, about 1.6 km west of the observation wells, and arable land in between. The transport time from the farm to the production wells was determined to 30 years and it was interpreted that this might been a very old problem and the elevated levels of nitrate could be a problem also in the future, depending on whether the contamination has ceased or not.

The flow path from Road 42 to the production wells was about 1 km and the transport time was assessed to 4 years. This could be compared to the transport time of to 30 years for the 1.6 km long path from the production well to the farm in the Siene. One likely reason regarding the shorter transportation time, might have been that the groundwater gradient along the pathway between Road 42 and the Säve River was steeper, due to lower hydraulic conductivity.

7.4 Evaluation of the use of GMS, MODFLOW and PEST

PEST and MODFLOW were used via GMS and not from terminal mode, because it was not fully understood how to use PEST and MODFLOW in that way. MODFLOW via GMS was thought to be a very elaborate and comprehensive groundwater simulation program as it allows modelling of almost any feature of interest. One disadvantage was however that it was rather time consuming to work with. For example when the extent of the model domain was changed the existing grid had to be erased and MODFLOW had to be initialized once again and from that it followed that all the MODFLOW settings had to be reformulated. PEST was believed to drastically reduce the calibration time, and was relatively easy to use. However it would be better if incorporated more fully in GMS, for example it was not completely clear how to incorporate a full weight matrix or prior information via GMS. Also it was not clear how to obtain the derivatives that constitute the Jacobian matrix. If obtained these could be used to calculate a number of fit-independent statistics that was described by Hill and Tiedeman (2007) for example leverage statistics.

When PEST, or any other indirect inverse modelling technique, is applied it was understood that the user is forced to deal with issues like parameter correlation and parameter insensitivity which is not the case when the technique of manual calibration is applied. When using automated calibration technique, model bias was also in some way highlighted. Account taken to these issues was believed to be vital in order to obtain a proper and unique model that truly represents the system..

7.1 Further improvements

One major uncertainty was the extent of the different material layers and the depth to bedrock. Further investigations of these properties are probably needed. It would also be beneficial concerning possible future modelling if an additional number observation wells were available, meaning that a greater amount of observations

would allow definition of more parameters. Regarding the model geometry and stratigraphy Hill and Tiedeman (2007) propose that the effect of potentially new information could be investigated by running the model with a new assumed geometry, and from that conclude what new field data to collect (this was to some extent done).

Location and type of additional observations could be investigated with regard to the information that they offer to the parameters. Fit-independent statistics that could be used are, according to Hill and Tiedeman (2007), parameter correlation coefficients, dimensionless scaled sensitivities, composite scaled sensitivities, and leverage statistics.

Concerning the soil conditions and the depth to bedrock little were known at the boundaries why effort preferably should be applied here in first place. Areas of certain interest are displayed in Figure 7.1.

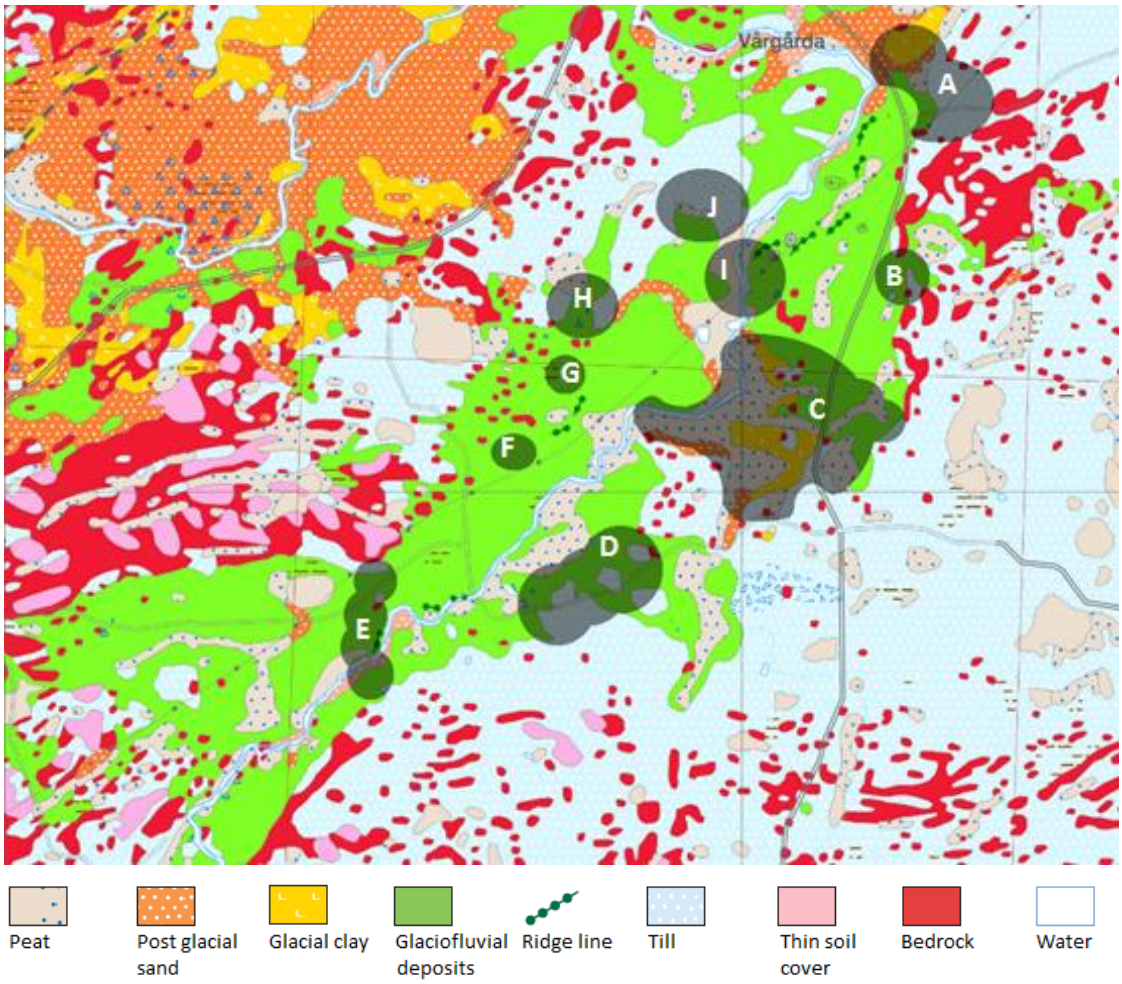

Figure 7.1 *Areas of interest considering future investigation of the aquifer depth and soil conditions*

Concerning the area north to northeast of Algutstorp (area A) high groundwater recharge was expected from the hill to the east. However, major uncertainties were the depth to bedrock and the magnitude of the denser materials. The till layer was assumed to be relatively thin (3 m) but it was suspected that the layer is of a greater

thickness. Also additional measurements of the water level in this area are preferable if a proper constant head boundary should be applied towards the dense materials.

At area B, the surroundings of the truck centre between Svenstorp and Svantetorp, additional information about the aquifer thickness is also needed.

The area that is encircled by Bänatorp, Storehagen and Ormentorp (area C) was believed to house low permeable material and it is of interest to find out more clearly the extent of this material but also the depth to bedrock.

In area D, the depth to firm bedrock was also a major issue, and has to be further investigated.

Area E characterizes the south west boundary, with an assumed constant head boundary condition. However little was known about the water level at the sides of the river and more investigations are needed.

The areas southwest and northwest of Storehagen were thought to be relatively effectively drained by the streams and with respect to the topography it was anticipated that the area yield relatively little water across the boundary. Instead the contribution to the groundwater recharge may be due to leakage of the streams in to the aquifer. Since relatively little groundwater recharge was expected due to the surrounding area to the west, major drawdown could emerge in this area and thus proper knowledge about the aquifer thickness is needed. It is therefore recommended that the areas denoted F, G, H and J should be investigated with regard to the depth.

Between Algutstorp and Storehagen (area I) very little information exists about the material properties and the hydraulic connection between the two abstraction areas. For example it was anticipated that the esker was once passing across here and has since them been eroded away by the Säve River. More knowledge about these properties and also the depth to firm bottom is desirable.

Moreover Hill and Tiedeman (2007) generally recommend that flow observations are used in the calibration process. It is here therefore recommended that a flow observation program should be implemented. The program could consist of one additional gauging station in the Säve River and measurements of the flow in the streams at their confluence with the Säve River and at the boundary of the aquifer, see Figure 2.1. It is of great interest to find whether the stream that passes through Algutstorp water treatment plant and the stream that passes by Storehagen, are draining the aquifer or if they contributes to the groundwater recharge. Apart from revealing the flow pattern, a more crucial incitement (not covered in this report) could be the risk of contamination, noting that the stream in Algutstorp passes a road and a truck centre.

Figure 7.2 *Proposed locations for measurements of the flow in the river and in the streams. © Lantmäteriet Gävle 2011. Consent I 2011/0072.*

To obtain a better understanding of the general hydraulic properties of the aquifer, additional pumping tests could be done at other locations than at Storehagen and Algutstorp. One aspect to understand better was the anisotropy. However note should be taken that when determining the anisotropy, a larger number of water level readings have in general to be conducted during the very first part of the pumping test.

The hydraulic conductivity of the low permeability materials like silt and clay has not been investigated individually, only the general or vertical average conductivity was obtained from the pumping tests. Neither was any grain size analysis conducted for these types of material, because no samples were available. It is thus recommended that if future borehole investigations are conducted, sampling of these materials should be carried out as well.

One last issue that also should be mentioned is the hydraulic conductance for the Säve River and the streams. The conductance was approximated very roughly why a more stringent analysis could be done. The conductance could be determined if the riverbed thickness, river width and the riverbed material conductivity is investigated, preferably at a number of locations.

The modelling could perhaps have been better made if a local model was applied at a specific area of particular interest, and using a solution of a regional model as boundary conditions. Nevertheless a global model has to be relatively correct for a local model to apply and there are still major uncertainties regarding the depth of the aquifer and the extent of the different material layers. Consequently these issues may have to be resolved before implementing a local model.

8 Conclusions

It was concluded that the model was sufficiently accurate in the area around Storehagen and in the area southwest of Storehagen, why the identified capture zone at this part of the aquifer also was reasonable. One motivation for this conclusion was that the base flow or surface runoff from the south west boundary was judged to be of a minor magnitude. Due to the calculated flow pattern in this area it was believed that the source of the nitrate originates from the area between the observation wells 12 and 13 and Siene.

Generally for the whole area the major uncertainties are due to the little knowledge about the extent of material layers, the aquifer depth and the boundary conditions.

The parameter estimation technique and the associated theory has served the purpose of identifying insensitive parameters, reducing parameter correlation thus increasing the uniqueness of the solution, and reducing the calibration time.

Based on this report the Vårgårda Water Board possesses a concrete indication of the aquifer behaviour in the area around Storehagen and the model's shortcomings, and could from it make interpretations and formulate actions.

8.1 Further improvements

The following points summarize the proposed improvements:

- Investigations of the aquifer geometry and stratigraphy are recommended. Proposed locations are described in Chapter 7, Section 7.5.
- Grain size analysis for the soil types; clay, silt and till.
- Investigate the porosity of the different soil types and the material originating from the different areas..
- Additional pumping tests, at other locations than Storehagen and Algutstorp,
- More groundwater head observations to allow the use of more parameters and more measurement readings at each observation to facilitate a more trustful assessment of the observation standard deviation.
- Stringent investigations of the boundary conditions.
- Observe the flows in the streams and in the river.

9 References

Allmäna Ingenjörsbyrån AB (1950). *Investigational borrings: Algutstorp och Tånga hed.* In Swedish. Allmäna Ingenjörsbyrån AB.

Allmäna Ingenjörsbyrån AB (1976) . *Investigational borrings and pumping tests: Storehagen.* In Swedish. Allmäna Ingenjörsbyrån AB. (Borehole protocoll)

Anderson M. and Woessner W (1992) . *Applied groundwater modeling. Simulation of Flow and Advective Transport.* San Diego, California: Academic Press Inc.

Andreasson P.-G (2006) . *Geobiosfären.* In Swedish. Lund: Studentliteratur.

Aquaveo (2011a) . *Groundwater Modelling System 7.1*. (Computer program)

Aquaveo (2009a) . GMS:BCF-package Dialog. *XMS wiki*. http://www.xmswiki.com. (3 Mar. 2011)

Aquaveo (2009b) . Boundary matching. *XMS wiki*. http://www.xmswiki.com. (5 May 2011)

Aquaveo (2011b) . GMS:Observations. *XMS wiki*. http://www.xmswiki.com. (18 Apr. 2011)

Aquaveo (2009c) . GMS:River Package. *XMS wiki*. http://www.xmswiki.com. (11 May 2011)

Aquaveo (2010) . *GMS 7.0 Tutorials. MODFLOW – Conceptual Model Approach.* Aquaveo.

Digitala Kartbiblioteket (2011). (Maps and topography models) © Lantmäteriet Gävle 2011. Consent I 2011/0072.

Division of GeoEngineering, Chalmers University of Technology (2000) *Kvartärgeologi.* Course compendium in Engineering Geology (VGE 370). In Swedish. Göteborg.

Fetter C.W. (1988). *Applied Hydrogeology*. Fourth Edition. New Jersey: Prentice Hall.

Fredén C. (1994). *Geology.* SNA Publishing. Department of Human Geography. Stockholm University.

Gustafson G. and Carlsson L. (1997). *Provpumpning som geohydrologisk undersöknings metodik.* In Swedish. Göteborg: Geologiska institutionen.

Halldin S. (1988). *Swedish evaporation research - A review.* Section of Hydrology. Uppsala University.

Harbaugh A. (2005). *MODFLOW-2005, The U.S. Geological Survey Modular Ground-Water Model – the Ground-Water Flow Process.* Virginia, USA: U.S. Geological Survey.

Hill M. (1998). *Methods and Guidelines for effective model calibration.* Colorado: U.S Geological Survey. Water-Resources Investigations Report: 98-4005

Hill M. and Tiedeman C. (2007). *Effective groundwater model calibration.* New Jersey: John Wiley & Sons.

Kjessler & Mannestråle AB (1990). *Investigational borrings: Algutstorp och Storehagen.* In Swedish. Uppdragnummer: 412469 (Grain size analysis and borehole protocoll)

Kresic N. (2007). *Hydrogeology and groundwater modeling.* Second edition. Rixeyville, Virginia, USA: Taylor & Francis Group.

Livsmedelsverket (2006) . *Vägledning dricksvattenföreskrifterna.* In Swedish. Livsmedelsverket. (SLVFS 2001:30)

Lång L.-O. and Persson T. (2011). *K130 Beskrivning till kartan Grundvattenförekomster i Vårgårda kommun.* In Swedish. Uppsala: Sveriges geologiska undersökning.

Naturvårdsverket (2011). *Handbok om vattenskyddsområde*. Handbok 2010:5. Utgåva1. In Swedish. Naturvårdsverket.

Pollock D. (1994). *User's Guide for MODPATH/MODPATH-PLOT, Version 3: A particle tracking post-processing package for MODFLOW, the U. S. Geological Survey finite-difference ground-water flow model*. U.S Geological Survey. Open-File Report: 94-464

Ramböll Sverige AB (2007) . *Reservvattentäkt Algutstorp.* In Swedish. Göteborg: Ramböll Sverige AB. Uppdragsnummer: 61450619712

Ramböll Sverige AB (2010). *Investigational borrings: Algutstorp vattentäkt.* In Swedish. (Borehole protocoll)

Ramböll Sverige AB (2011). *Vattentäkter Storehagen och Algutstorp. Tekniskt underlag med förslag till skyddsområde och skyddsföreskrifter.* In Swedish. Göteborg: Ramböll Sverige AB. Uppdragsnummer: 61470828899

SGU (2004) . *Investigational borrings and seismic surveys: Vårgårda kommun.* (Borehole protocoll)

SMHI (2009a). Dataserier med normalvärden för perioden 1961-1990. *Klimatdata.* In Swedish. http://www.smhi.se. (15 March 2011)

SMHI (2009b). Årsavdunstning medelvärde 1961-1990. *Klimatdata*. In Swedish. http://www.smhi.se. (25 March 2011)

SMHI (2010) . Modellberäknad vattenföring och vattenkvalitet. Produkter och tjänster. In Swedish. http://www.smhi.se (25 March 2001)

Stephens D., Hsu K.-C., Prieksat M., Ankeny M., Blandford N. and Roth T. (1998). A comparison of estimated and calculated effective porosity. *Hydrogeology Journal (1998) 6:156–165* , page 156–165.

Svenskt Vatten (2011). Vattenverk & reningsprocesser. *Vattentjänster*. In Swedish. http://www.svensktvatten.se/ (29 March 2011)

Vattenkartan (2011). http://www.vattenkartan.se. (2 Feb. 2011)

Virtual Insitute of Applied Science (2010). *Distrubution Calculator*. (Computer Program)

Watermark Numerical Computing (2005) . *PEST Model-Independent Parameter Estimation.* Fifth Eddition. Watermark Numerical Computing. (User Manual)

White F. (2009). *Fluid mechanics.* Sixth Edition. New York: McGraw-Hill.

Jordartskartan

Detaljerad undersökning

SGU
Sveriges geologiska undersökning
Geological Survey of Sweden

Kartan visar utbredningen av jordarter i eller nära markytan. Informationen är anpassad för visning i skala 1:50 000, vilket innebär att minsta ytorna som finns representerade har en diameter på 50m i naturen. Lägesnoggrannheten är vanligtvis bättre än 50 meter. Generaliseringar förekommer. Exempelvis kan områden med många, små, närliggande hällar presenteras som en sammanhängande häll på kartan, och avlagringar som bara täcker små ytor i verkligheten men som har stor betydelse för förståelsen av den geologiska utvecklingen i ett område, som isälvsavlagringar, kan ha överdrivits i kartbilden.

Ytterligare information, om till exempel jordarternas utbredning under ytan, finns lagrad i SGUs databas och kan, liksom bland annat kartbladsbeskrivningar, beställas från SGU.

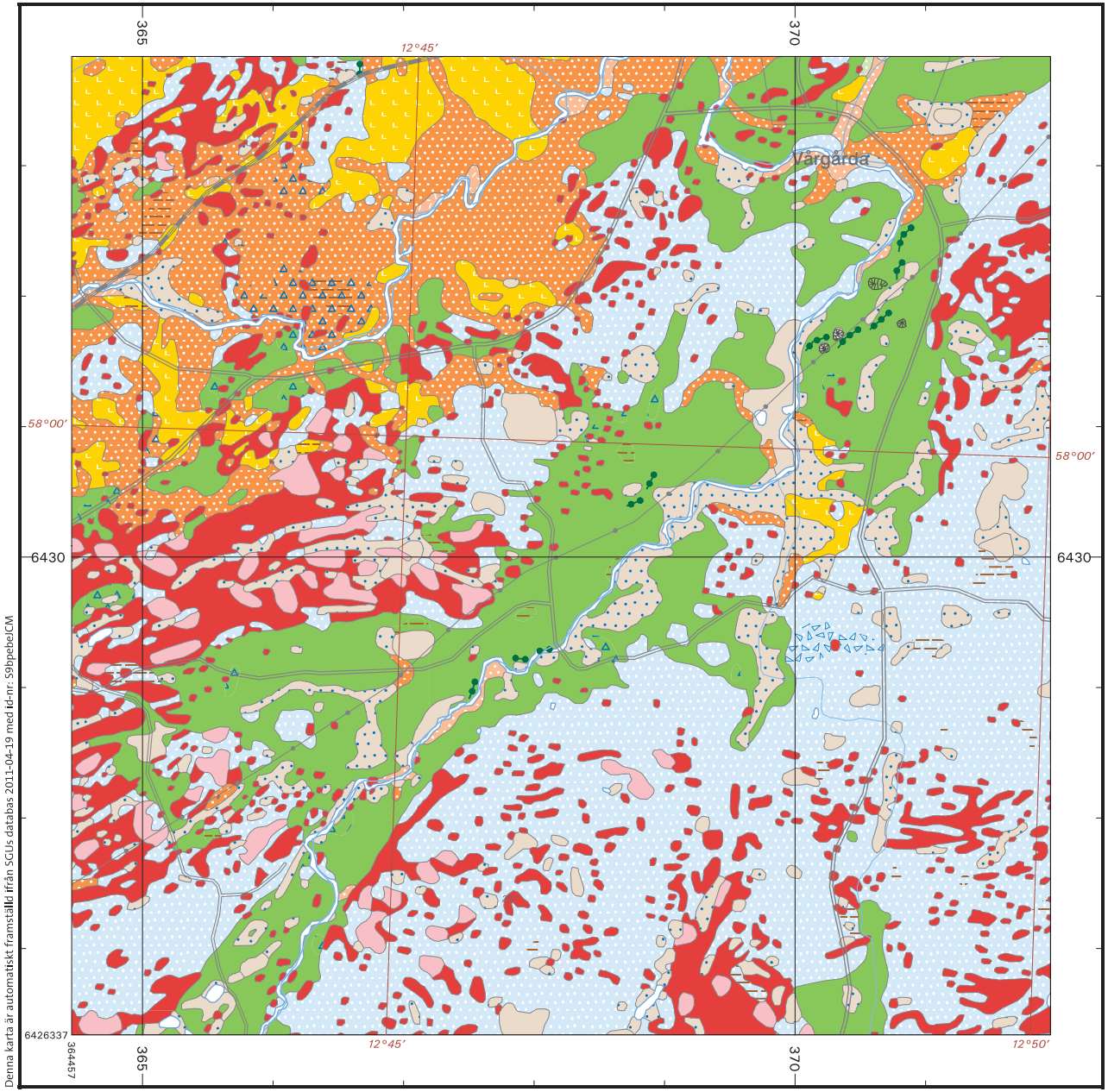

- Mossetorv
- Kärrtorv
- Tunt eller osammanhängande ytlager av torv
- Älvsediment, ler--silt
- Älvsediment, sand
- Postglacial sand
- Glacial lera
- Glacial grovsilt-finsand
- Isälvssediment
- Åskrön
- Sandig morän
- Hög blockfrekvens på annan jordart än morän
- Blockrik yta
- Tunt eller osammanhängande jordtäcke på berg
- Berggrund
- Vatten
- Jord- eller grustäkt

Denna karta är automatiskt framställd ifrån SGUs databas 2011-04-19 med id-nr: S9bpebeJCM

Huvudkontor:
Box 670
751 28 Uppsala
Tel: 018-17 90 00
E-post: kundservice@sgu.se
www.sgu.se

0 0,5 1,0 1,5 2,0 2,5 km

Skala 1:50 000

Topografiskt underlag: Ur GSD-Översiktskartan
© Lantmäteriet. MS2009/08799

Rutnät i svart anger koordinater i SWEREF 99 TM.
Gradnätet i brunt anger latitud och longitud
i referenssystemet SWEREF 99.

1 Aquifer analysis

The method is based on the Cooper-Jacob Straight Line solution of the Theis' equation. Generally if the pumping rate is constant and the aquifer is confined the drawdown is plotted against *t/t'* in a semi logarithmic diagram. In the diagram the time *t* is the time period between the initiations of the pumping to the point of time at which a particular drawdown is measured. *t'* is the time that has prevailed after the pumping has stopped to the point of time at which a particular drawdown is measured.

If a line is fitted to the straight part of the drawdown curve and the line is extend over a log-cycle, the difference in the drawdown over that log-cycle is denoted *Δs* and is used in the equation below to calculate the transmissivity.

$$T = \frac{0.183\,Q}{\Delta s} \tag{1}$$

where *Q* is the pumping rate.

However since the pumping rate varied, the transmissivity was calculated from

$$T = \frac{0.183\,Q_{last}}{\Delta s} \tag{2}$$

and the time *t* was modified as

$$t = t^* = Q_1 t_1 + Q_2 (t_2 - t_1) \ldots . Q_n (t_n - t_{n-1}) \tag{3}$$

Since it was assumed that the aquifer is unconfined the drawdown recovery data was corrected by means of

$$s' = s - \frac{s^2}{2h} \tag{4}$$

where

s is the recorded drawdown and *h* is the saturated thickness of the aquifer. The saturated thickness was approximately determined to 12 m and was calculated as the mean thickness of the aquifer subtracted by the mean distance between the water table and the ground surface measured before the initiation of the pumping test. The mean thickness of the aquifer was determined based the depth of a number of wells in the vicinity to the abstraction well.

The reason for the correction is that the above equation is based on the assumption that the aquifer is confined and to account for the transmissivity change that occur in a unconfined aquifer the drawdown has to be corrected (Kresic 2007).

Appendix 2 – Conductivity values

Pumping test carried out in 1976.

Table 1.1 Calculation of the adjusted time

Pumping rate, Q [m^3/s]	Duration, dt [min]	Q·dt [(m^3/s)·min]
0.029	540	15.66
0	1620	0
0.029	12240	354.96
0.027	4680	126.36
0.029	2340	67.86
0	90	0
0.027	90	2.43
0	120	0
0.027	1440	38.88
0.025	18660	466.5
0	120	0
0.02	720	14.4
0.023	540	12.42
0.02	6840	136.8
0.023	13860	318.78
Sum:	63900	1555.05

Total duration: 63900 min
44.4 days

Adjusted duration, t*: 67611 min
$\left(\frac{Last\ recorded\ Q}{Q \cdot dt}\right)$ 47.0 days

Appendix 2 – Conductivity values

Table 1.2 Observation well 2. Initial groundwater level is 34.75 m and adjusted duration (t) is 67611 min.*

Date and time	t' [min]	t*+t' [min]	(t*+t')/t' [-]	Groundwater level [m]	Drawdown [m]	Correction factor [m]	Corrected drawdown [m]
1976-05-14 09:00	1	67612	67612	33.12	-1.63	0.1107	-1.74
1976-05-14 18:00	540	68151	126	33.35	-1.40	0.0817	-1.48
1976-05-14 21:00	720	68331	95	33.40	-1.35	0.0759	-1.43
1976-05-15 00:00	900	68511	76	33.50	-1.25	0.0651	-1.32
1976-05-16 00:00	2340	69951	30	34.08	-0.67	0.0187	-0.69
1976-05-17 00:00	3780	71391	19	34.35	-0.40	0.0067	-0.41
1976-05-18 00:00	5220	72831	14	34.50	-0.25	0.0026	-0.25
1976-05-19 00:00	6660	74271	11	34.60	-0.15	0.0009	-0.15
1976-05-20 00:00	8100	75711	9	34.67	-0.08	0.0003	-0.08
1976-05-21 00:00	9540	77151	8	34.75	0.00	0.0000	0.00

Appendix 2 – Conductivity values

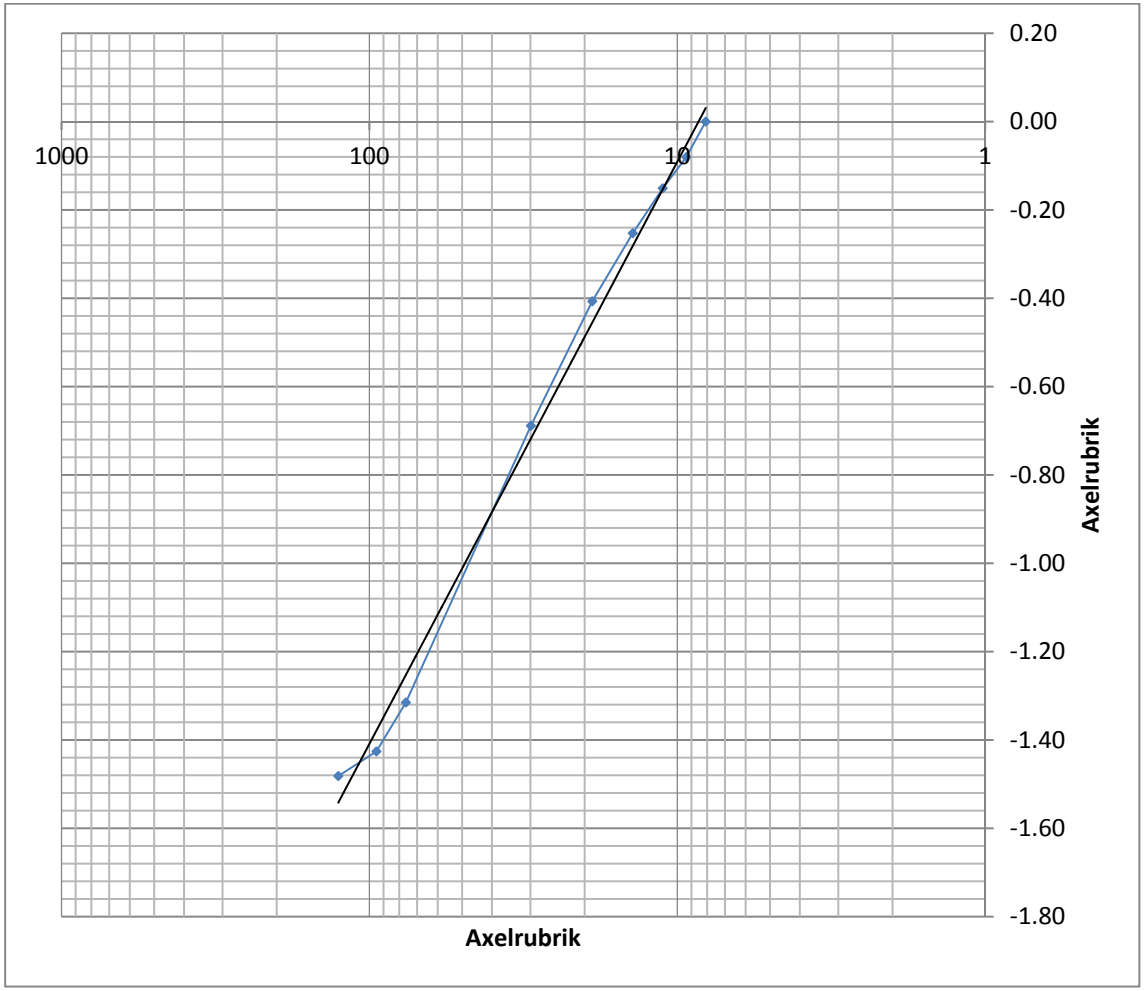

Figure 1.1 Observation well 2 – plotted drawdown.

From Figure 1.1 follow parameters is deduced: Δs=1.31 m and T=0.0032 m^2/s. For an overview of all transmissivity values see Table 3.1.

Table 1.3 Observation well 3. Initial groundwater level is 34.78 m and adjusted duration (t) is 67611 min.*

Date and time	t' [min]	t*+t' [min]	(t*+t')/t' [-]	Groundwater level [m]	Drawdown [m]	Correction factor [m]	Corrected drawdown [m]
1976-05-14 09:00	1	67612	67612	33.30	-1.48	0.0913	-1.57
1976-05-14 18:00	540	68151	126	33.40	-1.38	0.0794	-1.46
1976-05-14 21:00	720	68331	95	33.55	-1.23	0.0630	-1.29
1976-05-15 00:00	900	68511	76	33.66	-1.12	0.0523	-1.17
1976-05-16 00:00	2340	69951	30	34.17	-0.61	0.0155	-0.63
1976-05-17 00:00	3780	71391	19	34.41	-0.37	0.0057	-0.38
1976-05-18 00:00	5220	72831	14	34.54	-0.24	0.0024	-0.24
1976-05-19 00:00	6660	74271	11	34.64	-0.14	0.0008	-0.14
1976-05-20 00:00	8100	75711	9	34.70	-0.08	0.0003	-0.08
1976-05-21 00:00	9540	77151	8	34.78	0.00	0.0000	0.00

Appendix 2 – Conductivity values

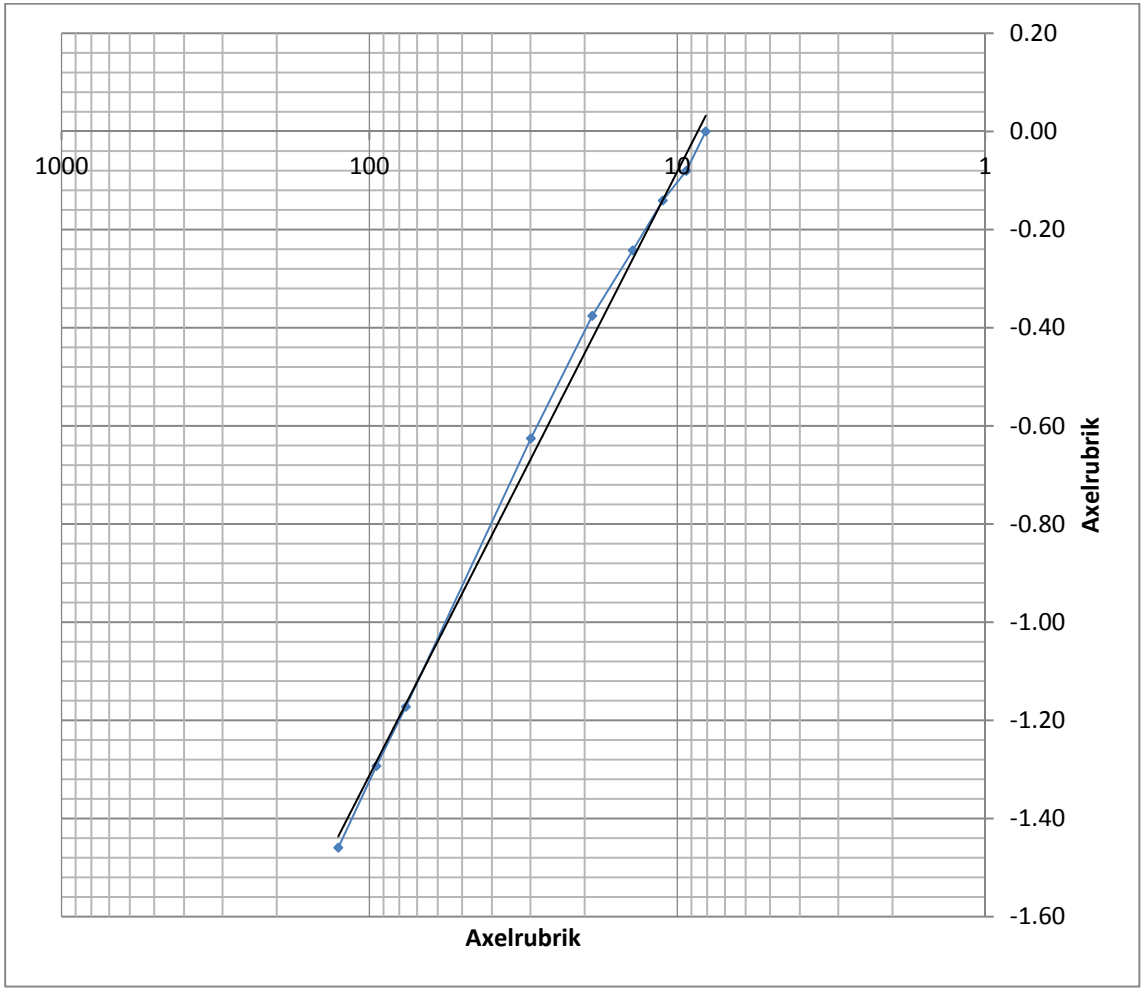

Figure 1.2 Observation well 3 – plotted drawdown.

From Figure 1.2 follow parameters is deduced: Δs=1.22 m and T=0.0034 m^2/s. For an overview of all transmissivity values see Table 3.1.

Table 1.4 Observation well 4. Initial groundwater level is 34.74 m and adjusted duration (t) is 67611 min.*

Date and time	t' [min]	t*+t' [min]	(t*+t')/t' [-]	Groundwater level [m]	Drawdown [m]	Correction factor [m]	Corrected drawdown [m]
1976-05-14 09:00	1	67612	67612	33.10	-1.64	0.1121	-1.75
1976-05-14 18:00	540	68151	126	33.20	-1.54	0.0988	-1.64
1976-05-14 21:00	720	68331	95	33.30	-1.44	0.0864	-1.53
1976-05-15 00:00	900	68511	76	33.42	-1.32	0.0726	-1.39
1976-05-16 00:00	2340	69951	30	34.14	-0.60	0.0150	-0.62
1976-05-17 00:00	3780	71391	19	34.36	-0.38	0.0060	-0.39
1976-05-18 00:00	5220	72831	14	34.48	-0.26	0.0028	-0.26
1976-05-19 00:00	6660	74271	11	34.60	-0.14	0.0008	-0.14
1976-05-20 00:00	8100	75711	9	34.68	-0.06	0.0002	-0.06
1976-05-21 00:00	9540	77151	8	34.74	0.00	0.0000	0.00

Appendix 2 – Conductivity values

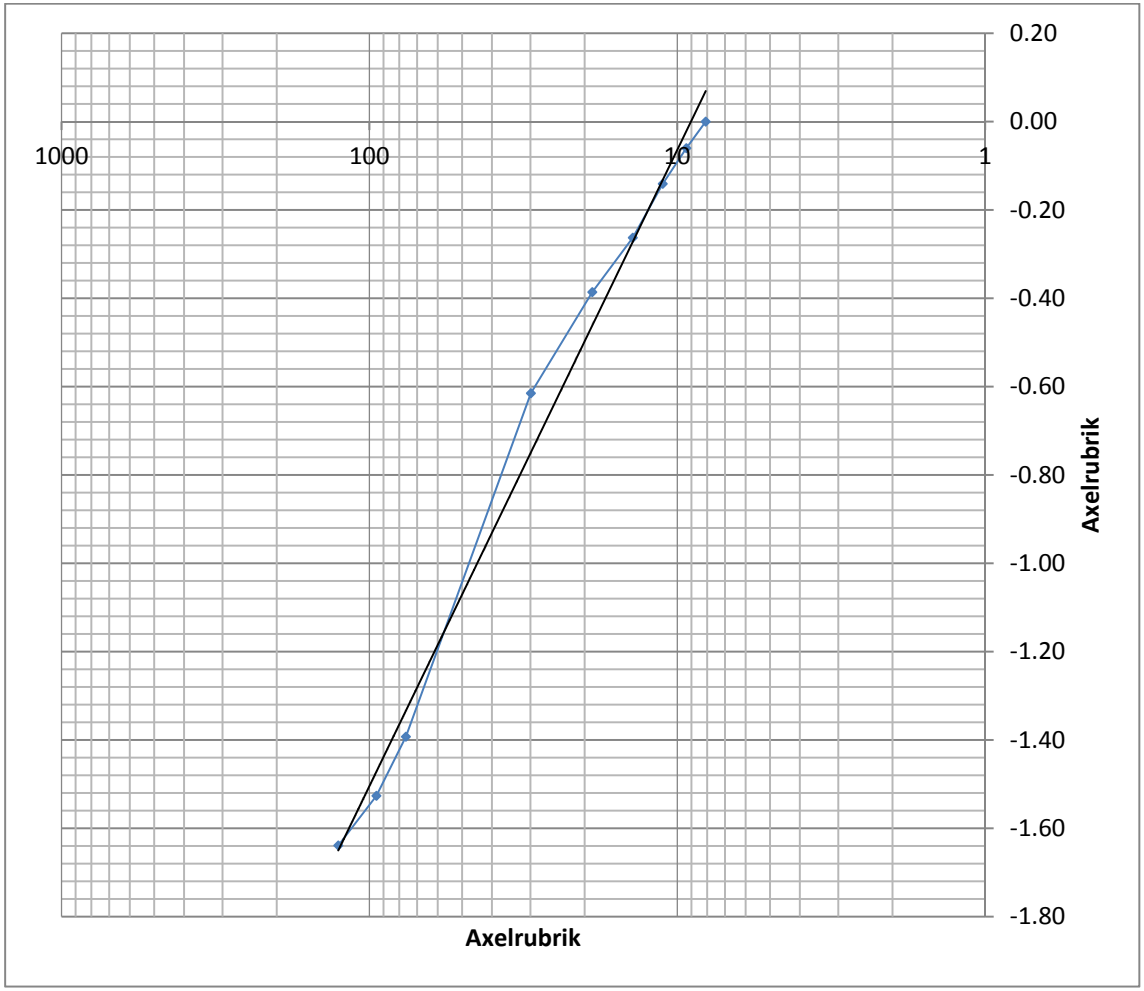

Figure 1.3 Observation well 4 – plotted drawdown.

From Figure 1.3 follow parameters is deduced: Δs=1.42 m and T=0.0030 m^2/s. For an overview of all transmissivity values see Table 3.1.

Table 1.5 Observation well 5. Initial groundwater level is 34.72 m and adjusted duration (t) is 67611 min.*

Date and time	t' [min]	t*+t' [min]	(t*+t')/t' [-]	Groundwater level [m]	Drawdown [m]	Correction factor [m]	Corrected drawdown [m]
1976-05-14 09:00	1	67612	67612	33.23	-1.49	0.0925	-1.58
1976-05-14 18:00	540	68151	126	33.35	-1.37	0.0782	-1.45
1976-05-14 21:00	720	68331	95	33.42	-1.30	0.0704	-1.37
1976-05-15 00:00	900	68511	76	33.53	-1.19	0.0590	-1.25
1976-05-16 00:00	2340	69951	30	34.05	-0.67	0.0187	-0.69
1976-05-17 00:00	3780	71391	19	34.32	-0.40	0.0067	-0.41
1976-05-18 00:00	5220	72831	14	34.48	-0.24	0.0024	-0.24
1976-05-19 00:00	6660	74271	11	34.59	-0.13	0.0007	-0.13
1976-05-20 00:00	8100	75711	9	34.67	-0.05	0.0001	-0.05
1976-05-21 00:00	9540	77151	8	34.72	0.00	0.0000	0.00

Appendix 2 – Conductivity values

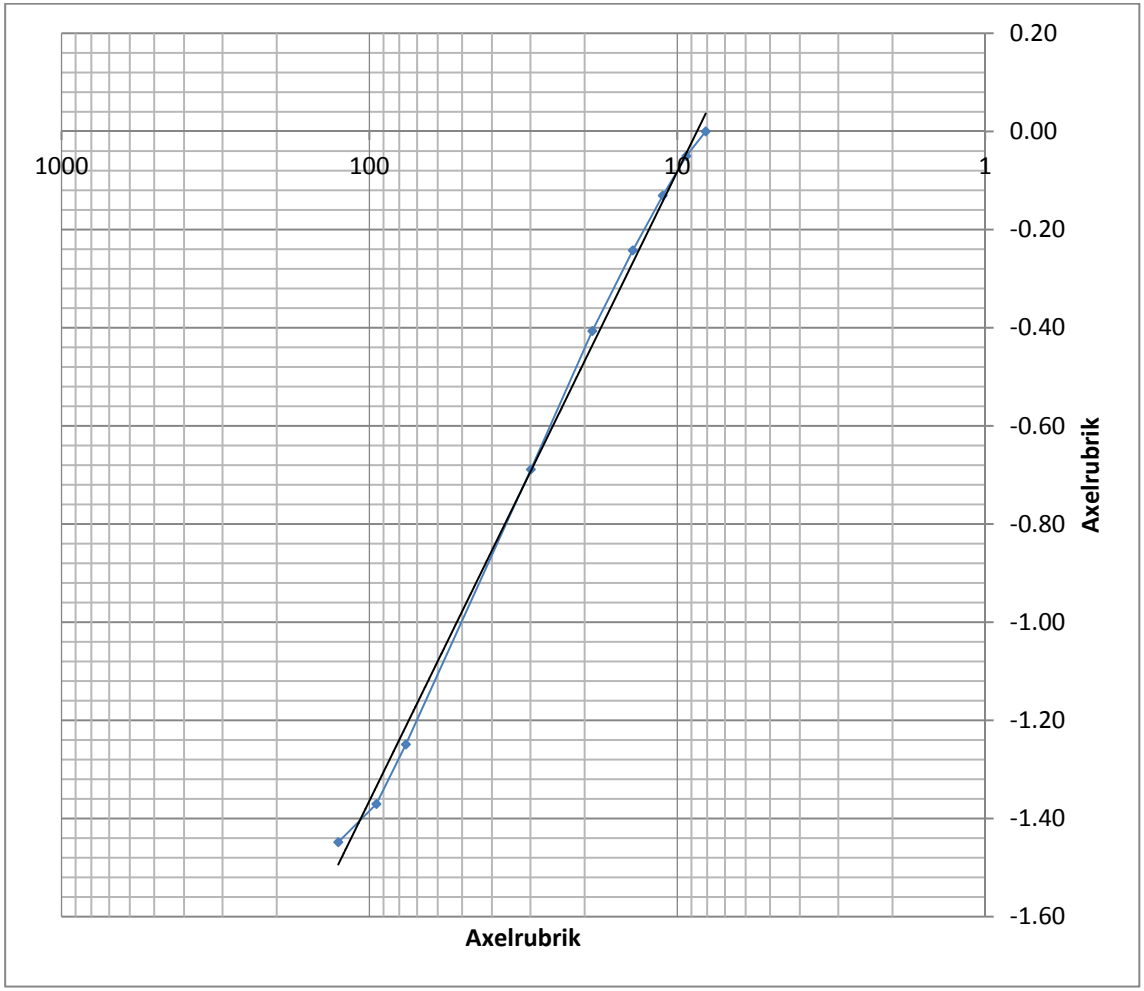

Figure 1.4 Observation well 5 – plotted drawdown.

From Figure 1.4 follow parameters is deduced: Δs=1.28 m and T=0.0033 m^2/s. For an overview of all transmissivity values see Table 3.1.

Table 1.6 Observation well 6. Initial groundwater level is 34.74 m and adjusted duration (t) is 67611 min.*

Date and time	t' [min]	t*+t' [min]	(t*+t')/t' [-]	Groundwater level [m]	Drawdown [m]	Correction factor [m]	Corrected drawdown [m]
1976-05-14 09:00	1	67612	67612	33.75	34.74	-0.99	0.0408
1976-05-14 18:00	540	68151	126	33.80	34.74	-0.94	0.0368
1976-05-14 21:00	720	68331	95	33.84	34.74	-0.90	0.0337
1976-05-15 00:00	900	68511	76	33.88	34.74	-0.86	0.0308
1976-05-16 00:00	2340	69951	30	34.15	34.74	-0.59	0.0145
1976-05-17 00:00	3780	71391	19	34.36	34.74	-0.38	0.0060
1976-05-18 00:00	5220	72831	14	34.51	34.74	-0.23	0.0022
1976-05-19 00:00	6660	74271	11	34.60	34.74	-0.14	0.0008
1976-05-20 00:00	8100	75711	9	34.68	34.74	-0.06	0.0002
1976-05-21 00:00	9540	77151	8	34.74	34.74	0.00	0.0000

Appendix 2 – Conductivity values

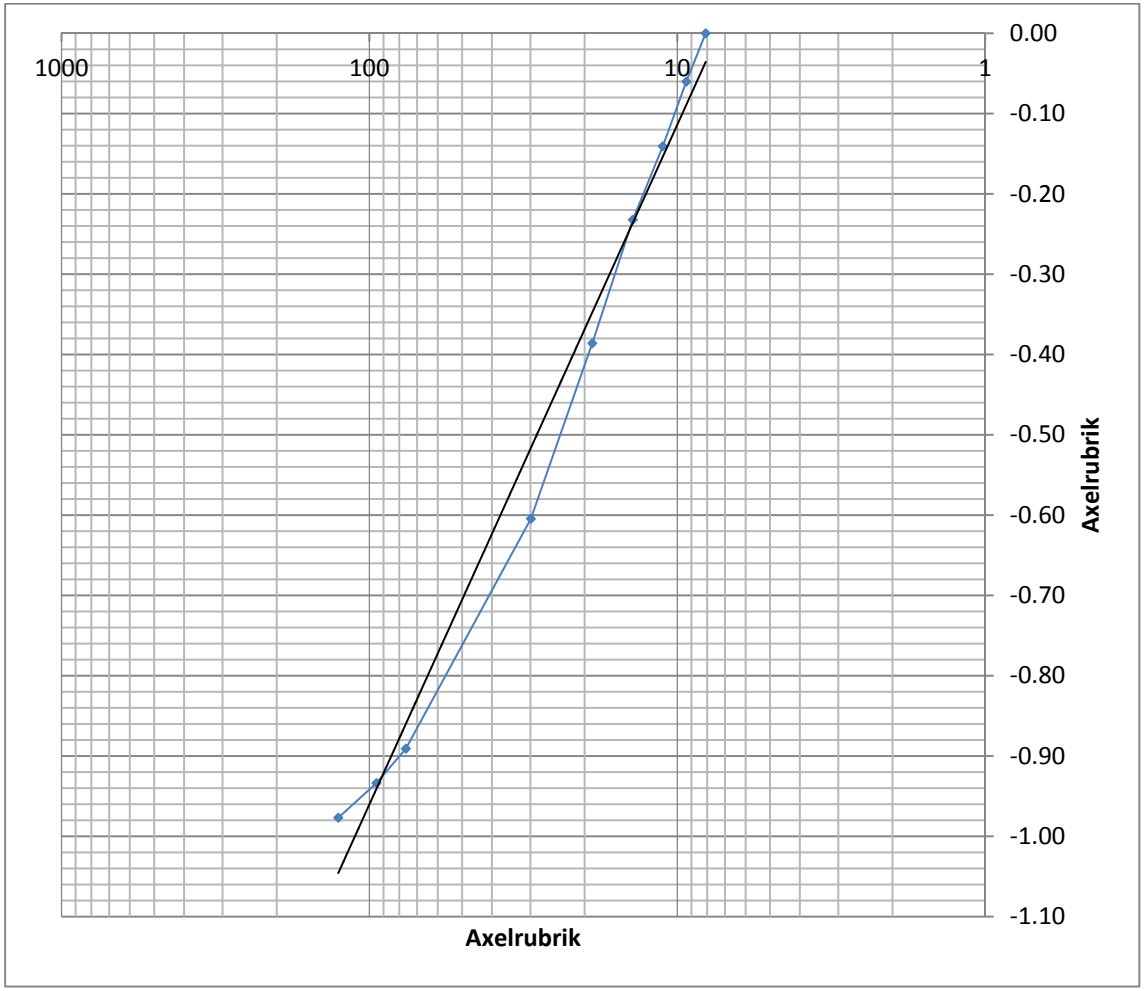

Figure 1.5 Observation well 6 – plotted drawdown.

From Figure 1.5 follow parameters is deduced: Δs=0.85 m and T=0.0050 m^2/s. For an overview of all transmissivity values see Table 3.1.

Table 1.7 Observation well "Brunn 1". Initial groundwater level is 34.74m and adjusted duration (t) is 67611 min.*

Date and time	t' [min]	t*+t' [min]	(t*+t')/t' [-]	Groundwater level [m]	Drawdown [m]	Correction factor [m]	Corrected drawdown [m]
1976-05-14 09:00	1	67612	67612	32.10	-2.64	0.2904	-2.93
1976-05-14 18:00	540	68151	126	32.32	-2.42	0.2440	-2.66
1976-05-14 21:00	720	68331	95	32.55	-2.19	0.1998	-2.39
1976-05-15 00:00	900	68511	76	32.94	-1.80	0.1350	-1.94
1976-05-16 00:00	2340	69951	30	34.11	-0.63	0.0165	-0.65
1976-05-17 00:00	3780	71391	19	34.38	-0.36	0.0054	-0.37
1976-05-18 00:00	5220	72831	14	34.52	-0.22	0.0020	-0.22
1976-05-19 00:00	6660	74271	11	34.61	-0.13	0.0007	-0.13
1976-05-20 00:00	8100	75711	9	34.68	-0.06	0.0002	-0.06
1976-05-21 00:00	9540	77151	8	34.74	0.00	0.0000	0.00

Appendix 2 – Conductivity values

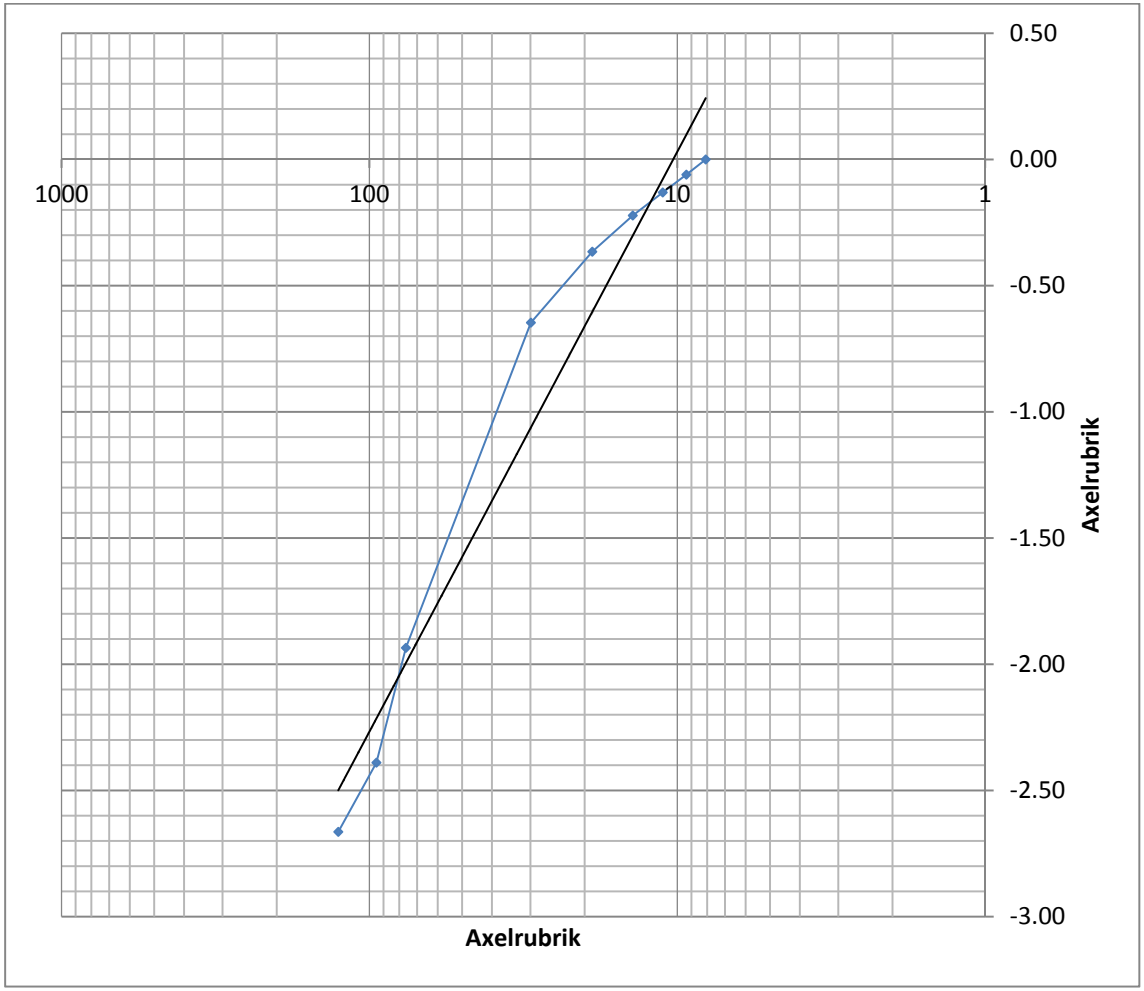

Figure 1.6 Observation well "Brunn 1" – plotted drawdown.

From Figure 1.6 follow parameters is deduced: Δs=2.26 m and T=0.0019 m^2/s. For an overview of all transmissivity values see Table 3.1.

Table 1.8 Observation well ”Brunn 8”. Initial groundwater level is 34.66 m and adjusted duration (t) is 67611 min.*

Date and time	t' [min]	t*+t' [min]	(t*+t')/t' [-]	Groundwater level [m]	Drawdown [m]	Correction factor [m]	Corrected drawdown [m]
1976-05-14 09:00	1	67612	67612	34.43	-0.23	0.0022	-0.23
1976-05-14 18:00	540	68151	126	34.43	-0.23	0.0022	-0.23
1976-05-14 21:00	720	68331	95	34.43	-0.23	0.0022	-0.23
1976-05-15 00:00	900	68511	76	34.43	-0.23	0.0022	-0.23
1976-05-16 00:00	2340	69951	30	34.43	-0.23	0.0022	-0.23
1976-05-17 00:00	3780	71391	19	34.46	-0.20	0.0017	-0.20
1976-05-18 00:00	5220	72831	14	34.48	-0.18	0.0014	-0.18
1976-05-19 00:00	6660	74271	11	34.52	-0.14	0.0008	-0.14
1976-05-20 00:00	8100	75711	9	34.60	-0.06	0.0001	-0.06
1976-05-21 00:00	9540	77151	8	34.66	0.00	0.0000	0.00

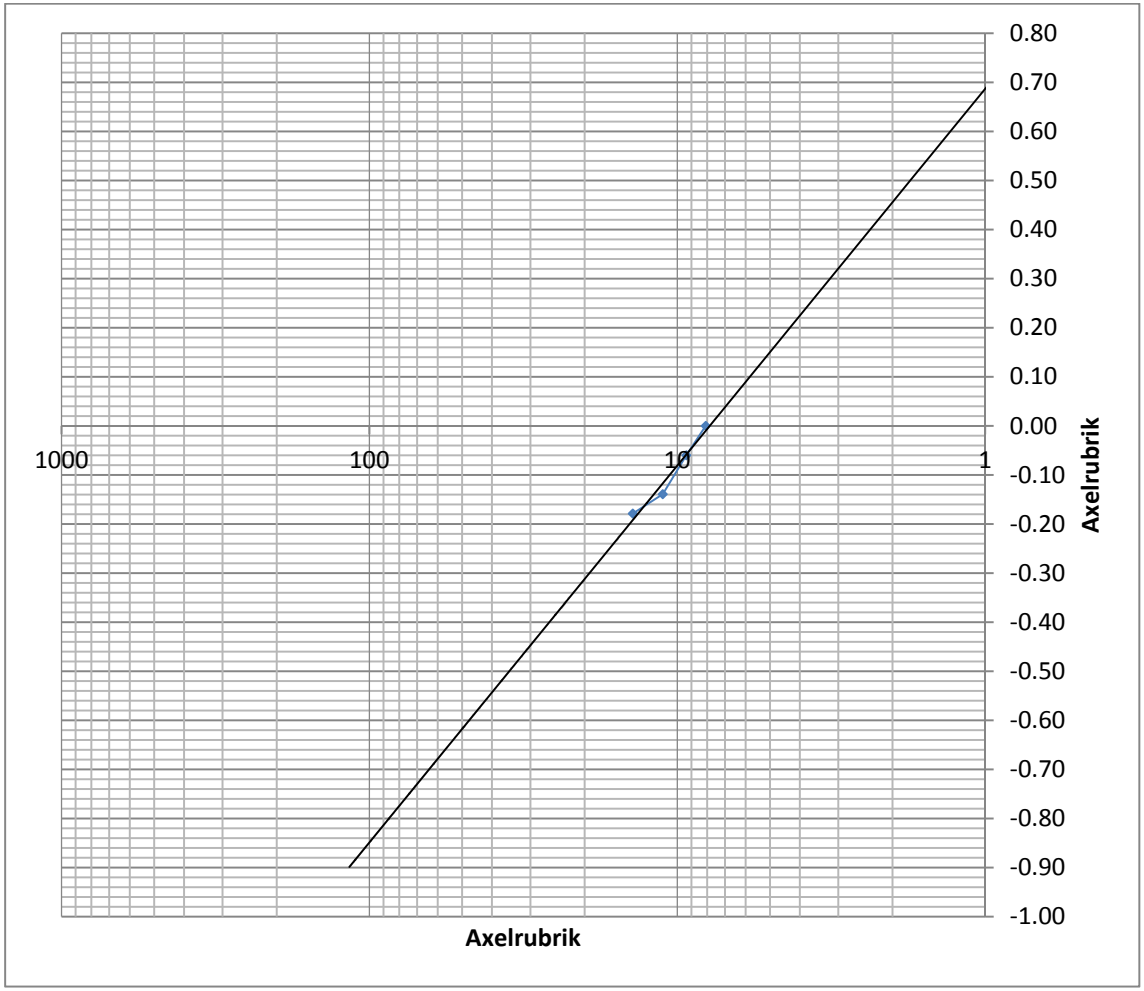

Figure 1.7 Observation well "Brunn 8" – plotted drawdown. Only the last four observations is plotted in the diagram.

From Figure 1.7 follow parameters is deduced: Δs=0.77 m and T=0.0055 m^2/s. For an overview of all transmissivity values see Table 3.1.

2 Saturated thickness

2.1 Storehagen

According to Table 2.1the average aquifer thickness is 14.9 meters and according to

Appendix 2 – Conductivity values

Table 2.2 the average distance from water table to ground surface is 3.0 meters. The average saturated thickness is therefore assumed to be 11.9 meters.

Table 2.1 Aquifer thickness, Storehagen

Observation well	Ground elevation [m]	Elevation of firm bottom [m]	Aquifer thickness [m]
11	98	81	17
12	98.5	75	23.5
13	99.5	91.5	8
16	103	89	14
17	99.5	84.5	15
18	97	82	15
20	99	82	17
21	98.5	81.5	17
22	98	83.5	14.5
8903	100.7	85	15.7
8905	99.2	91.2	8
9001	102.8	88.8	14

Table 2.2 Distance from water table to ground surface, Storehagen

Observation well	Ground elevation [m]	Initial water table [m]	Distance from water table to ground surface [m]
2	38.7	35.3	3.4
3	37.5	35.4	2.1
4	36	35.32	0.68
5	41.5	35.35	6.15
6	38	35.46	2.54
Brunn 1	40.1	35.46	4.64
Brunn 7	37.9	36.43	1.47
Brunn 8	38	34.95	3.05

2.2 Algutstorp

Table 2.3 Aquifer thickness, Algutstorp

Observation well	Ground elevation [m]	Elevation of firm bottom [m]	Aquifer thickness [m]
R13	98.2	85.7	12.5
R14	98.33	90.83	7.5
R15	101.7	93.7	8
R16	99.74	89.99	9.75
R17	98.06	88.81	9.25
R18	98.65	88.4	10.25
R19	98.56	88.06	10.5

Table 2.4 Distance from water table to ground surface, Algutstorp

Observation well	Ground elevation [m]	Initial water table [m]	Distance from water table to ground surface [m]
B1	99.5	1.8	97.7

B2	99	1.24	97.76
B3	98.8	0.92	97.88

According to Table 2.3 the average aquifer thickness is 9.7 meters and according to Table 2.4 the average distance from water table to ground surface is 1.3 meters. The average saturated thickness is therefore assumed to be 8.4 meters.

3 Overview of transmissivity values, aquifer analysis

3.1 Storehagen

Table 3.1 *Transmissivity[1] and conductivity values, Storehagen. Saturated thickness is assumed to be 11.9 meters according to previous Chapter.*

Observation well	Transmissivity [m^2/s]	Conductivity [m/s]
2	0.0032	$2.7 \cdot 10^{-4}$
3	0.0035	$2.9 \cdot 10^{-4}$
4	0.0030	$2.5 \cdot 10^{-4}$
5	0.0033	$2.7 \cdot 10^{-4}$
6	0.0050	$4.1 \cdot 10^{-4}$
Brunn 1	0.0019	$1.6 \cdot 10^{-4}$
Brunn 8	0.0055	$4.6 \cdot 10^{-4}$
Average	0.0036	$3.0 \cdot 10^{-4}$

3.2 Algutstorp

Table 3.2 *Transmissivity[2] and conductivity values, aquifer field test 1 drawdown phase, Algutstorp. Saturated thickness is assumed to be 8.4 meters according to previous Chapter.*

Observation well	Transmissivity [m^2/s]	Conductivity [m/s]
B1	0.0040	$4.8 \cdot 10^{-4}$
B2	0.0042	$5.0 \cdot 10^{-4}$
B3	0.0031	$3.7 \cdot 10^{-4}$
R8902	0.0045	$5.4 \cdot 10^{-4}$
Average	0.0040	$4.7 \cdot 10^{-4}$

[1] Transmissivity values from Chapter 2
[2] Transmissivity values from (Ramböll Sverige AB 2007)

Appendix 2 – Conductivity values

Table 3.3 *Transmissivity[2] and conductivity values, aquifer field test 1 recovery phase, Algutstorp. Saturated thickness is assumed to be 8.4 meters according to previous Chapter.*

Observation well	Transmissivity [m^2/s]	Conductivity [m/s]
B1	0.0032	$3.8 \cdot 10^{-4}$
B2	0.0029	$3.5 \cdot 10^{-4}$
B3	0.0039	$4.6 \cdot 10^{-4}$
R8902	0.0037	$4.4 \cdot 10^{-4}$
Average	0.0034	$4.1 \cdot 10^{-4}$

Table 3.4 *Transmissivity[2] and conductivity values, aquifer field test 2 drawdown phase, Algutstorp. Saturated thickness is assumed to be 8.4 meters according to previous Chapter.*

Observation well	Transmissivity [m^2/s]	Conductivity [m/s]
B1	0.0031	$3.7 \cdot 10^{-4}$
B2	0.0038	$4.5 \cdot 10^{-4}$
B3	0.0018	$2.1 \cdot 10^{-4}$
R8902	0.0050	$6.0 \cdot 10^{-4}$
Average	0.0034	$4.1 \cdot 10^{-4}$

Table 3.5 *Transmissivity[2] and conductivity values, aquifer field test 2 drawdown recovery phase, Algutstorp. Saturated thickness is assumed to be 8.4 meters according to previous Chapter.*

Observation well	Transmissivity [m^2/s]	Conductivity [m/s]
B1	0.0038	$4.5 \cdot 10^{-4}$
B2	0.0056	$6.7 \cdot 10^{-4}$
B3	0.0056	$6.7 \cdot 10^{-4}$
R8902	0.0072	$8.6 \cdot 10^{-4}$
Average	0.0056	$6.6 \cdot 10^{-4}$

4 Conductivity calculations by Hazen's formula

The Hazen formula is an empirical formula that uses grain size analysis as a base for calculations. Like other empirical formulas in this context, the Hazen formula renders only approximate values of the hydraulic conductivity for small sample series. (Kresic, 2007) However in the perspective of initial hydraulic conductivity it was assumed here that that it was sufficient enough. The Hazen formula is given as

$$K = C \cdot d_{10}^2$$

where

C is a constant which ranges from 400 to 1200 depending on the type of soil. The lower number the finer grain size. Here a value of the constant C was chosen to 1157.

The samples were all taken in rather coarse material. Considering all the samples D_{10} ranged from 0.05 to 0.25 and D_{60} from 0.2 to 1.8.

The average conductivity for the sand in the two areas, Storehagen and Algutstorp is $5.1 \cdot 10^{-4}$ m/s.

4.1 Storehagen

The grain size distribution where mainly preformed for layers of coarse sand. The sand in Storehagen has a conductivity of about $6.7 \cdot 10^{-4}$ m/s according to Hazen's formula, see Table 4.1.

Table 4.1 Conductivity values in Storehagen for soil fraction coarse sand, calculated with Hazen's formula.

Observation well	Conductivity [m/s]	Average conductivity [m/s]
8903-1	$3.7 \cdot 10^{-4}$	$5.5 \cdot 10^{-4}$
8903-2	$7.2 \cdot 10^{-4}$	
12-7	$2.6 \cdot 10^{-4}$	$7.4 \cdot 10^{-4}$
12-8	$1.2 \cdot 10^{-4}$	
12-9	$7.2 \cdot 10^{-4}$	
12-10	$1.9 \cdot 10^{-3}$	
Average	$6.7 \cdot 10^{-4}$	$6.4 \cdot 10^{-4}$

4.2 Algutstorp

The sand in Algutstorp has a conductivity of about $3.8 \cdot 10^{-4}$ m/s according to Hazen's formula, see Table 4.2.

Appendix 2 – Conductivity values

Table 4.2 Conductivity values in Algutstorp for soil fraction coarse sand, calculated with Hazen's formula.

Observation well	Conductivity [m/s]	Average conductivity [m/s]
0801-1	$2.6 \cdot 10^{-4}$	$3.6 \cdot 10^{-4}$
0801-2	$3.0 \cdot 10^{-4}$	
0801-3	$5.1 \cdot 10^{-4}$	
0802-1	$6.1 \cdot 10^{-4}$	$5.4 \cdot 10^{-4}$
0802-2	$4.6 \cdot 10^{-4}$	
0802-3	$5.6 \cdot 10^{-4}$	
0803-1	$2.0 \cdot 10^{-4}$	$4.4 \cdot 10^{-4}$
0803-2	$3.0 \cdot 10^{-4}$	
0803-3	$2.3 \cdot 10^{-4}$	
0803-4	$7.8 \cdot 10^{-4}$	
0803-5	$6.7 \cdot 10^{-4}$	
0803-6	$7.2 \cdot 10^{-4}$	
0803-7	$4.2 \cdot 10^{-4}$	
0803-8	$2.0 \cdot 10^{-4}$	
0804-1	$2.9 \cdot 10^{-5}$	$1.5 \cdot 10^{-4}$
0804-2	$2.9 \cdot 10^{-5}$	
0804-3	$5.7 \cdot 10^{-5}$	
0804-4	$1.2 \cdot 10^{-4}$	
0804-5	$2.6 \cdot 10^{-4}$	
0804-6	$5.6 \cdot 10^{-4}$	
0804-7	$5.7 \cdot 10^{-5}$	
0804-8	$4.9 \cdot 10^{-5}$	
0804-9	$2.3 \cdot 10^{-4}$	
8907-1	$1.8 \cdot 10^{-4}$	$4.2 \cdot 10^{-4}$

Appendix 2 – Conductivity values

8907-2	$5.1 \cdot 10^{-4}$	
8907-3	$4.2 \cdot 10^{-4}$	
8907-4	$5.6 \cdot 10^{-4}$	
Average	$3.4 \cdot 10^{-4}$	$3.8 \cdot 10^{-4}$

5 Confidence interval for conductivity values

Table 5.1 Mean values for conductivity Storehagen

	Average conductivity [m/s]
Cooper-Jacob (Table 2.3)	$3.0 \cdot 10^{-4}$

Table 5.2 Mean values for conductivity Algutstorp

	Average conductivity [m/s]
Aquifer field test 1 drawdown phase (Table 3.2)	$4.7 \cdot 10^{-4}$
Aquifer field test 1 drawdown recovery phase (Table 3.3)	$4.1 \cdot 10^{-4}$
Aquifer field test 2 drawdown phase (Table 3.4)	$4.1 \cdot 10^{-4}$
Aquifer field test 2 drawdown recovery phase (Table 3.5)	$6.6 \cdot 10^{-4}$

Table 5.3 Conductivity values, Storehagen and Algutstorp

	Storehagen [m/s]	Algutstorp [m/s]
Sample mean, μx	$3.0 \cdot 10^{-4}$	$4.9 \cdot 10^{-4}$
Sample standard deviation, s	$1.1 \cdot 10^{-4}$	$1.5 \cdot 10^{-4}$
Two sided 95% confidence interval	$9.8 \cdot 10^{-5}$	$8.2 \cdot 10^{-5}$

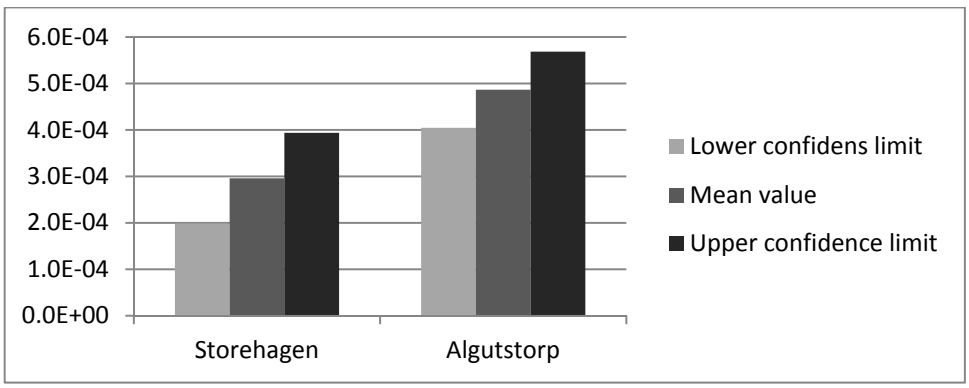

Figure 8 Confidence interval for conductivity values

Drawdown data recorded in the production well B1 when water was extracted from the well B2. (Ramböll Sverige AB 2007)

The drawdown was plotted against the pumping time in a double logarithmic diagram, see Figure 1, and the type curve that was giving the best match was Theis-Boulton, r/D=1.25.

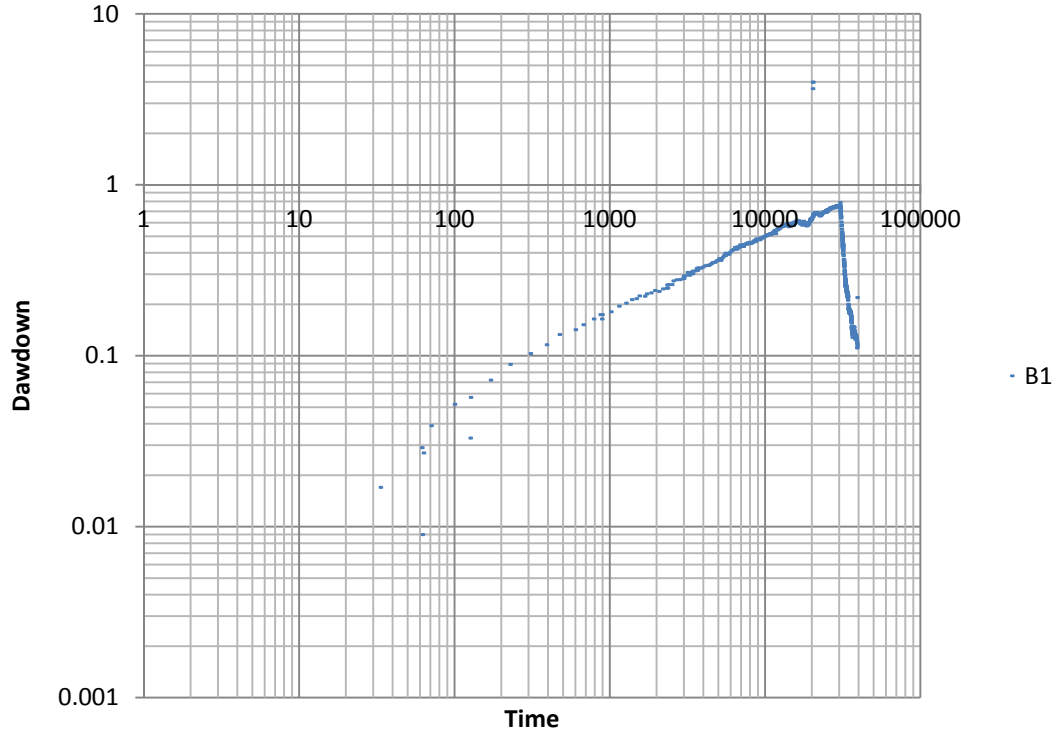

Figure 1 *Drawdown verses pumping time.*

The horizontal transmissivity was calculated by the means of

$$T = \frac{7.95Q}{100}\frac{W(1/u, r/D)}{s_m} \quad (1)$$

where

s_m is the drawdown at the match point and was measured to 0.21

Q is the withdrawal rate and was 0.0074m^3/s

W(1/u,r/D) is at the match point equal to 1

The horizontal transmissivity was in this way calculated to $2.8 \cdot 10^{-3}$ m^2/s. The horizontal hydraulic conductivity was calculated by dividing the horizontal transmissivity with the approximately saturated thickness and was determined to $3.3 \cdot 10^{-4}$ m^2/s.

The vertical transmissivity was calculated using

$$K_Z = \frac{Kb_0 * b_a}{r^2}\left(\frac{r}{D}\right)^2 \quad (2)$$

where

Appendix 3 – Anisotropy of the hydraulic conductivity

K is the horizontal transmissivity

b_0 is the initial saturated thickness of the aquifer and was approximated to be 8.4m

r is the distance between the observation well B1 and the pumping well B2 and was given as 25m

b_a was assumed to equal $b_0/3$

The vertical transmissivity was calculated to $1.6 \cdot 10^{-4}$ m^2/s and the anisotropy factor defined as K_r/K_z was determined to 2. (Gustafson & Gustafson 1997)

1.1 Input parameters

Catchment area

$CA_{Kärtared - Algutstorp}$ 48200525 m^2 *(Vattenkartan 2011)*

Annual mean flow for the period 1995-2009

$Q_{Kärtared}$ 4.2 m^3/s *(SMHI 2010)*

$Q_{Algutstorp}$ 4.9 m^3/s *(SMHI 2010)*

Year	**Flow rate [m³/s]**	**Flow rate [m³/s]**
1990	5.7	4.88
1991	4.2	3.62
1992	5.5	4.65
1993	3.9	3.31
1994	5.6	4.72
1995	5.6	4.81
1996	2.8	2.39
1997	3.5	2.99
1998	6.0	5.09
1999	5.9	5.04
2000	6.4	5.44
2001	4.0	3.45
2002	4.7	4.02
2003	2.8	2.35
2004	5.2	4.44
2005	3.9	3.35
2006	5.8	4.89
2007	6.2	5.28
2008	7.0	5.98
2009	3.7	3.14
2010	4.3	3.68
Mean	4.9	4.17
STDAV	1.20	1.03

1.2 Calculated parameters

Recharge

$$R = \frac{Q_{Algutstorp} - Q_{Kärtared}}{CA_{Kärtared-Algutstorp}} = \frac{1.5 \cdot 10^{-8}\ m/s}{472\ mm/year}$$

Standard deviation for the recharge

μ recharge [m/s]	$1.50 \cdot 10^{-8}$
σ recharge [m/s]	$2.60 \cdot 10^{-8}$
μ recharge [m/yr]	0.47
σ recharge [m/yr]	0.82
Two sided 95% confidence intervall [m/yr]	0.26

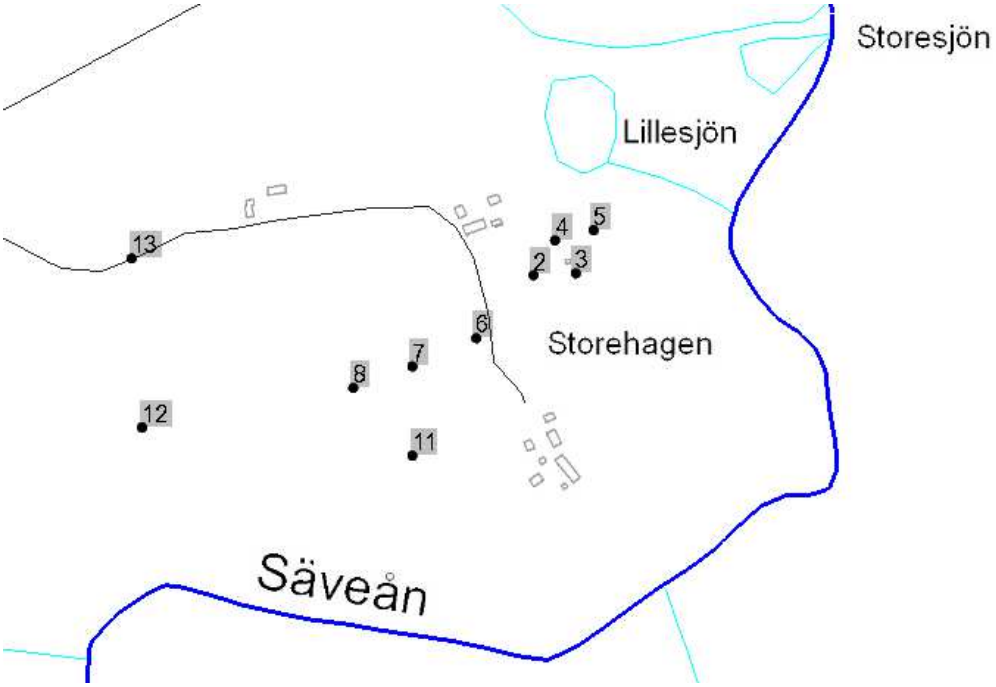

Figure 1 *Location of observation wells in Storehagen*

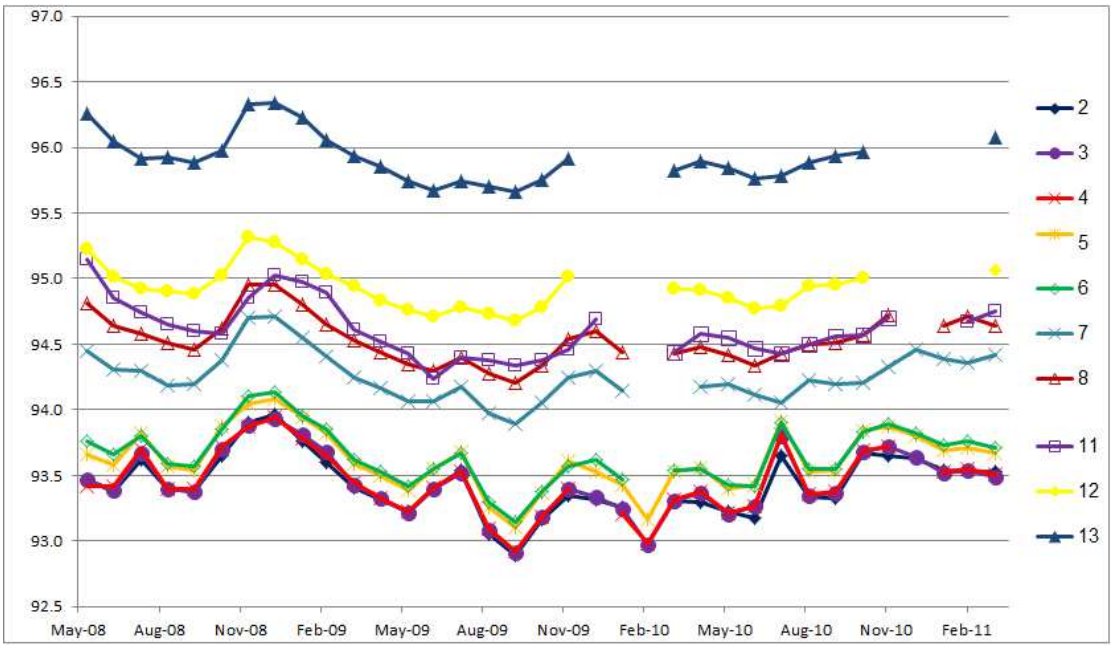

Figure 2 *Temporal variations in groundwater head May 2008 – April 2011, Storehagen*

Data obtained from Algutstorps water treatment plant.

Excel file: Grundvatten nivå.xls

Updated 2011-03-31 by Per-Olof Lennartsson

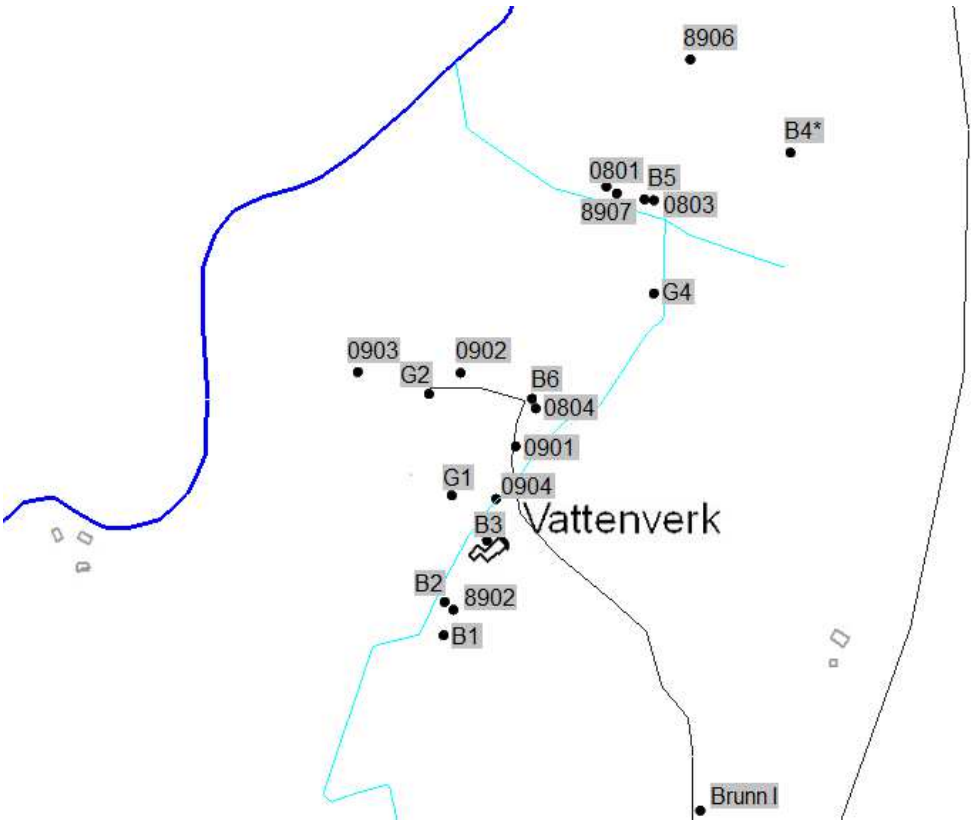

Figure 3 *Location of observation wells in Algutstorp*

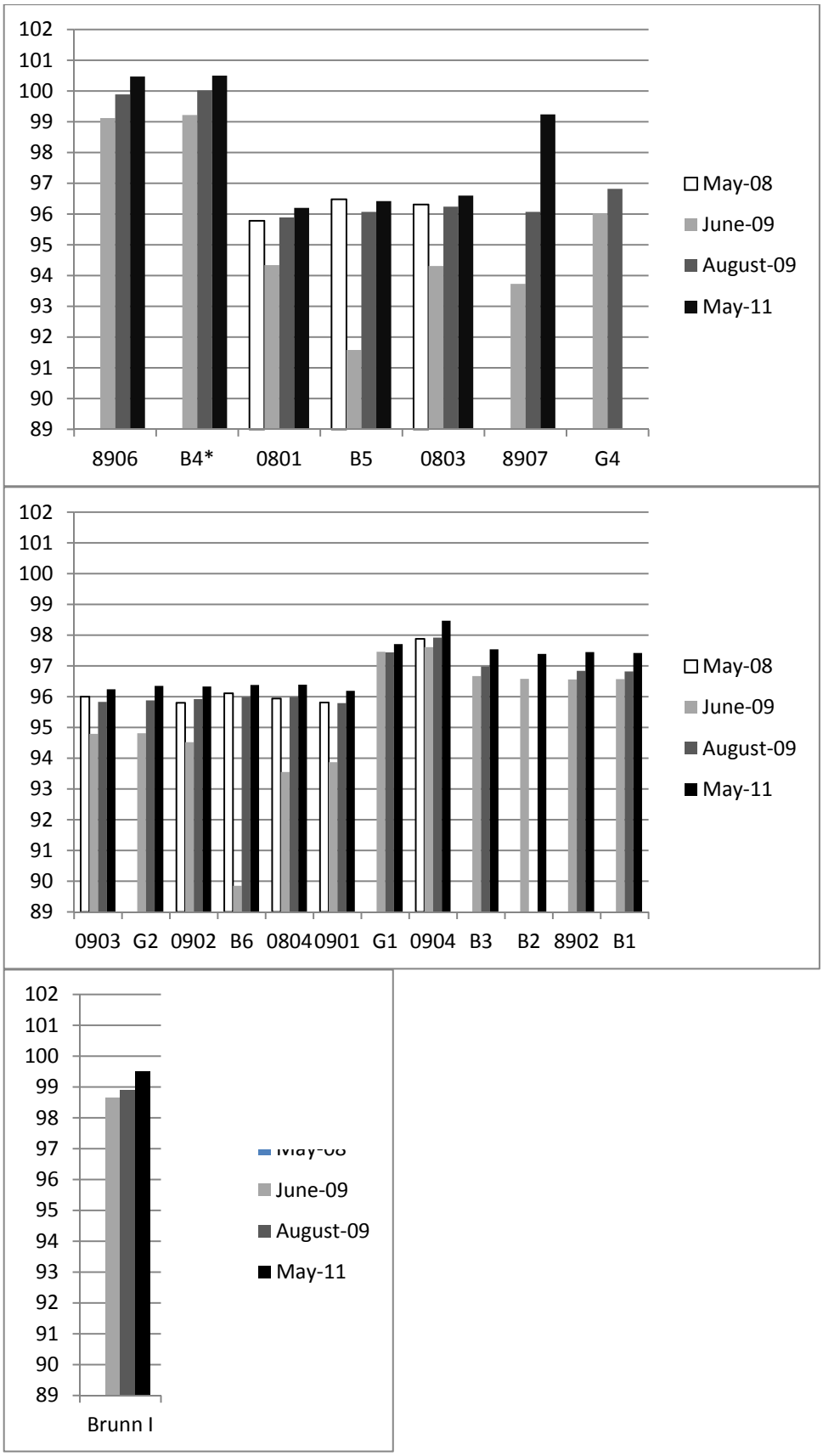

Figure 4 *Temporal variations in groundwater head, Algutstorp*

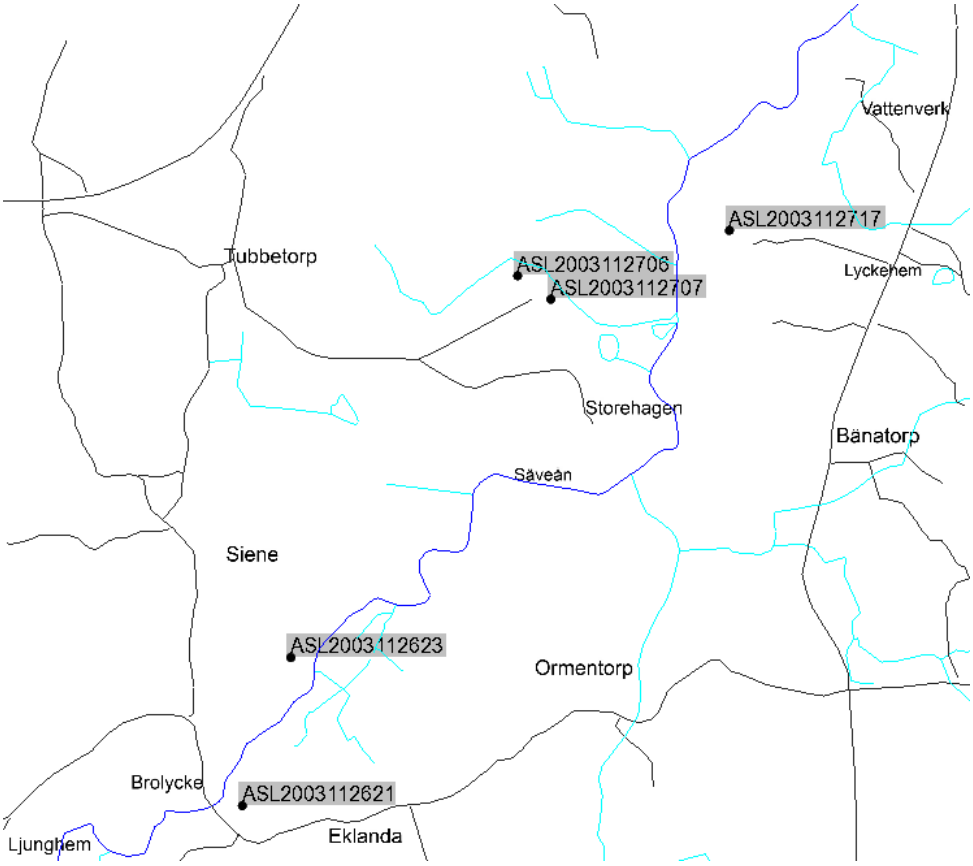

Figure 5 *Location of wells observed by SGU*

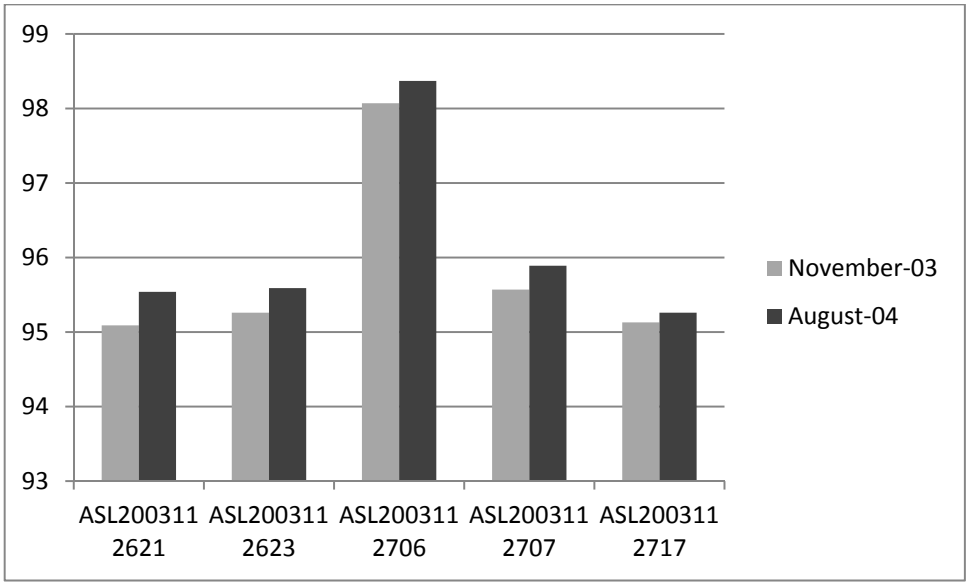

Figure 6 *Temporal variations in groundwater head, observed by SGU*

Data obtained from Sweden's Geological Survey (SGU).

Excel file: Nivaer_vargarda.xls

Created 2006-12-04 by Åsa Lindh

Appendix 6 – Classification of soil types

HGU	1 - Bedrock	2 - Till	3 - Clay	4 - Silt	5 - Sand
Notation from the borehole protocol	Berg Berg eller block Block eller berg	Morän stenig morän sandig morän finsand/morän	Lera, finsand och finmo Lera växl. Silt - lera siltig lera Siltig lera/lerig silt	Lerblandad finsand Lera och finsand Lerblandad sand Lerblandad sand och finmo siltig sand silt siltig finsand lerig silt silt/finsand	Finsand Lerblandad sand och grus Sand Strid sand Sand med finmtrl (silt) Siltig sand Lerig-siltig sand Finsand-mellansand Finsand/silt (mo) Strid sand och grus Grovt grus Sand och grus Kraftigt stenblandad grovt grus Finsand och grus Stenblandad sand och grus Grusig sand Sand, med grus/sten Grusig sand-mellansand

Appendix 6 – Classification of soil types

HGU	1 - Bedrock	2 - Till	3 - Clay	4 - Silt	5 - Sand
Notation from the borehole protocol					Sten Mellansand Sandigt grus fyllning mellansand/grovsand grovsand grusig grovsand stenig , grusig sand grusig , stenig sandStenig grus

1 Forward run

File name: vargarda2011-05-13.gpr

1.1 Settings

Run options: Forward run

Layer property entry method: Use material IDs

Layer type: Convertible

Vertical hydraulic conductivity: Specify anisotrophy factors

Cell wetting parameters: Allow wetting of cells

Wetting factor: 1

Wetting iter. Interval: 5

Maximum outer iterations: 100

Maximum inner iterations: 50

Head change criterion for convergence: 0.05 m

Residual criterion for convergence: 0.05 m^3/s

1.2 Parameters

Table 1.1 Parameters for forward run

Parameter	Value
Conductivity, sand	$1 \cdot 10^{-4}$ m/s
Conductivity, silt	$1 \cdot 10^{-5}$ m/s
Conductivity, clay	$1 \cdot 10^{-5}$ m/s
Conductivity, till	$1 \cdot 10^{-5}$ m/s
Vertical anisotropy, hydraulic conductivity	1
Recharge, main aquifer	0.475 mm/year
Recharge, border	1.425 mm/year
Hydraulic conductance, Säveån River	0.00175 m^2/s
Hydraulic conductance, streams	0.0005 m^2/s
Hydraulic conductance, drains	0.0005 m^2/s

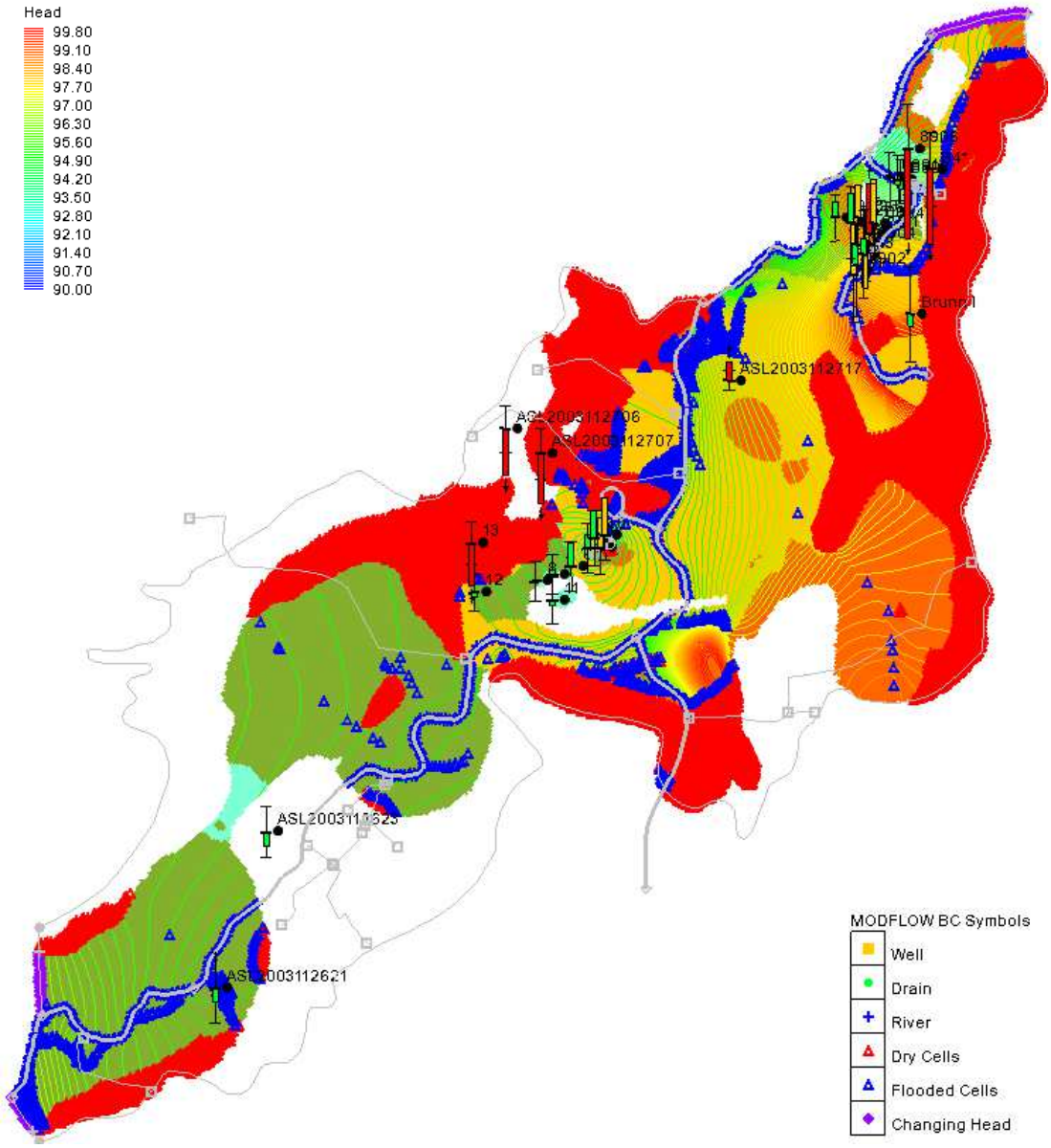

Figure 1.1

Sum of squared weighted residuals: 205.12

2 Parameter estimation

File name: vargarda2011-05-13PEST.gpr

2.1 Settings

Only settings different from the file “vargarda2011-05-13.gpr” is accounted for.

Run options: Parameter estimation

Residual criterion for convergence: 0.008 m^3/s

2.2 Parameters

Only parameters different from the file “vargarda2011-05-13.gpr” is accounted for.

Table 2.1 Starting values for PEST-parameters first run.

Parameter	Start value [m/s]	Min value [m/s]	Max value [m/s]
Sand	$5 \cdot 10^{-4}$	$1 \cdot 10^{-7}$	0.1
Silt	$1 \cdot 10^{-5}$	$1 \cdot 10^{-12}$	0.01
Clay	$1 \cdot 10^{-5}$	$1 \cdot 10^{-12}$	0.01
Till	$1 \cdot 10^{-5}$	$1 \cdot 10^{-12}$	0.01

2.3 Optimisation result

Table 2.2 Optimal value from the inverse modelling

Parameter	Conductivity [m/s]
Sand	4.93E-04
Silt	2.00E-06
Clay	1.09E-05
Till	3.72E-05

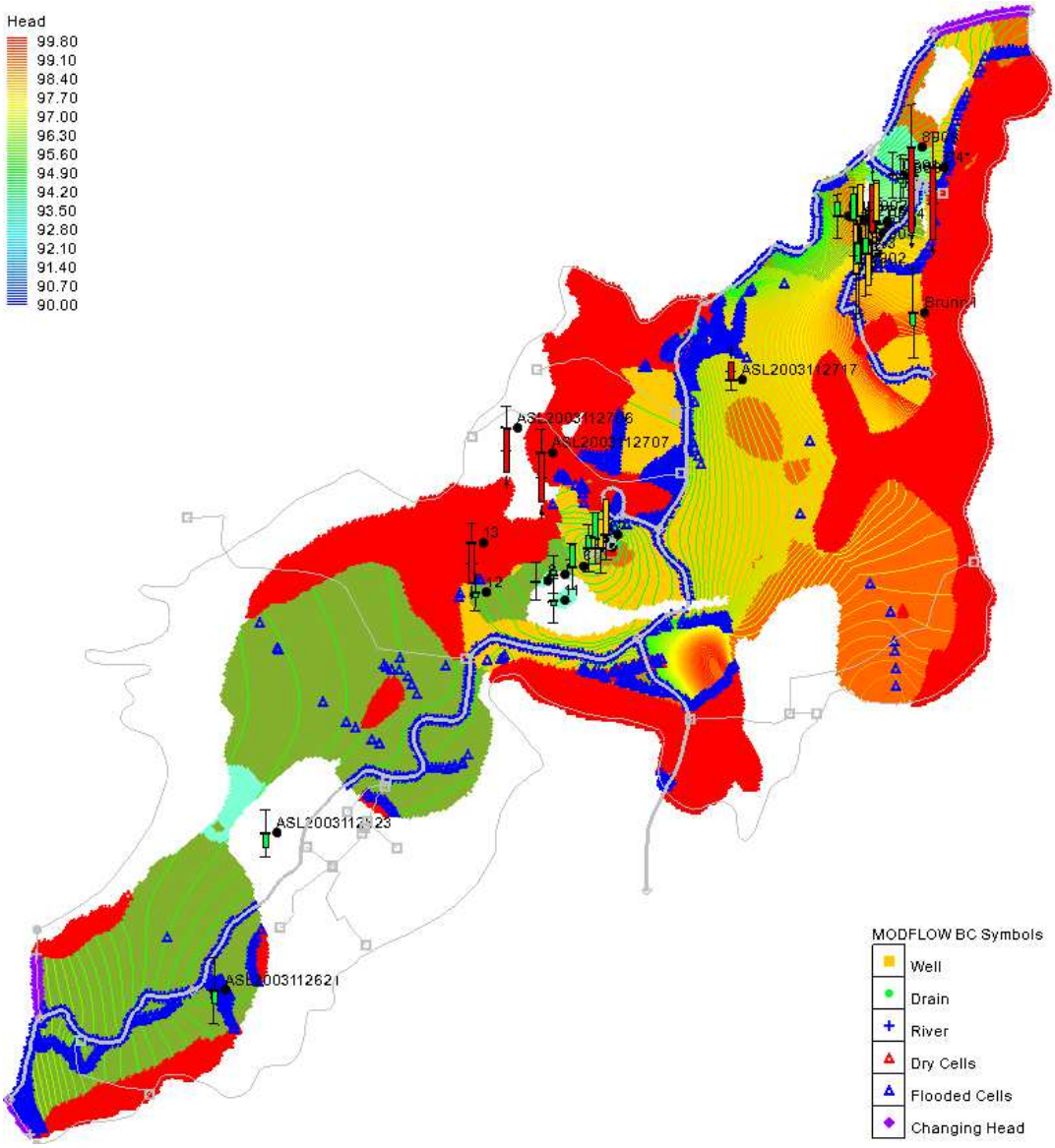

Table 2.3 Residuals for observation group "head"

Number of residuals with non-zero weight	32
Mean value of non-zero weighted residuals	9.97E-02
Maximum weighted residual [observation "hed12"]	6.779
Minimum weighted residual [observation "hed22"]	-6.728
Variance of weighted residuals	7.549
Standard error of weighted residuals	2.747
Contribution to phi from observation group "head"	241.6

Sum of squared weighted residuals: 241.6

Table 2.4 Parameter correlation coefficient matrix

	Sand	Silt	Clay	Till
Sand	1.0000	-0.5671	-0.3842	-0.0608
Silt	-0.5671	1.0000	-0.0535	0.0345
Clay	-0.3842	-0.0535	1.0000	0.0234
Till	-0.0608	0.0345	0.0234	1.0000

The sensitivity for the parameters is described in Table 2.5, where the sensitivity indicates the factor of how much a simulated value would change in relation to the changed parameter (Hill & Tiedeman 2007).

Table 2.5 Composite sensitivities

Parameter	Composite sensitivities for	
	observation group "head"	all observations/prior info
Sand	8.5	3.9
Silt	18.5	8.6
Clay	102.8	47.7
Till	18.4	8.5

Appendix 7 – Calibration process

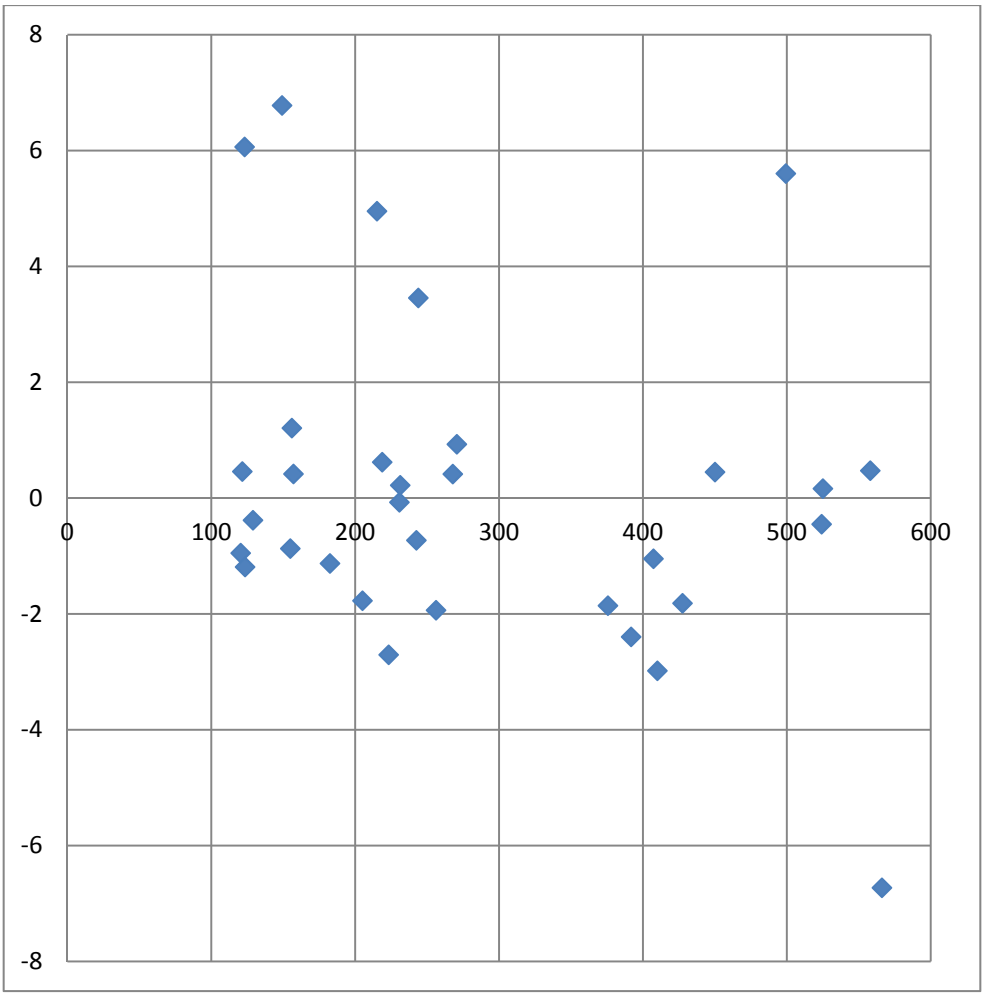

Figure 2.1 *Weight*Modelled versus Weight*Residual*